Lecture notes on
Computational Fluid Dynamics

Dan S. Henningson
Martin Berggren

January 13, 2005

Contents

Preface

These lecture notes has evolved from a CFD course (5C1212) and a Fluid Mechanics course (5C1214) at the department of Mechanics and the department of Numerical Analysis and Computer Science (NADA) at KTH. Erik Stålberg and Ori Levin has typed most of the LaTeXformulas and has created the electronic versions of most figures.

Stockholm, August 2004
Dan Henningson
Martin Berggren

Chapter 1

Derivation of the Navier-Stokes equations

1.1 Notation

The Navier-Stokes equations in vector notation has the following form

$$
\begin{cases}
\dfrac{\partial \mathbf{u}}{\partial t} + (\mathbf{u} \cdot \nabla)\,\mathbf{u} & = & -\dfrac{1}{\rho}\nabla p + \nu \nabla^2 \mathbf{u} \\[2mm]
\nabla \cdot \mathbf{u} & = & 0
\end{cases}
$$

where the velocity components are defined

$$
\mathbf{u} = (u, v, w) = (u_1, u_2, u_3)
$$

the nabla operator is defined as

$$
\nabla = \left(\frac{\partial}{\partial x}, \frac{\partial}{\partial y}, \frac{\partial}{\partial z} \right) = \left(\frac{\partial}{\partial x_1}, \frac{\partial}{\partial x_2}, \frac{\partial}{\partial x_3} \right)
$$

the Laplace operator is written as

$$
\nabla^2 = \frac{\partial^2}{\partial x^2} + \frac{\partial^2}{\partial y^2} + \frac{\partial^2}{\partial z^2}
$$

and the following definitions are used

$$
\begin{array}{ccl}
\nu & - & \text{kinematic viscosity} \\
\rho & - & \text{density} \\
p & - & \text{pressure}
\end{array}
$$

see figure 1.1 for a definition of the coordinate system and the velocity components.
The Cartesian tensor form of the equations can be written

$$
\begin{cases}
\dfrac{\partial u_i}{\partial t} + u_j \dfrac{\partial u_i}{\partial x_j} & = & -\dfrac{1}{\rho}\dfrac{\partial p}{\partial x_i} + \nu \dfrac{\partial^2 u_i}{\partial x_j \partial x_j} \\[3mm]
\dfrac{\partial u_i}{\partial x_i} & = & 0
\end{cases}
$$

where the summation convention is used. This implies that a repeated index is summed over, from 1 to 3, as follows

$$
u_i u_i = u_1 u_1 + u_2 u_2 + u_3 u_3
$$

Thus the first component of the vector equation can be written out as
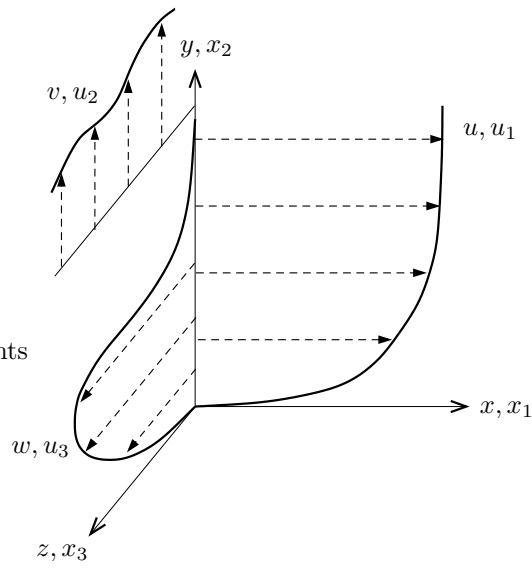
Figure 1.1: Definition of coordinate system and velocity components
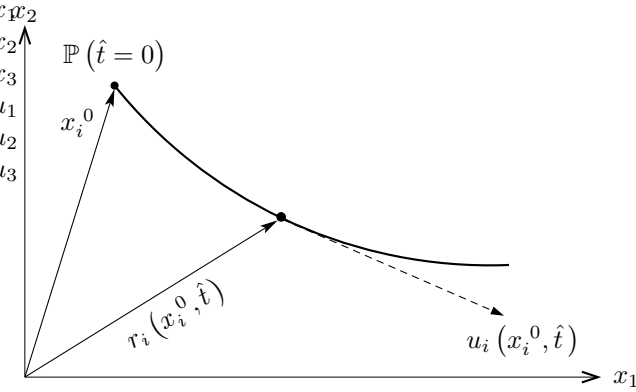
Figure 1.2: Particle path.

$$i = 1 \quad \frac{\partial u_1}{\partial t} + u_1 \frac{\partial u_1}{\partial x_1} + u_2 \frac{\partial u_1}{\partial x_2} + u_3 \frac{\partial u_1}{\partial x_3} = -\frac{1}{\rho} \frac{\partial p}{\partial x_1} + \nu \left(\frac{\partial^2 u_1}{\partial x_1^2} + \frac{\partial^2 u_1}{\partial x_2^2} + \frac{\partial^2 u_1}{\partial x_3^2} \right)$$

$$\text{or} \quad \frac{\partial u}{\partial t} + u \frac{\partial u}{\partial x} + v \frac{\partial u}{\partial y} + w \frac{\partial u}{\partial z} = -\frac{1}{\rho} \frac{\partial p}{\partial x} + \nu \underbrace{\left(\frac{\partial^2 u}{\partial x^2} + \frac{\partial^2 u}{\partial y^2} + \frac{\partial^2 u}{\partial z^2} \right)}_{\nabla^2 u}$$

1.2   Kinematics

Lagrangian and Euler coordinates

Kinematics is the description of motion without regard to forces. We begin by considering the motion of a fluid particle in Lagrangian coordinates, the coordinates familiar from classical mechanics.

<u>Lagrange coordinates</u>: every particle is marked and followed in flow. The independent variables are

$$x_i^0 \quad - \quad \text{initial position of fluid particle}$$

$$\hat{t} \quad - \quad \text{time}$$

where the particle path of $\mathbb{P}$, see figure 1.2, is

$$r_i = r_i \left(x_i^0, \hat{t} \right)$$

and the velocity of the particle is the rate of change of the particle position, i.e.

$$u_i = \frac{\partial r_i}{\partial \hat{t}}$$

Note here that when $x_i{}^0$ changes we consider new particles. Instead of marking every fluid particle it is most of the time more convenient to use Euler coordinates.

Euler coordinates: consider fixed point in space, fluid flows past point. The independent variables are

$$x_i \quad - \quad \text{space coordinates}$$

$$t \quad - \quad \text{time}$$

Thus the fluid velocity $u_i = u_i(x_i, t)$ is now considered as a function of the coordinate x_i and time t.

The relation between Lagrangian and Euler coordinates, i.e. $(x_i{}^0, \hat{t})$ and (x_i, t), is easily found by noting that the particle position is expressed in fixed space coordinates x_i, i.e.

$$\begin{cases} x_i &= r_i\left(x_i{}^0, \hat{t}\right) \qquad \text{at the time} \\[2mm] t &= \hat{t} \end{cases}$$

Material derivative

Although it is usually most convenient to use Euler coordinates, we still need to consider the rate of change of quantities following a fluid particle. This leads to the following definition.

Material derivative: rate of change in time following fluid particle expressed in Euler coordinates.

Consider the quantity F following fluid particle, where

$$F = F_{\mathrm{L}}\left(x_i{}^0, \hat{t}\right) = F_{\mathrm{E}}\left(x_i, t\right) = F_{\mathrm{E}}\left(r_i\left(x_i, \hat{t}\right), t\right)$$

The rate of change of F following a fluid particle can then be written

$$\frac{\partial F}{\partial \hat{t}} = \frac{\partial F_{\mathrm{E}}}{\partial x_i} \cdot \frac{\partial r_i}{\partial \hat{t}} + \frac{\partial F_{\mathrm{E}}}{\partial t} \cdot \frac{\partial t}{\partial \hat{t}} = \frac{\partial F_{\mathrm{E}}}{\partial t} + u_i \frac{\partial F_{\mathrm{E}}}{\partial x_i}$$

Based on this expression we define the material derivative $\dfrac{D}{Dt}$ as

$$\frac{\partial}{\partial \hat{t}} \equiv \frac{D}{Dt} = \frac{\partial}{\partial t} + u_i \frac{\partial}{\partial x_i} = \frac{\partial}{\partial t} + (\mathbf{u} \cdot \nabla)$$

In the material or substantial derivative the first term measures the local rate of change and the second measures the change due to the motion with velocity u_i.

As an example we consider the acceleration of a fluid particle in a steady converging river, see figure 1.3. The acceleration is defined

$$a_j = \frac{Du_i}{Dt} = \frac{\partial u_i}{\partial t} + u_j \frac{\partial u_i}{\partial x_j}$$

which can be simplified in 1D for stationary case to

$$a = \frac{Du}{Dt} = \frac{\partial u}{\partial t} + u \frac{\partial u}{\partial x}$$

Note that the acceleration $\neq 0$ even if velocity at fixed x does not change. This has been experienced by everyone in a raft in a converging river. The raft which is following the fluid is accelerating although the flow field is steady.

Description of deformation

Evolution of a line element

Consider the two nearby particles in figure 1.4 during time $d\hat{t}$. The position of $\mathbb{P}_2$ can by Taylor expansion be expressed as

$$\begin{aligned} \mathbb{P}_2 \quad : \quad & r_i\left(d\hat{t}\right) + dr_i\left(d\hat{t}\right) = \\ & = r_i(0) + \frac{\partial r_i}{\partial \hat{t}}(0)\, d\hat{t} + dr_i(0) + \frac{\partial}{\partial \hat{t}}\left(dr_i\right)\Big|_0 d\hat{t} \\ & = x_i{}^0 + dx_i{}^0 + u_i(0)\, d\hat{t} + du_i(0)\, d\hat{t} \end{aligned}$$

x, x_1
y, x_2
z, x_3
u, u_1
v, u_2
w, u_3
x_1
x_2
$x_i^{\,0}$
$r_i\left(x_i^{\,0}, \hat{t}\right)$
$u_i\left(x_i^{\,0}, \hat{t}\right)$
$\mathbb{P}\left(\hat{t}=0\right)$
x

u_1

$u_2 > u_1$
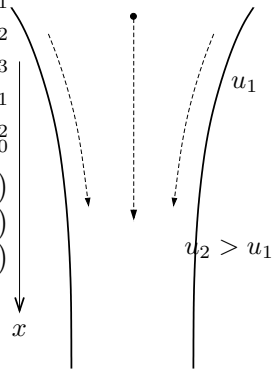
Figure 1.3: Acceleration of fluid particles in converging river.

x, x_1
y, x_2
z, x_3
u, u_1
v, u_2
w, u_3
x_1
x_2
$x_i^{\,0}$
$r_i\left(x_i^{\,0}, \hat{t}\right)$
$u_i\left(x_i^{\,0}, \hat{t}\right)$
$\mathbb{P}\left(\hat{t}=0\right)$
x
u_1
$u_2 > u_1$

x_2

$\mathrm{d}x_i^{\,0}$

$\mathrm{d}u_i\,\mathrm{d}\hat{t}$

$\mathbb{P}_2$

$u_i\,\mathrm{d}\hat{t}$

$\mathrm{d}r_i\!\left(\mathrm{d}\hat{t}\right)$

$\mathbb{P}_1$

$x_i^{\,0}$

$r_i\!\left(\mathrm{d}\hat{t}\right)$

x_1

x_3
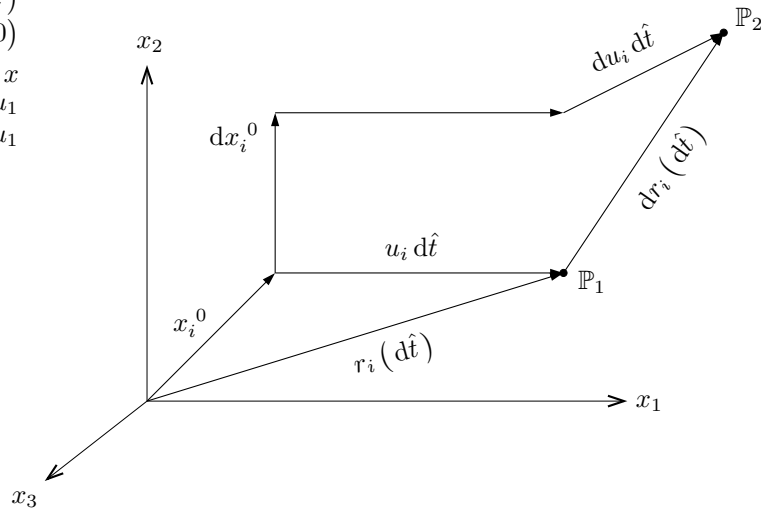
Figure 1.4: Relative motion of two nearly particles.

where we have used

$$
\begin{aligned}
\frac{\partial}{\partial \hat{t}}(\mathrm{d}r_i) &= \frac{\partial}{\partial \hat{t}}\left(\frac{\partial r_i}{\partial x_j{}^0}\right) \mathrm{d}x_j{}^0 = \frac{\partial}{\partial x_j{}^0}\left(\frac{\partial r_i}{\partial \hat{t}}\right) \mathrm{d}x_j{}^0 \\
&= \frac{\partial u_i}{\partial x_j{}^0} \mathrm{d}x_j{}^0 = \mathrm{d}u_i
\end{aligned}
$$

and where

$$
\begin{array}{lcl}
\dfrac{\partial u_i}{\partial x_j{}^0} & - & \text{change of } u_i \text{ with initial pos.} \\
\mathrm{d}x_j{}^0 & - & \text{difference in initial pos.} \\
\mathrm{d}u_i & - & \text{difference in velocity}
\end{array}
$$

We can transform the expression $\dfrac{\partial}{\partial \hat{t}}(\mathrm{d}r_i) = \mathrm{d}u_i$ in Lagrange coordinates to an equation for a material line element in Euler coordinates

$$
\begin{aligned}
\frac{D}{Dt}(\mathrm{d}r_i) &= \mathrm{d}u_i \\
&= \{\text{expand in Euler coordinates}\} \\
&= \frac{\partial u_i}{\partial x_j}\,\mathrm{d}r_j
\end{aligned}
$$

where

$$
\begin{array}{lcl}
\dfrac{\partial u_i}{\partial x_j} & - & \text{change in velocity with spatial position} \\
\mathrm{d}r_j & - & \text{difference in spatial pos. of particles}
\end{array}
$$

Relative motion associated with invariant parts

We consider the relative motion $\mathrm{d}u_i = \dfrac{\partial u_i}{\partial x_j}\,\mathrm{d}r_j$ by dividing $\dfrac{\partial u_i}{\partial x_j}$ in its invariant parts, i.e.

$$
\frac{\partial u_i}{\partial x_j} = \xi_{ij} + \underbrace{\overline{e}_{ij} + \overline{\overline{e}}_{ij}}_{e_{ij}}
$$

where e_{ij} is the deformation rate tensor and

$$
\begin{array}{lcll}
\xi_{ij} &=& \dfrac{1}{2}\left(\dfrac{\partial u_i}{\partial u_j} - \dfrac{\partial u_j}{\partial x_i}\right) & \text{anti-symmetric part} \\[3mm]
\overline{e}_{ij} &=& \dfrac{1}{2}\left(\dfrac{\partial u_i}{\partial x_j} + \dfrac{\partial u_j}{\partial x_i} - \dfrac{2}{3}\dfrac{\partial u_r}{\partial u_r}\delta_{ij}\right) & \text{traceless part} \\[3mm]
\overline{\overline{e}}_{ij} &=& \dfrac{1}{3}\dfrac{\partial u_r}{\partial u_r}\delta_{ij} & \text{isotropic part}
\end{array}
$$

The symmetric part of $\dfrac{\partial u_i}{\partial x_j}$, e_{ij}, describes the deformation and is considered in detail below, whereas the anti-symmetric part can be written in terms of the vorticity ω_k and is associated with solid body rotation, i.e. no deformation.

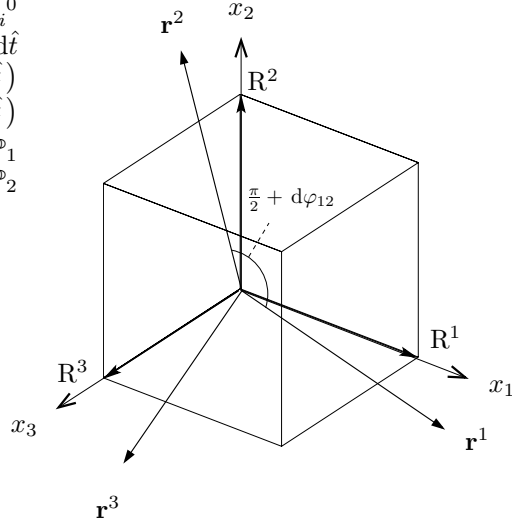The anti-symmetric part can be written

Figure 1.5: Deformation of a cube.

$$
[\xi_{ij}] \;=\; \begin{bmatrix} 0 & \frac{1}{2}\left(\frac{\partial u_1}{\partial x_2}-\frac{\partial u_2}{\partial x_1}\right) & \frac{1}{2}\left(\frac{\partial u_1}{\partial x_3}-\frac{\partial u_3}{\partial x_1}\right) \\[2mm] -\frac{1}{2}\left(\frac{\partial u_1}{\partial x_2}-\frac{\partial u_2}{\partial x_1}\right) & 0 & \frac{1}{2}\left(\frac{\partial u_2}{\partial x_3}-\frac{\partial u_3}{\partial x_2}\right) \\[2mm] -\frac{1}{2}\left(\frac{\partial u_1}{\partial x_3}-\frac{\partial u_3}{\partial x_1}\right) & -\frac{1}{2}\left(\frac{\partial u_2}{\partial x_3}-\frac{\partial u_3}{\partial x_2}\right) & 0 \end{bmatrix}
$$

$$
= \{\text{use } \boldsymbol{\omega}=\nabla\times\mathbf{u}\,,\ \omega_k=\epsilon_{kji}\frac{\partial}{\partial x_j}u_i\}
$$

$$
= \begin{bmatrix} 0 & -\frac{1}{2}\omega_3 & \frac{1}{2}\omega_2 \\[2mm] \frac{1}{2}\omega_3 & 0 & -\frac{1}{2}\omega_1 \\[2mm] \frac{1}{2}\omega_2 & \frac{1}{2}\omega_1 & 0 \end{bmatrix}
$$

Deformation of a small cube

Consider the deformation of the small cube in figure 1.5, where we define

$$
\mathrm{R}^l_k \;=\; \mathrm{R}\delta_{kl} \qquad \text{component } k \text{ of side } l
$$

$$
r^l_k \;=\; \mathrm{R}^l_k + \underbrace{\frac{\partial u_k}{\partial x_j}\mathrm{R}^l_j\,\mathrm{d}t}_{\mathrm{d}u^l_k} \qquad \text{relative motion of side } l
$$

$$
= \; \mathrm{R}\left(\delta_{kl}+\frac{\partial u_k}{\partial x_l}\,\mathrm{d}t\right) \qquad \text{deformed cube}
$$

First, we consider the deformation on side 1, which can be expressed as

$$
\mathrm{d}R^1 = \left|\mathbf{r}^1\right| - \mathrm{R} = \sqrt{r^1_k r^1_k} - \mathrm{R}
$$

The inner product can be expanded as

$$
r^1_k r^1_k \;=\; \left[\left(1+\frac{\partial u_1}{\partial x_1}\,\mathrm{d}t\right)^2 + \left(\frac{\partial u_2}{\partial x_1}\,\mathrm{d}t\right)^2 + \left(\frac{\partial u_3}{\partial x_1}\,\mathrm{d}t\right)^2\right]\mathrm{R}^2
$$

$$
= \{\text{drop quadratic terms}\}
$$

$$
= \mathrm{R}^2\left(1+2\frac{\partial u_1}{\partial x_1}\,\mathrm{d}t\right)
$$

We have dropped the quadratic terms since we are assuming that dt is small. dR^1 becomes

$$
\begin{aligned}
dR^1 &= R\sqrt{1 + 2\frac{\partial u_1}{\partial x_1}dt} - R = R\left(1 + \frac{\partial u_1}{\partial x_1}dt + ...\right) - R \\
&= R\frac{\partial u_1}{\partial x_1}dt = Re_{11}\,dt
\end{aligned}
$$

which implies that

$$
\frac{dR^1}{dt} = Re_{11}
$$

Thus the deformation rate of side 1 depends on e_{11}, both traceless and isotropic part of $\frac{\partial u_i}{\partial x_j}$.

Second, we consider the deformation of the angle between side 1 and side 2. This can be expressed as

$$
\begin{aligned}
\cos\left(\frac{\pi}{2} + d\phi_{12}\right) &= \frac{\mathbf{r}^1 \cdot \mathbf{r}^2}{|\mathbf{r}^1||\mathbf{r}^2|} = r_k^1 r_k^2 \cdot \left(r_m^1 r_m^1 \cdot r_n^2 r_n^2\right)^{-1/2} \\
&= \left(\delta_{k1} + \frac{\partial u_k}{\partial x_1}dt\right)\left(\delta_{k2} + \frac{\partial u_k}{\partial x_2}dt\right) \cdot \left(1 + 2\frac{\partial u_1}{\partial x_1}dt\right)^{-1/2}\left(1 + 2\frac{\partial u_2}{\partial x_2}dt\right)^{-1/2} \\
&= \left(\frac{\partial u_1}{\partial x_2}dt + \frac{\partial u_2}{\partial x_1}dt\right)\left(1 - \frac{\partial u_1}{\partial x_1}dt\right)\left(1 - \frac{\partial u_2}{\partial x_2}dt\right) \\
&= \left(\frac{\partial u_1}{\partial x_2} + \frac{\partial u_2}{\partial x_1}\right)dt = 2\bar{e}_{12}\,dt
\end{aligned}
$$

where we have dropped quadratic terms. We use the trigonometric identity

$$
\cos\left(\frac{\pi}{2} + d\varphi_{12}\right) = \cos\frac{\pi}{2}\cdot\cos d\varphi_{12} - \sin\frac{\pi}{2}\cdot\sin d\varphi_{12} \approx -d\varphi_{12}
$$

which allow us to obtain the finial expression

$$
\frac{d\varphi_{12}}{dt} = -2\bar{e}_{12}
$$

Thus the deformation rate of angle between side 1 and side 2 depends only on traceless part of $\frac{\partial u_i}{\partial x_j}$.

Third, we consider the deformation of the volume of the cube. This can be expressed as

$$
\begin{aligned}
dV &= \left|\mathbf{r}^1 \ \ \mathbf{r}^2 \ \ \mathbf{r}^3\right| - R^3 \\
&= R^3\begin{vmatrix} 1 + \frac{\partial u_1}{\partial x_1}dt & \frac{\partial u_1}{\partial x_2}dt & \frac{\partial u_1}{\partial x_3}dt \\ \frac{\partial u_2}{\partial x_1}dt & 1 + \frac{\partial u_2}{\partial x_2}dt & \frac{\partial u_2}{\partial x_3}dt \\ \frac{\partial u_3}{\partial x_1}dt & \frac{\partial u_3}{\partial x_2}dt & 1 + \frac{\partial u_3}{\partial x_3}dt \end{vmatrix} - R^3 \\
&= R^3\left(1 + \frac{\partial u_1}{\partial x_1}dt\right)\left(1 + \frac{\partial u_2}{\partial x_2}dt\right)\left(1 + \frac{\partial u_3}{\partial x_3}dt\right) - R^3 \\
&= R^3\left(\frac{\partial u_1}{\partial x_1} + \frac{\partial u_2}{\partial x_2} + \frac{\partial u_3}{\partial x_3}\right)dt \\
&= R^3\frac{\partial u_k}{\partial x_k}dt
\end{aligned}
$$

where we have again omitted quadratic terms. Thus we have

$$
\frac{dV}{dt} = R^3\bar{\bar{e}}_{rr}
$$

and the deformation rate of volume of cube (or expansion rate) depends on isotropic part of $\frac{\partial u_i}{\partial x_j}$.

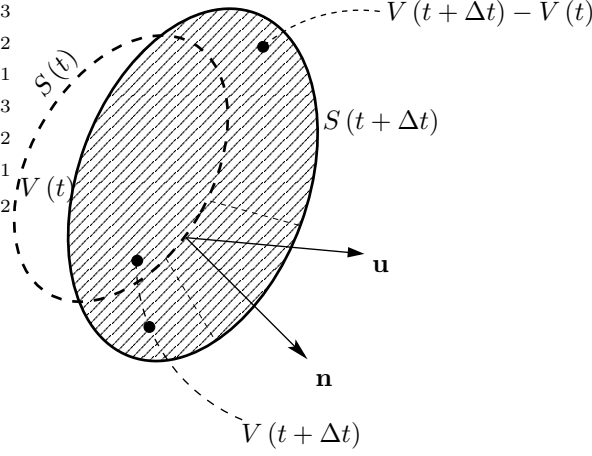In summary, the motion of a fluid particle with velocity u_i can be divided into the following invariant parts

Figure 1.6: Volume moving with the fluid.

i) $\quad u_i \quad$ solid body translation

ii) $\quad \xi_{ij} = \frac{1}{2}\left(\dfrac{\partial u_i}{\partial x_j} - \dfrac{\partial u_j}{\partial x_i}\right) = -\frac{1}{2}\epsilon_{kij}\omega_k \quad$ solid body rotation

iii) $\quad \overline{e}_{ij} = \frac{1}{2}\left(\dfrac{\partial u_i}{\partial x_j} + \dfrac{\partial u_j}{\partial x_i} - \dfrac{2}{3}\dfrac{\partial u_r}{\partial u_r}\delta_{ij}\right) \quad$ volume constant deformation

iv) $\quad \overline{\overline{e}}_{ij} = \frac{1}{3}\dfrac{\partial u_r}{\partial u_r}\delta_{ij} \quad$ volume expansion rate

1.3   Reynolds transport theorem

Volume integral following with the fluid

Consider the time derivative of a <u>material</u> volume integral, i.e. a volume integral where the volume is moving with the fluid. We obtain the following expressions

$$
\begin{aligned}
\frac{D}{Dt}\int_{V(t)} T_{ij}\,\mathrm{d}V &= \lim_{\Delta t \to 0}\left\{\frac{1}{\Delta t}\left[\int_{V(t+\Delta t)} T_{ij}(t+\Delta t)\,\mathrm{d}V - \int_{V(t)} T_{ij}(t)\,\mathrm{d}V\right]\right\} \\
&= \lim_{\Delta t \to 0}\left\{\frac{1}{\Delta t}\left[\int_{V(t+\Delta t)} T_{ij}(t+\Delta t)\,\mathrm{d}V - \int_{V(t)} T_{ij}(t+\Delta t)\,\mathrm{d}V\right.\right. \\
&\qquad\qquad\left.\left. + \frac{1}{\Delta t}\left[\int_{V(t)} T_{ij}(t+\Delta t)\,\mathrm{d}V - \int_{V(t)} T_{ij}(t)\,\mathrm{d}V\right]\right]\right\} \\
&= \lim_{\Delta t \to 0}\left\{\frac{1}{\Delta t}\int_{V(t+\Delta t)-V(t)} T_{ij}(t+\Delta t)\,\mathrm{d}V\right\} + \int_{V(t)} \frac{\partial T_{ij}}{\partial t}\,\mathrm{d}V
\end{aligned}
$$

The volume in the first integral on the last line is represented in figure 1.6, where a volume element describing the change in volume between V at time t and $t+\Delta t$ can be written as

$$\mathbf{u}\cdot\mathbf{n}\Delta t = u_k n_k \Delta t \Rightarrow \mathrm{d}V = u_k n_k \Delta t\,\mathrm{d}S$$

This implies that the volume integral can be converted to a surface integral. This surface integral can in turn be changed back to a volume integral by the use of Gauss (or Greens) theorem. We have

$$
\frac{D}{Dt} \int_{V(t)} T_{ij} \, dV = \lim_{\Delta t \to 0} \left[\oint_{S(t)} T_{ij} \left(t + \Delta t \right) u_k n_k \, dS \right] + \int_{V(t)} \frac{\partial T_{ij}}{\partial t} \, dV
$$

$$
= \oint_{S(t)} T_{ij} u_k n_k \, dS + \int_{V(t)} \frac{\partial T_{ij}}{\partial t} \, dV = \{\text{Gauss/Green's theorem}\}
$$

$$
= \int_{V(t)} \left[\frac{\partial T_{ij}}{\partial t} + \frac{\partial}{\partial x_k} \left(u_k T_{ij} \right) \right] dV
$$

which is the Reynolds transport theorem.

Conservation of mass

By the substitution $T_{ij} \to \rho$ and the use of the Reynolds transport theorem above we can derive the equation for the conservation of mass. We have

$$
\frac{D}{Dt} \int_{V(t)} \rho \, dV = \int_{V(t)} \left[\frac{\partial \rho}{\partial t} + \frac{\partial}{\partial x_k} \left(u_k \rho \right) \right] = 0
$$

Since the volume is arbitrary, the following must hold for the integrand

$$
0 = \underbrace{\frac{\partial \rho}{\partial t}}_{\text{①}} + \underbrace{\frac{\partial}{\partial x_k} \left(u_k \rho \right)}_{\text{②}} = \frac{\partial \rho}{\partial t} + u_k \frac{\partial \rho}{\partial x_k} + \rho \frac{\partial u_k}{\partial x_k} = \underbrace{\frac{D\rho}{Dt}}_{\text{③}} + \underbrace{\rho \frac{\partial u_k}{\partial x_k}}_{\text{④}}
$$

where we have used the definition of the material derivative in order to simplify the expression. The terms in the expression can be given the following interpretations:

①	:	accumulation of mass in fixed element
②	:	net flow rate of mass out of element
③	:	rate of density change of material element
④	:	volume expansion rate of material element

By considering the transport of a quantity given per unit mass, i.e. $T_{ij} = \rho t_{ij}$, we can simplify Reynolds transport theorem. The integrand in the theorem can then be written

$$
\frac{\partial}{\partial t} \left(\rho t_{ij} \right) + \frac{\partial}{\partial x_k} \left(u_k \rho t_{ij} \right) = t_{ij} \overbrace{\frac{\partial \rho}{\partial t}}^{0 \, (\text{cont. eq.})} + \rho \frac{\partial t_{ij}}{\partial t} + t_{ij} \frac{\partial}{\partial x_k} \overbrace{\left(u_k \rho \right)}^{0} + \rho u_k \frac{\partial t_{ij}}{\partial x_k} = \rho \frac{D t_{ij}}{Dt}
$$

which implies that Reynolds transport theorem becomes

$$
\frac{D}{Dt} \int_{V(t)} \rho \, t_{ij} \, dV = \int_{V(t)} \rho \frac{D t_{ij}}{Dt} \, dV
$$

where $V(t)$ again is a material volume.

1.4 Momentum equation

Conservation of momentum

The momentum equation is based on the principle of conservation of momentum, i.e. that the time rate of change of momentum in a material region = sum of the forces on that region. The quantities involved are:

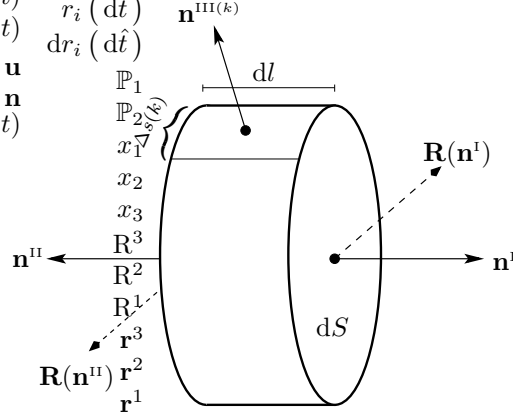|		
F_i	-	body forces per unit mass
R_i	-	surface forces per unit area
ρu_i	-	momentum per unit volume

Figure 1.7: Momentum balance for fluid element

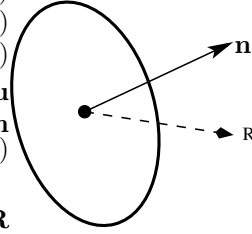Figure 1.8: Surface force and unit normal.

We can put the momentum conservation in integral form as follows

$$\frac{D}{Dt} \int_{V(t)} \rho u_i \, dV = \int_{V(t)} \rho F_i \, dV + \int_{S(t)} R_i \, dS$$

Using Reynolds transport theorem this can be written

$$\int_{V(t)} \rho \frac{Du_i}{Dt} \, dV = \int_{V(t)} \rho F_i \, dV + \int_{S(t)} R_i \, dS$$

which is Newtons second law written for a volume of fluid: mass $\cdot$ acceleration = sum of forces. To proceed R_i must be investigated so that the surface integral can be transformed to a volume integral. In order to do that we have to define the stress tensor.

The stress tensor

Remove a fluid element and replace outside fluid by surface forces as in figure 1.7. Here $\mathbf{R}(\mathbf{n})$ is the surface force per unit area on surface dS with normal $\mathbf{n}$, see figure 1.8. Momentum conservation for the small fluid particle leads to

$$\rho \frac{Du_i}{Dt} \, dS \, dl = \rho F_i \, dS \, dl + R_i \left(n_j^{\mathrm{I}}\right) \, dS + R_i \left(n_j^{\mathrm{II}}\right) \, dS + \sum_k R_i \left(n_j^{\mathrm{III}(k)}\right) \Delta s^{(k)} \, dl$$

Letting $dl \to 0$ gives

$$0 = R_i \left(n_j^{\mathrm{I}}\right) \, dS + R_i \left(n_j^{\mathrm{II}}\right) \, dS$$

Now $n_j = n_j^{\mathrm{I}} = -n_j^{\mathrm{II}}$ which leads to

$$R_i \left(n_j\right) = -R_i \left(-n_j\right)$$

implying that a surface force on one side of a surface is balanced by an equal an opposite surface force at the other side of that surface. Note that it is a general principle that the terms proportional to the volume of a small fluid particle approaches zero faster than the terms proportional to the surface area of the particle. Thus the surface forces acting on a small fluid particle has to balance, irrespective of volume forces or acceleration terms.
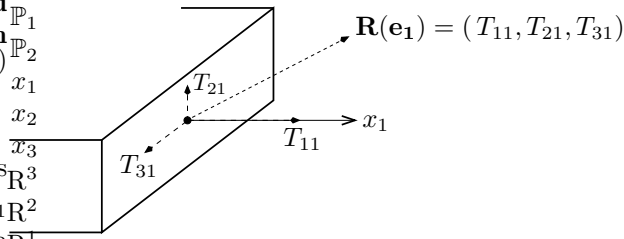
$\mathbf{u}_{\mathbb{P}_1}$
$\mathbf{n}_{\mathbb{P}_2}$
$V(t+\Delta t)$
x_1
x_2
x_3

$\mathbf{R(e_1)} = (T_{11}, T_{21}, T_{31})$

T_{21}

x_1

T_{11}

PSfrag replacements
R^3
$x, x_1 \mathrm{R}^2$
$y, x_2 \overline{\mathrm{R}}^1$
$z, x_3 \; \mathbf{r}^3$
$u, u_1 \; \mathbf{r}^2$

T_{31}

Figure 1.9: Definition of surface force components on a surface with a normal in the 1-direction.

$v, u_2 \; \mathbf{r}^1$
$\frac{\pi}{2} + \mathrm{d}\varphi_{12}$
$V_1(t)$
$S_2(t)$
$V(t+\Delta t) - V(t)$
$r_i \, \delta(x, t+\Delta t)$
$u_i\left(x_i^0, \hat{t}\right) \; \mathbf{u}$
$\mathbb{P}\left(\hat{t}=0\right) \; \mathbf{n}$
$V(t+\Delta t)$

x_2

$\mathbf{R(e_2)} = (T_{12}, T_{22}, T_{32})$

T_{22}

T_{12}

T_{32}

u_1
$u_2 > u_1$
x_1
x_2
x_3
x_i^0
$u_i \, \mathrm{d}t$
$\mathrm{d}x_i^0$
$\mathrm{d}u_i \, \mathrm{d}\hat{t}$
$r_i\left(\mathrm{d}t\right)$
$\mathrm{d}r_i\left(\mathrm{d}t\right)$
$\mathbb{P}$
$\mathbb{P}$
x_1
x_2
x_3
R^3
R^2
R^1
$\mathbf{r}^3$
$\mathbf{r}^2$
$\mathbf{r}^1$
$\frac{\pi}{2} + \mathrm{d}\varphi_{12}$
$V(t)$
$S(t)$
$V(t+\Delta t) - V(t)$
$S(t+\Delta t)$
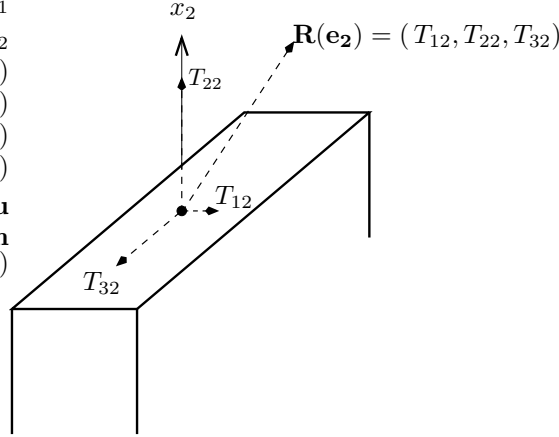$\mathbf{u}$
$\mathbf{n}$
$V(t+\Delta t)$

Figure 1.10: Definition of surface force components on a surface with a normal in the 2-direction.

We now divide the surface forces into components along the coordinate directions, as in figures 1.9 and 1.10, with corresponding definitions for the force components on a surface with a normal in the 3-direction. Thus, T_{ij} is the i-component of the surface force on a surface $\mathrm{d}S$ with a normal in the j-direction.

Consider a fluid particle with surfaces along the coordinate directions cut by a slanted surface, as in figure 1.11. The areas of the surface elements are related by

$$\mathrm{d}S_j = \mathbf{e}_j \cdot \mathbf{n} \, \mathrm{d}S = n_j \, \mathrm{d}S$$

where $\mathrm{d}S$ is the area of the slanted surface. Momentum balance require the surface forces to balance in the element, we have

$$0 = R_1 \, \mathrm{d}S - T_{11} n_1 \, \mathrm{d}S - T_{12} n_2 \, \mathrm{d}S - T_{13} n_3 \, \mathrm{d}S$$

which implies that the total surface force R_i can be written in terms of the components of the stress tensor T_{ij} as

$$R_i = T_{i1} n_1 + T_{i2} n_2 + T_{i3} n_3 = T_{ij} n_j$$

$\mathbf{e_2}$
$\mathbf{R}$
$\mathbf{n}$
R_1
$\mathrm{d}S_1$
$\mathrm{d}S_3$
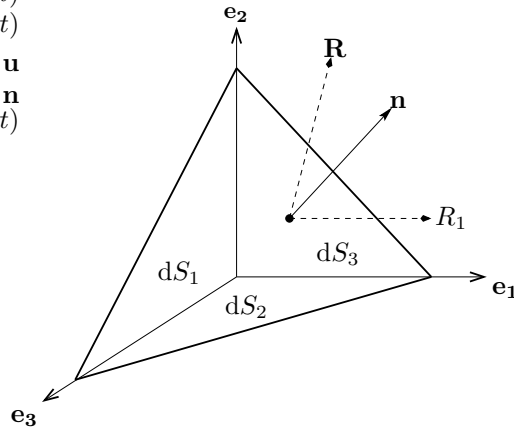$\mathrm{d}S_2$
$\mathbf{e_1}$
$\mathbf{e_3}$

Figure 1.11: Surface force balance on a fluid particle with a slanted surface.

Here the diagonal components are <u>normal stresses</u> off-diagonal components are <u>shear</u> stresses.

Further consideration of the moment balance around a fluid particle show that T_{ij} is a symmetric tensor, i.e.

$$T_{ij} = T_{ji}$$

Momentum equation

Using the definition of the surface force in terms of the stress tensor, the momentum equation can now be written

$$\int_{V(t)} \rho \frac{Du_i}{Dt}\, dV = \int_{V(t)} \rho F_i\, dV + \int_{S(t)} T_{ij} n_j\, dS = \int_{V(t)} \left[\rho F_i + \frac{\partial T_{ij}}{\partial x_j} \right] dV$$

The volume is again arbitrary implying that the integrand must itself equal zero. We have

$$\rho \frac{Du_i}{Dt} = \rho F_i + \frac{\partial T_{ij}}{\partial x_j}$$

Pressure and viscous stress tensor

For fluid at rest only normal stresses present otherwise fluid element would deform. We thus divide the stress tensor into an isotropic part, the hydrodynamic pressure p, and a part depending on the motion of the fluid. We have

$$T_{ij} = -p\delta_{ij} + \tau_{ij}$$

p - hydrodynamic pressure, directed inward
τ_{ij} - viscous stress tensor, depends on fluid motion
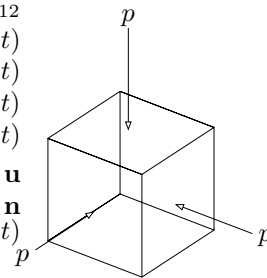
Newtonian fluid

It is natural to assume that the viscous stresses are functions of deformation rate e_{ij} or strain. Recall that the invariant symmetric parts are

$$e_{ij} = \underbrace{\frac{1}{2}\left(\frac{\partial u_i}{\partial x_j} + \frac{\partial u_j}{\partial x_i} - \frac{2}{3}\frac{\partial u_r}{\partial x_r}\delta_{ij} \right)}_{\bar{e}_{ij}} + \underbrace{\frac{1}{3}\frac{\partial u_r}{\partial x_r}\delta_{ij}}_{\bar{\bar{e}}_{ij}}$$

where $\bar{e}_{ij}$ is the volume constant deformation rate and $\bar{\bar{e}}_{ij}$ is the uniform rate of expansion. For an isotropic fluid, the viscous stress tensor is a linear function of the invariant parts of e_{ij}, i.e.

$$\tau_{ij} = \lambda \bar{\bar{e}}_{ij} + 2\mu \bar{e}_{ij}$$

where we have defined the two viscosities as

$\mu(T)$: dynamic viscosity (here T is the temperature)
$\lambda(T)$: second viscosity, often=0

For a Newtonian fluid, we thus have the following relationship between the viscous stress and the strain (deformation rate)

$$\tau_{ij} = 2\mu \bar{e}_{ij} = \mu \left(\frac{\partial u_i}{\partial x_j} + \frac{\partial u_j}{\partial x_i} - \frac{2}{3}\frac{\partial u_r}{\partial x_r}\delta_{ij} \right)$$

which leads to the momentum equation

$$\rho \frac{Du_i}{Dt} = -\frac{\partial p}{\partial x_i} + \frac{\partial}{\partial x_j}\left[\mu \left(\frac{\partial u_i}{\partial x_j} + \frac{\partial u_j}{\partial x_i} - \frac{2}{3}\frac{\partial u_r}{\partial x_r}\delta_{ij} \right) \right] + \rho F_i$$

1.5   Energy equation

The energy equation is a mathematical statement which is based on the physical law that the rate of change of energy in material particle = rate that energy is received by heat and work transfers by that particle. We have the following definitions

$$\rho \left[e + \tfrac{1}{2} u_i u_i \right] \, dV \quad \text{energy of particle, with } e \text{ the internal energy}$$

$$\rho u_i F_i \, dV \qquad \underbrace{\text{work rate}}_{\text{force} \cdot \text{velocity}} \text{ of } F_i \text{ on particle}$$

$$u_j R_j \, dS \qquad \text{work rate of } R_j \text{ on particle}$$

$$n_i q_i \, dS \qquad \text{heat loss from surface, with } q_i \text{ the heat flux vector, directed outward}$$

Using Reynolds transport theorem we can put the energy conservation in integral form as

$$\frac{D}{Dt} \int_{V(t)} \rho \left[e + \frac{1}{2} u_i u_i \right] \, dV = \int_{V(t)} \rho F_i u_i \, dV + \int_{S(t)} \left[n_i T_{ij} u_j - n_i q_i \right] \, dS = \int_{V(t)} \left[\rho F_i u_i + \frac{\partial}{\partial x_i} \left(T_{ij} u_j - q_i \right) \right] \, dV$$

Compare the expression in classical mechanics, where the momentum equation is $m\dot{\mathbf{u}} = \mathbf{F}$ and the associated kinetic energy equation is

$$
\begin{array}{lcl}
\frac{m}{2} \frac{d}{dt} (\mathbf{u} \cdot \mathbf{u}) & = & \mathbf{F} \cdot \mathbf{u} \\
\text{work rate} & = & \text{force} \cdot \text{velocity} \\
(\text{ work} & = & \text{force} \cdot \text{dist. })
\end{array}
$$

From the integral energy equation we obtain the total energy equation by the observation that the volume is arbitrary and thus that the integrand itself has to be zero. We have

$$\rho \frac{D}{Dt} \left(e + \frac{1}{2} u_i u_i \right) = \rho F_i u_i - \frac{\partial}{\partial x_i} (p u_i) + \frac{\partial}{\partial x_i} (\tau_{ij} u_j) - \frac{\partial q_i}{\partial x_i}$$

The mechanical energy equation is found by taking the dot product between the momentum equation and $\mathbf{u}$. We obtain

$$\rho \frac{D}{Dt} \left(\frac{1}{2} u_i u_i \right) = \rho F_i u_i - u_i \frac{\partial p}{\partial x_i} + u_i \frac{\partial \tau_{ij}}{\partial x_j}$$

Thermal energy equation is then found by subtracting the mechanical energy equation from the total energy equation, i.e.

$$\rho \frac{De}{Dt} = -p \frac{\partial u_i}{\partial x_i} + \tau_{ij} \frac{\partial u_i}{\partial x_j} - \frac{\partial q_i}{\partial x_i}$$

The work of the surface forces divides into viscous and pressure work as follows

$$
\begin{array}{lcccc}
-\dfrac{\partial}{\partial x_i} (p u_i) & = & -p \dfrac{\partial u_i}{\partial x_i} & - & u_i \dfrac{\partial p}{\partial x_i} \\
& & \text{①} & & \text{②}
\end{array}
$$

$$
\begin{array}{lcccc}
\dfrac{\partial}{\partial x_i} (\tau_{ij} u_j) & = & \tau_{ij} \dfrac{\partial u_i}{\partial x_j} & + & u_j \dfrac{\partial \tau_{ij}}{\partial x_i}
\end{array}
$$

where following interpretations can be given to the thermal and the mechanical terms

①: thermal terms
      (force · deformation): heat generated by compression and viscous dissipation
②: mechanical terms
      (velocity · force gradients): gradients accelerate fluid and increase kinetic energy

The heat flux need to be related to the temperature gradients with Fouriers law

$$q_i = -\kappa \frac{\partial T}{\partial x_i}$$

where $\kappa = \kappa(T)$ is the thermal conductivity. This allows us to write the thermal energy equation as

$$\rho \frac{De}{Dt} = -p \frac{\partial u_i}{\partial x_i} + \Phi + \frac{\partial}{\partial x_i}\left(\kappa \frac{\partial T}{\partial x_i}\right)$$

where the positive definite dissipation function Φ is defined as

$$
\begin{aligned}
\Phi &= \tau_{ij} \frac{\partial u_i}{\partial x_j} = 2\mu \left[e_{ij} e_{ij} - \frac{1}{3}\left(\frac{\partial u_k}{\partial x_k}\right)^2 \right] \\
&= 2\mu \left(e_{ij} - \frac{1}{3}\frac{\partial u_k}{\partial x_k}\delta_{ij} \right)^2 > 0
\end{aligned}
$$

Alternative form of the thermal energy equation can be derived using the definition of the enthalpy

$$h = e + \frac{p}{\rho}$$

We have

$$\frac{Dh}{Dt} = \frac{De}{Dt} + \frac{1}{\rho}\frac{Dp}{Dt} - \underbrace{\frac{p}{\rho^2}\frac{D\rho}{Dt}}_{-\left(p\frac{\partial u_i}{\partial x_i}\right)}$$

which gives the final result

$$\rho \frac{Dh}{Dt} = \frac{Dp}{Dt} + \Phi + \frac{\partial}{\partial x_i}\left(\kappa \frac{\partial T}{\partial x_i}\right)$$

To close the system of equations we need a

    i)   thermodynamic equation $e = e(T, p)$ simplest case: $e = c_v T$ or $h = c_p T$

    ii)   equation of state $p = \rho R T$

where c_v and c_p are the specific heats at constant volume and temperature, respectively. At this time we also define the ratio of the specific heats as

$$\gamma = \frac{c_p}{c_v}$$

1.6   Navier-Stokes equations

The derivation is now completed and we are left with the Navier-Stokes equations. They are the equation describing the conservation of mass, the equation describing the conservation of momentum and the equation describing the conservation of energy. We have

$$\frac{D\rho}{Dt} + \rho \frac{\partial u_k}{\partial x_k} = 0$$

$$\rho \frac{Du_i}{Dt} = -\frac{\partial p}{\partial x_i} + \frac{\partial \tau_{ij}}{\partial x_j} + \rho F_i$$

$$\rho \frac{De}{Dt} = -p \frac{\partial u_i}{\partial x_i} + \Phi + \frac{\partial}{\partial x_i}\left(\kappa \frac{\partial T}{\partial x_i}\right)$$

where

$$
\begin{cases}
\Phi &= \tau_{ij}\dfrac{\partial u_i}{\partial x_j} \\
\tau_{ij} &= \mu\left(\dfrac{\partial u_i}{\partial x_j} + \dfrac{\partial u_j}{\partial x_i} - \dfrac{2}{3}\dfrac{\partial u_r}{\partial x_r}\delta_{ij}\right)
\end{cases}
$$

and the thermodynamic relation and the equation of state for a gas

$$
e = e\,(T,p)
$$

$$
p = \rho RT
$$

We have 7 equations and 7 unknowns and therefore the necessary requirements to obtain a solution of the system of equations.

unknown		equations	
ρ	1	continuity	1
u_i	3	momentum	3
p	1	energy	1
e	1	thermodyn.	1
T	1	gas law	1
	$\sum 7$		$\sum 7$

Equations in conservative form

A slightly different version of the equations can be found by using the identity

$$
\rho\frac{Dt_{ij}}{Dt} = \frac{\partial}{\partial t}\left(\rho t_{ij}\right) + \frac{\partial}{\partial x_k}\left(u_k \rho t_{ij}\right)
$$

to obtain the system

$$
\begin{cases}
\dfrac{\partial \rho}{\partial t} + \dfrac{\partial}{\partial x_k}\left(u_k\rho\right) = 0 \\[2mm]
\dfrac{\partial}{\partial t}\left(\rho u_i\right) + \dfrac{\partial}{\partial x_k}\left(\rho u_k u_i\right) = -\dfrac{\partial p}{\partial x_i} + \dfrac{\partial \tau_{ij}}{\partial x_j} + \rho F_i \\[2mm]
\dfrac{\partial}{\partial t}\left(e + \dfrac{1}{2}u_i u_i\right) + \dfrac{\partial}{\partial x_k}\left[\rho u_k\left(e + \dfrac{1}{2}u_i u_i\right)\right] = \rho F_i u_i - \dfrac{\partial}{\partial x_i}\left(p u_i\right) + \dfrac{\partial}{\partial x_i}\left(\tau_{ij} u_j\right) + \dfrac{\partial}{\partial x_i}\left(\kappa\dfrac{\partial T}{\partial x_i}\right)
\end{cases}
$$

These are all of the form

$$
\frac{\partial \mathbf{U}}{\partial t} + \frac{\partial \mathbf{G}^{(i)}}{\partial x_i} = \mathbf{J} \qquad \text{or} \qquad \frac{\partial \mathbf{U}}{\partial t} + \frac{\partial \mathbf{G}}{\partial x} + \frac{\partial \mathbf{G}}{\partial y} + \frac{\partial \mathbf{G}}{\partial z} = \mathbf{J}
$$

where

$$
\mathbf{U} = \left(\rho, \rho u_1, \rho u_2, \rho u_3, \rho\left(e + u_i u_i/2\right)\right)^T
$$

is the vector of unknowns,

$$
\mathbf{J} = \left(0, \rho F_1, \rho F_2, \rho F_3, \rho u_i F_i\right)^T
$$

is the vector of the right hand sides and

$$
\mathbf{G}^{(i)} = \begin{bmatrix}
\rho u_i \\
\rho u_1 u_i + p\delta_{1i} - \tau_{1i} \\
\rho u_2 u_i + p\delta_{2i} - \tau_{2i} \\
\rho u_3 u_i + p\delta_{3i} - \tau_{3i} \\
\rho\left(e + u_i u_i/2\right)u_i + p u_i + \kappa\frac{\partial T}{\partial x_i} - u_j\tau_{ij}
\end{bmatrix}
$$

is the flux of mass, momentum and energy, respectively. This form of the equation is usually termed the conservative form of the Navier-Stokes equations.

1.7 Incompressible Navier-Stokes equations

The conservation of mass and momentum can be written

$$\begin{cases} \dfrac{D\rho}{Dt} + \rho \dfrac{\partial u_i}{\partial x_i} = 0 \\[2mm] \rho \dfrac{Du_i}{Dt} = -\dfrac{\partial p}{\partial x_i} + \dfrac{\partial \tau_{ij}}{\partial x_j} + \rho F_i \\[2mm] \tau_{ij} = \mu \left(\dfrac{\partial u_i}{\partial x_j} + \dfrac{\partial u_j}{\partial x_i} - \dfrac{2}{3}\dfrac{\partial u_k}{\partial u_k}\delta_{ij} \right) \end{cases}$$

for incompressible flow $\rho = $ constant, which from the conservation of mass equation implies

$$\frac{\partial u_i}{\partial x_i} = 0$$

implying that a fluid particle experiences no change in volume. Thus the conservation of mass and momentum reduce to

$$\begin{cases} \dfrac{\partial u_i}{\partial t} + u_j \dfrac{\partial u_i}{\partial x_j} = -\dfrac{1}{\rho}\dfrac{\partial p}{\partial x_i} + \nu \nabla^2 u_i + F_i \\[2mm] \dfrac{\partial u_i}{\partial x_i} = 0 \end{cases}$$

since the components of the viscous stress tensor can now be written

$$\frac{\partial}{\partial x_j}\left(\frac{\partial u_i}{\partial x_j} + \frac{\partial u_j}{\partial x_i} - \frac{2}{3}\frac{\partial u_k}{\partial x_k}\delta_{ij}\right) = \frac{\partial^2 u_i}{\partial x_j \partial x_j} = \nabla^2 u_i$$

We have also introduced the kinematic viscosity, ν, above, defined as

$$\nu = \mu/\rho$$

The incompressible version of the conservation of mass and momentum equations are usually referred to as the incompressible Navier-Stokes equations, or just the Navier-Stokes equations in case it is evident that the incompressible limit is assumed. The reason that the energy equation is not included in the incompressible Navier-Stokes equations is that it decouples from the momentum and conservation of mass equations, as we will see below. In addition it can be worth noting that the conservation of mass equation is sometimes referred to as the continuity equation.

The incompressible Navier-Stokes equations need boundary and initial conditions in order for a solution to be possible. Boundary conditions (BC) on solid surfaces are $u_i = 0$. They are for obvious reasons usually referred to as the no slip conditions. As initial condition (IC) one needs to specify the velocity field at the initial time $u_i\,(t = 0) = u_i^0$. The pressure field does not need to be specified as it can be obtained once the velocity field is specified, as will be discussed below.

Integral form of the Navier-Stokes eq.

We have derived the differential form of the Navier-Stokes equations. Sometimes, for example when a finite-volume discretization is derived, it is convenient to use an integral form of the equations.

An integral from of the continuity equation is found by integrating the divergence constraint over a fixed volume V_F and using the Gauss theorem. We have

$$\int_V \frac{\partial}{\partial x_i}(u_i)\,\mathrm{d}V_F = \int_S u_i n_i\,\mathrm{d}S_F = 0$$

An integral form of the momentum equation is found by taking the time derivative of a fixed volume integral of the velocity, substituting the differential form of the Navier-Stokes equation, using the continuity equation and Gauss theorem. We have

$$\frac{\partial}{\partial t}\int_{V_F} u_i\,\mathrm{d}V = \int_{V_F} \frac{\partial u_i}{\partial t}\,\mathrm{d}V = -\int_{V_F}\left[\frac{\partial}{\partial x_j}(u_j u_i) + \frac{1}{\rho}\frac{\partial p}{\partial x_i} - \nu\frac{\partial^2 u_i}{\partial x_j \partial x_j}\right]\mathrm{d}V =$$

$$-\int_{V_F}\frac{\partial}{\partial x_j}\left[u_j u_i + \frac{1}{\rho}p\delta_{ij} - \nu\frac{\partial u_i}{\partial x_j}\right]\mathrm{d}V = -\int_{S_F}\left[u_i u_j n_j + \frac{p}{\rho}n_i - \nu\frac{\partial u_i}{\partial x_j}n_j\right]\mathrm{d}S$$
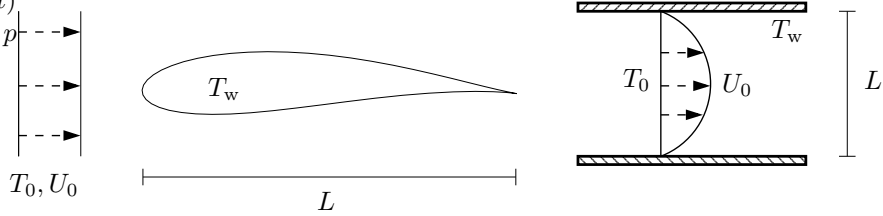
Figure 1.12: Examples of length, velocity and temperature scales.

Note that the integral from of the continuity equation is a compatibility condition for BC in incompressible flow.

Dimensionless form

It is often convenient to work with a non-dimensional form of the Navier-Stokes equations. We use the following scales and non-dimensional variables

$$x_i^* = \frac{x_i}{L} \qquad t^* = \frac{tU_0}{L} \qquad u_i^* = \frac{u_i}{U_0} \qquad p^* = \frac{p}{p_0} \qquad \frac{\partial}{\partial x_i} = \frac{1}{L}\frac{\partial}{\partial x_i^*} \qquad \frac{\partial}{\partial t} = \frac{U_0}{L}\frac{\partial}{\partial t^*} \qquad \Rightarrow$$

where * signifies a non-dimensional variable. The length and velocity scales have to be chosen appropriately from the problem under investigation, so that they represent typical lengths and velocities present. See figure 1.12 for examples.

If we introduce the non-dimensional variables in the Navier-Stokes equations we find

$$\begin{cases} \dfrac{U_0^2}{L} \cdot \dfrac{\partial u_i^*}{\partial t^*} + \dfrac{U_0^2}{L} u_j^* \dfrac{\partial u_i^*}{\partial x_j^*} = -\dfrac{p_0}{\rho L}\dfrac{\partial p^*}{\partial x_i^*} + \dfrac{\nu U_0}{L^2}\dfrac{\partial^2 u_i^*}{\partial x_j^* \partial x_j^*} \\[2mm] \dfrac{U_0}{L} \cdot \dfrac{\partial u_i^*}{\partial x_i^*} = 0 \end{cases}$$

Now drop * as a sign of non-dimensional variables and divide through with U_0^2/L, we find

$$\begin{cases} \dfrac{\partial u_i}{\partial t} + u_j\dfrac{\partial u_i}{\partial x_j} = -\dfrac{p_0}{\rho U_0^2}\dfrac{\partial p}{\partial x_i} + \dfrac{\nu}{U_0 L}\nabla^2 u_i \\[2mm] \dfrac{\partial u_i}{\partial x_i} = 0 \end{cases}$$

We have defined the Reynolds number Re as

$$Re = \frac{U_0 L}{\nu} = \frac{U_0^2/L}{\nu U_0/L^2} \qquad \frac{\text{``inertial forces''}}{\text{``viscous forces''}}$$

which can be interpreted as a measure of the inertial forces divided by the viscous forces. The Reynolds number is by far the single most important non-dimensional number in fluid mechanics. We also define the pressure scale as

$$p_0 = \rho U_0^2$$

which leaves us with the final form of the non-dimensional incompressible Navier-Stokes equations as

$$\begin{cases} \dfrac{\partial u_i}{\partial t} + u_j\dfrac{\partial u_i}{\partial x_j} = -\dfrac{\partial p}{\partial x_i} + \dfrac{1}{Re}\nabla^2 u_i \\[2mm] \dfrac{\partial u_i}{\partial x_i} = 0 \end{cases}$$

Non-dimensional energy equation

We stated above that the energy equation decouple from the rest of the Navier-Stokes equations for incompressible flow. This can be seen from a non-dimensionalization of the energy equation. We use the definition of the enthalpy ($h = c_p T$) to write the thermal energy equation as

$$\rho c_p \frac{DT}{Dt} = \frac{Dp}{Dt} + \Phi + \kappa \nabla^2 T$$

and use the following non-dimensional forms of the temperature and dissipation function

$$T^* = \frac{T - T_0}{T_w - T_0} \qquad \Phi^* = \frac{L^2}{U_0^2 \mu} \Phi$$

This leads to

$$
\begin{aligned}
\frac{DT^*}{Dt^*} &= \frac{\mu}{\rho U_0 L} \cdot \frac{\kappa}{\mu c_p} \cdot \nabla^{*2} T^* + \frac{U_0^2}{c_p (T_w - T_0)} \left[\frac{Dp^*}{Dt^*} + \frac{\mu}{\rho U_0 L} \phi^* \right] \\
&= \frac{1}{Re} \cdot \frac{1}{Pr} \cdot \nabla^{*2} T^* + \underbrace{\frac{U_0^2}{c_p (T_w - T_0)}}_{Ma^2 \frac{a_0^2}{c_p (T_w - T_0)}} \left(\frac{Dp^*}{Dt^*} + \frac{1}{R} \Phi^* \right)
\end{aligned}
$$

where a_0 speed of sound in free-stream and $Ma = \dfrac{U_0}{a_0}$ is Mach number. We now drop * and let $Ma \to 0$ to obtain

$$\frac{DT}{Dt} = \frac{1}{Re} \cdot \frac{1}{Pr} \cdot \nabla^2 T$$

where the Prandtl number $Pr = \frac{\mu c_p}{\kappa}$, which takes on a value of ≈ 0.7 for air.

As the Mach number approaches zero, the fluid behaves as an incompressible medium, which can be seen from the definition of the speed of sound. We have

$$a_0 = \frac{\gamma}{\rho \alpha}, \qquad \alpha = \frac{1}{\rho} \frac{\partial \rho}{\partial p} \bigg|_T$$

where α is the isothermal compressibility coefficient. If the density is constant, not depending on p, we have that $\alpha \to 0$ and $a_0 \to \infty$, which implies that $Ma \to 0$.

1.8   Role of the pressure in incompressible flow

The role of the pressure in incompressible flow is special due to the absence of a time derivative in the continuity equation. We will illustrate this in two different ways.

Artificial compressibility

First we discuss the artificial compressibility version of the equations, used sometimes for solution of the steady equations. We define a simplified continuity equation and equation of state as

$$\frac{\partial \rho}{\partial t} + \frac{\partial u_i}{\partial x_i} = 0 \qquad \text{and} \qquad p = \beta \rho$$

This allows us to write the Navier-Stokes equations as

$$
\begin{cases}
\dfrac{\partial u_i}{\partial t} + \dfrac{\partial}{\partial x_j} (u_j u_i) &= -\dfrac{\partial p}{\partial x_i} + \dfrac{1}{Re} \nabla^2 u_i \\
\dfrac{\partial p}{\partial t} + \beta \dfrac{\partial u_i}{\partial x_i} &= 0
\end{cases}
$$

Let

$$
\mathbf{u} = \begin{bmatrix} p \\ u \\ v \\ w \end{bmatrix} \qquad
\mathbf{e} = \begin{bmatrix} \beta u \\ p + u^2 \\ uv \\ uw \end{bmatrix} \qquad
\mathbf{f} = \begin{bmatrix} \beta v \\ uv \\ p + v^2 \\ vw \end{bmatrix} \qquad
\mathbf{g} = \begin{bmatrix} \beta w \\ uw \\ vw \\ p + \beta^2 \end{bmatrix}
$$

be the vector of unknowns and their fluxes. The Navier-Stokes equations can then be written

$$\frac{\partial \mathbf{u}}{\partial t} + \frac{\partial \mathbf{e}}{\partial x} + \frac{\partial \mathbf{f}}{\partial y} + \frac{\partial \mathbf{g}}{\partial z} = \frac{1}{Re} \nabla^2 \mathbf{D} \mathbf{u}$$

$$\text{or} \qquad \frac{\partial \mathbf{u}}{\partial t} + \mathbf{A} \frac{\partial \mathbf{u}}{\partial \mathbf{x}} + \mathbf{B} \frac{\partial \mathbf{u}}{\partial \mathbf{y}} + \mathbf{C} \frac{\partial \mathbf{u}}{\partial \mathbf{z}} = \frac{1}{R} \nabla^2 \mathbf{D} \mathbf{u}$$

where the matrices above are defined

$$\mathbf{A} = \frac{\partial \mathbf{e}}{\partial \mathbf{u}} = \begin{bmatrix} 0 & \beta & 0 & 0 \\ 1 & 2u & 0 & 0 \\ 0 & v & u & 0 \\ 0 & w & 0 & u \end{bmatrix}, \quad \mathbf{B} = \frac{\partial \mathbf{f}}{\partial \mathbf{u}} = \begin{bmatrix} 0 & 0 & \beta & 0 \\ 0 & v & u & 0 \\ 1 & 0 & 2v & 0 \\ 0 & 0 & w & v \end{bmatrix}$$

$$\mathbf{C} = \frac{\partial \mathbf{g}}{\partial \mathbf{u}} = \begin{bmatrix} 0 & 0 & 0 & \beta \\ 0 & v & u & 0 \\ 1 & 0 & 2v & 0 \\ 0 & 0 & w & v \end{bmatrix}, \quad \mathbf{D} = \begin{bmatrix} 0 & 0 & 0 & 0 \\ 0 & 1 & 0 & 0 \\ 0 & 0 & 1 & 0 \\ 0 & 0 & 0 & 1 \end{bmatrix}$$

the eigenvalues of $\mathbf{A}, \mathbf{B}, \mathbf{C}$ are the wave speeds of plane waves in the respective coordinate directions, they are

$$\left(u, u, u \pm \sqrt{u^2 + \beta} \right), \qquad \left(v, v, v \pm \sqrt{v^2 + \beta} \right) \text{ and } \qquad \left(w, w, w \pm \sqrt{w^2 + \beta} \right)$$

Note that the effective acoustic or pressure wave speed $\sim \sqrt{\beta} \to \infty$ for incompressible flow.

Projection on a divergence free space

Second we discuss the projection of the velocity field on a divergence free space. We begin by the following theorem.

Theorem 1. Any w_i in Ω can uniquely be decomposed into

$$w_i = u_i + \frac{\partial p}{\partial x_i}$$

$$\text{where} \qquad \frac{\partial u_i}{\partial x_i} = 0, \quad u_i \cdot n_i = 0 \qquad \text{on} \qquad \partial \Omega.$$

i.e. into a function u_i that is divergence free and parallel to the boundary and the gradient of a function, here called p.

Proof. We start by showing that u_i and $\frac{\partial p}{\partial x_i}$ is orthogonal in the L_2 inner product.

$$\left(u_i, \frac{\partial p}{\partial x_i} \right) = \int_\Omega u_i \frac{\partial p}{\partial x_i} \, dV = \int_\Omega \frac{\partial}{\partial x_i} (u_i p) \, dV = \oint_{\partial \Omega} p u_i n_i \, dS = 0$$

The uniqueness of the decomposition can be seen by assuming that we have two different decompositions and showing that they have to be equivalent. Let

$$w_i = u_i^{(1)} + \frac{\partial p^{(1)}}{\partial x_i} = u_i^{(2)} + \frac{\partial p^{(2)}}{\partial x_i}$$

The inner product between

$$u_i^{(1)} - u_i^{(2)} + \frac{\partial}{\partial x_i} \left(p^{(1)} - p^{(2)} \right) \qquad \text{and} \quad u_i^{(1)} - u_i^{(2)}$$

gives

$$0 = \int_\Omega \left[\left(u_i^{(1)} - u_i^{(2)} \right)^2 + \left(u_i^{(1)} - u_i^{(2)} \right) \frac{\partial}{\partial x_i} \left(p^{(1)} - p^{(2)} \right) \right] dV = \int_\Omega \left(u_i^{(1)} - u_i^{(2)} \right)^2 dV$$

Thus we have

$$u_i^{(1)} = u_i^{(2)}, \qquad p^{(1)} = p^{(2)} + C$$

$\frac{\pi}{2} + d\varphi_{12}$

$V(t)$

$S(t)$

$V(t + \Delta t) - V(t)$

$S(t + \Delta t)$

$\mathbf{u}$

$\mathbf{n}$

$V(t + \Delta t)$

p

T_0, U_0

T_w

L

T_0

U_0

Gradient fields

$\frac{\partial p}{\partial x_i}$

w_i

u_i

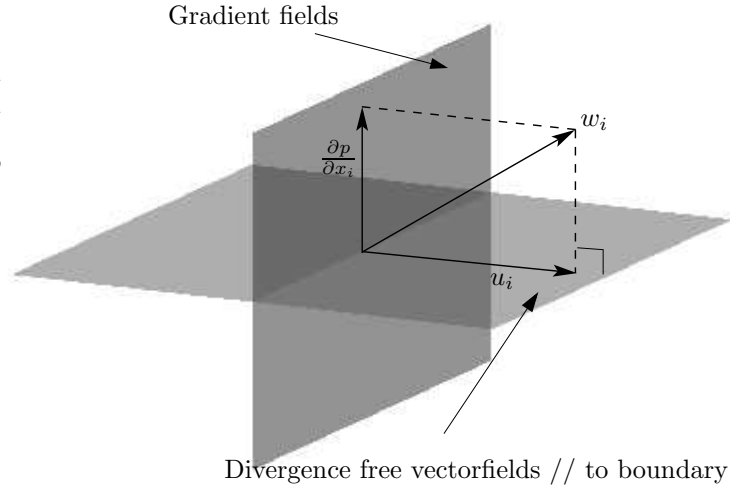Divergence free vectorfields // to boundary

Figure 1.13: Projection of a function on a divergence free space.

We can find an equation for a p with above properties by noting that

$$\nabla^2 p = \frac{\partial w_i}{\partial x_i} \qquad \text{in } \Omega \text{ with} \qquad \frac{\partial p}{\partial n} = w_i n_i \text{ on } \partial\Omega$$

has a unique solution. Now, if

$$u_i = w_i - \frac{\partial p}{\partial x_i} \Rightarrow$$

we have

$$0 = \frac{\partial u_i}{\partial x_i} = \frac{\partial w_i}{\partial x_i} - \frac{\partial^2 p}{\partial x_i \partial x_i}; \quad \text{and} \qquad 0 = u_i n_i = w_i n_i - \frac{\partial p}{\partial n}$$

$\square$

To sum up, to project w_i on divergence free space let $w_i = u_i + \dfrac{\partial p}{\partial x_i}$

1) solve for $p : \dfrac{\partial w_i}{\partial x_i} = \nabla^2 p, \qquad \dfrac{\partial p}{\partial n} = 0$

2) let $u_i = w_i - \dfrac{\partial p}{\partial x_i}$

This is schematically shown in figure 1.13. Note also that $(w_i - u_i) \perp u_i$.

Apply to Navier-Stokes equations

Let $\mathbb{P}$ be orthogonal projector which maps w_i on divergence free part u_i, i.e. $\mathbb{P}w_i = u_i$. We then have the following relations

$$w_i = \mathbb{P}w_i + \frac{\partial p}{\partial x_i}$$

$$\mathbb{P}u_i = u_i, \qquad \mathbb{P}\frac{\partial p}{\partial x_i} = 0$$

Applying the orthogonal projector to the Navier-Stokes equations, we have

$$\mathbb{P}\left(\frac{\partial u_i}{\partial t} + \frac{\partial p}{\partial x_i}\right) = \mathbb{P}\left(-u_j \frac{\partial u_i}{\partial x_j} + \frac{1}{Re}\nabla^2 u_i\right)$$

Now, u_i is divergence free and parallel to boundary, thus

$$\mathbb{P}\frac{\partial u_i}{\partial t} = \frac{\partial u_i}{\partial t}$$

However,

$$\mathbb{P}\nabla^2 u_i \neq \nabla^2 u_i$$

since $\nabla^2 u_i$ need not be parallel to the boundary. Thus we find an evolution equation without the pressure, we have

$$\frac{\partial u_i}{\partial t} = \mathbb{P}\left(\underbrace{-u_j\frac{\partial u_i}{\partial x_j} + \frac{1}{Re}\nabla^2 u_i}_{w_i}\right)$$

The pressure term in the Naiver-Stokes equations ensures that the right hand side w_i is divergence free. We can find a Poisson equation for the pressure by taking the divergence of w_i, according to the result above. We find

$$\nabla^2 p = \frac{\partial}{\partial x_i}\left(\underbrace{-u_j\frac{\partial u_i}{\partial x_j} + \frac{1}{Re}\nabla^2 u_i}_{w_i}\right) = -\frac{\partial u_j}{\partial x_i}\frac{\partial u_i}{\partial x_j}$$

thus the pressure satisfies elliptic Poisson equation, which links the velocity field in the whole domain instantaneously. This can be interpreted such that the information in incompressible flow spreads infinitely fast, i.e. we have an infinite wave speed for pressure waves, something seen in the analysis of the artificial compressibility equations.

Evolution equation for the divergence

It is common in several numerical solution algorithms for the Naiver-Stokes equations to discard the divergence constraint and instead use the pressure Poisson equation derived above as the second equation in the incompressible Naiver-Stokes equations. If this is done we may encounter solutions that are not divergence free.

Consider the equation for the evolution of the divergence, found by taking the divergence of the momentum equations and substituting the Laplacian of the pressure with the right hand side of the Poisson equation. We have

$$\frac{\partial}{\partial t}\left(\frac{\partial u_i}{\partial x_i}\right) = \frac{1}{Re}\nabla^2\left(\frac{\partial u_i}{\partial x_i}\right)$$

Thus the divergence is not automatically zero, but satisfies a heat equation. For the stationary case the solution obeys the maximum principle. This states that the maximum of a harmonic function, a function satisfying the Laplace equation, has its maximum on the boundary. Thus, the divergence is zero inside the domain, if and only if it is zero everywhere on the boundary.

Since it is the pressure term in the Navier-Stokes equations ensures that the velocity is divergence free, this has implications for the boundary conditions for the pressure Poisson equation. A priori we have none specified, but they have to be chosen such that the divergence of the velocity field is zero on the boundary. This may be a difficult constraint to satisfy in a numerical solution algorithm.

z, x_3
u, u_1
v, u_2
w, u_3
x_1
x_2
x_i^0

Chapter 2

$u_i\left(\mathbf{x}_i, \hat{t}\right)$
$u_i\left(x_i{}^0, \hat{t}\right)$
$\mathbb{P}\left(\hat{t}=0\right)$

Flow $\overset{x}{\underset{u_1}{}}$ physics

$u_2 > u_1$
x_1
x_2
x_3
x_i

$u_i\,\mathrm{d}\hat{t}$

2.1   Exact solutions

Plane Pouseuille flow - exact solution for channel flow

$\mathrm{d}u_i\,\mathrm{d}\hat{t}$

The flow inside the two-dimensional channel, see figure 2.1, is driven by a pressure difference $p_0 - p_1$ between the inlet and the outlet of the channel. We will assume two-dimensional, steady flow, i.e.
$r_i\left(\mathrm{d}\hat{t}\right)$
$\mathrm{d}r_i\left(\mathrm{d}t\right)$

$\mathbb{P}_1$
$\mathbb{P}_2$

$$\frac{\partial}{\partial t} = 0, \qquad u_3 = 0$$

x_1
x_2

and that the flow is fully developed, meaning that effects of inlet conditions have disappeared. We have

x_3
R^3

$$u_1 = u_1\left(x_2\right), \quad u_2 = u_2\left(x_2\right)$$

R^2
R

The boundary conditions are $u_1 = u_2 = 0$ at $x_2 = \pm h$. The continuity equation reads

$\mathbf{r}^3$
$\mathbf{r}^2$
$\mathbf{r}^1$
$\frac{\pi}{2} + \mathrm{d}\varphi_{12}$

$$\frac{\overset{0}{\cancel{\partial u_1}}}{\cancel{\partial x_1}} + \frac{\partial u_2}{\partial x_2} + \frac{\overset{0}{\cancel{\partial u_3}}}{\cancel{\partial x_3}} = 0$$

$V\left(t\right)$
$S\left(t\right)$

$V\left(t+\Delta t\right) - V\left(t\right)$

where the first and the last term disappears due to the assumption of two-dimensional flow and that the flow is fully developed. This implies that $u_2 = C = 0$, where the constant is seem to be zero from the boundary conditions.
$S\left(t+\Delta t\right)$

The steady momentum equations read

$\mathbf{u}$
$\mathbf{n}$

$V\left(t+\Delta t\right)$
p
T_0, U_0
T_{w}

$$\begin{cases} \rho u_1 \dfrac{\partial u_1}{\partial x_1} + \rho u_2 \dfrac{\partial u_1}{\partial x_2} = -\dfrac{\partial p}{\partial x_1} + \mu \nabla^2 u_1 \\[2mm] \rho u_1 \dfrac{\partial u_2}{\partial x_1} + \rho u_2 \dfrac{\partial u_2}{\partial x_2} = -\dfrac{\partial p}{\partial x_2} + \mu \nabla^2 u_2 - \rho g \end{cases}$$

which, by applying the assumptions above, reduce to

L
T_0
U_0

Gradient fields
w_i
$\frac{\partial p}{\partial x_i}$
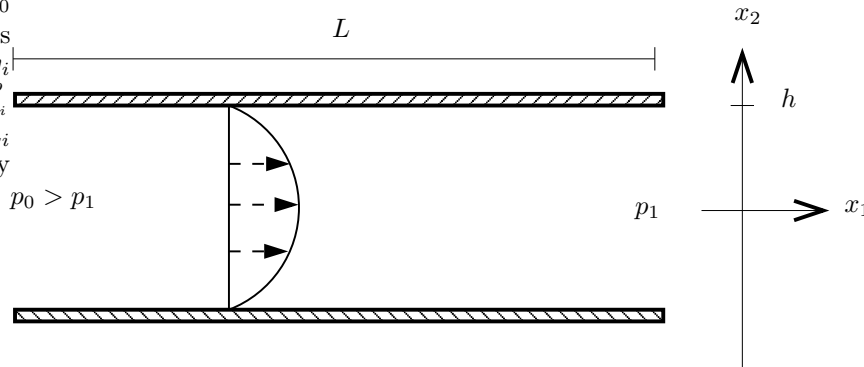u_i

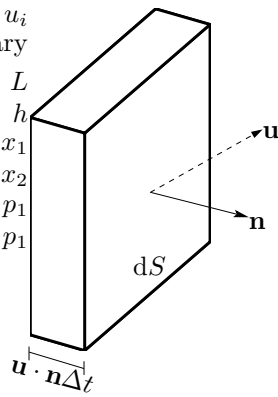ree vectorfields // to boundary

Figure 2.1: Plane channel geometry.

Figure 2.2: Volume of fluid flowing through surface dS in time Δt

$$0 = -\frac{\partial p}{\partial x_1} + \mu \frac{\mathrm{d}^2 u_1}{\mathrm{d} x_2^2}$$

$$0 = -\frac{\partial p}{\partial x_2} - \rho g$$

The momentum equation in the x_2-direction (or normal direction) implies

$$p = -\rho g x_2 + P(x_1) \qquad \Rightarrow \qquad \frac{\partial p}{\partial x_1} = \frac{\mathrm{d}P}{\mathrm{d}x_1}$$

showing that the pressure gradient in the x_1-direction (or streamwise direction) is only a function of x_1. The momentum equation in the streamwise direction implies

$$0 = -\frac{\mathrm{d}P}{\mathrm{d}x_1} + \mu \frac{\mathrm{d}^2 u_1}{\mathrm{d}x_2^2}$$

Since $P(x_1)$ and $u_1(x_2)$ we have

$$\frac{\mathrm{d}^2 u_1}{\mathrm{d}x_2^2} = \frac{1}{\mu} \frac{\mathrm{d}P}{\mathrm{d}x_1} = \text{const. (independent of } x_1, x_2)$$

We can integrate u_1 in the normal direction to obtain

$$u_1 = \frac{1}{2\mu} \frac{\mathrm{d}P}{\mathrm{d}x_1} x_2^2 + C_1 x_2 + C_2$$

The constants can be evaluated from the boundary conditions $u_1(\pm h) = 0$, giving the parabolic velocity profile

$$u_1 = \frac{h^2}{2\mu} \cdot \frac{\mathrm{d}P}{\mathrm{d}x_1} \left[1 - \left(\frac{x_2}{h} \right)^2 \right]$$

Evaluating the maximum velocity at the center of the channel we have

$$u_{\max} = -\frac{h^2}{2\mu} \cdot \frac{\mathrm{d}P}{\mathrm{d}x_1} > 0$$

if flow is in the positive x_1-direction. The velocity becomes

$$\frac{u_1}{u_{\max}} = 1 - \left(\frac{x_2}{h} \right)^2$$

Flow rate

From figure 2.2 we can evaluate the flow rate as $\mathrm{d}Q = \mathbf{u} \cdot \mathbf{n} \, \mathrm{d}S$. Integrating over the channel we find

$$Q = \int_S u_i n_i \, \mathrm{d}S = \{\text{channel}\} = \int_{-h}^{h} u_1 \, \mathrm{d}x_2 = -\frac{2h^3}{3\mu} \cdot \frac{\mathrm{d}P}{\mathrm{d}x_1} = \frac{4}{3} h u_{\max}$$
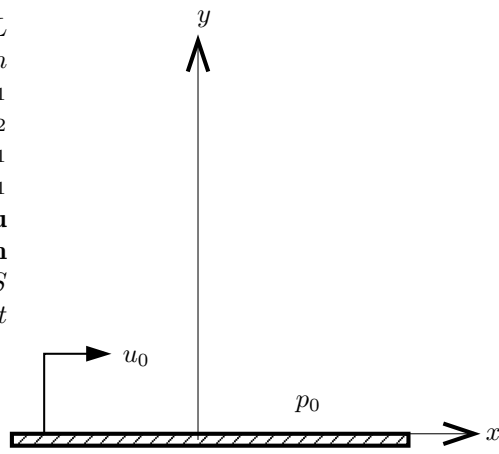
Figure 2.3: Stokes instantaneously plate.

Wall shear stress

The wall shear stress can be evaluated from the velocity gradient at the wall. We have

$$\tau_{12} = \tau_{21} = \mu \frac{\mathrm{d}u_1}{\mathrm{d}x_2} = -\frac{2\mu \cdot u_{\max} \cdot x_2}{h^2}$$

implying that

$$\tau_{\text{wall}} = \tau\big|_{x_2=-h} = \frac{2\mu\, u_{\max}}{h}$$

Vorticity

The vorticity is zero in the streamwise and normal directions, i.e. $\omega_1 = \omega_2 = 0$ and has the following expression in the x_3-direction (or spanwise direction)

$$\omega_3 = \frac{\partial u_2}{\partial x_1} - \frac{\partial u_1}{\partial x_2} = -\frac{\mathrm{d}u_1}{\mathrm{d}x_2} = \frac{2u_{\max} \cdot x_2}{h^2}$$

Stokes 1:st problem: instantaneously started plate

Consider the instantaneously starting plate of infinite horizontal extent shown in figure 2.3. This is a time dependent problem where plate velocity is set to $u = u_0$ at time $t = 0$. We assume that the velocity can be written $u = u(y, t)$ which using continuity and the boundary conditions imply that normal velocity $v = 0$. The momentum equations reduce to

$$\frac{\partial u}{\partial t} = -\frac{1}{\rho}\frac{\partial p}{\partial x} + \nu \frac{\partial^2 u}{\partial y^2}$$

$$0 = -\frac{1}{\rho}\frac{\partial p}{\partial y} - g$$

The normal momentum equation implies that $p = -\rho g y + p_0$, where p_0 is the atmospheric pressure at the plate surface. This gives us the following diffusion equation, initial and boundary conditions for u

$$\frac{\partial u}{\partial t} = \nu \frac{\partial^2 u}{\partial y^2}$$
$$u(y, 0) = 0 \quad 0 \le y \le \infty$$
$$u(0, t) = u_0 \quad t > 0$$
$$u(\infty, t) = 0 \quad t > 0$$

We look for a similarity solution, i.e. we introduce a new dependent variable which is a combination of y and t such that the partial differential equation reduces to an ordinary differential equation. Let

$$f(\eta) = \frac{u}{u_0} \qquad \eta = C \cdot y \cdot t^b$$

where C and b are constants to be chosen appropriately. We transform the time and space derivatives according to

$$\frac{\partial}{\partial t} = \frac{\partial \eta}{\partial t}\frac{d}{d\eta} = Cbyt^{b-1}\frac{d}{d\eta}$$

$$\frac{\partial}{\partial y} = \frac{\partial \eta}{\partial y}\frac{d}{d\eta} = Ct^b\frac{d}{d\eta}$$

$$\frac{\partial^2}{\partial y^2} = C^2 t^{2b}\frac{d^2}{d\eta^2}$$

If we substitute this into the equation for u and use the definition of η, we find an equation for f

$$bt^{-1}\eta\frac{df}{d\eta} = \nu C^2 t^{2b}\frac{d^2 f}{d\eta^2}$$

where no explicit dependence on y and t can remain if a similarity solution is to exist. Thus, the coefficient of the two η-dependent terms have to be proportional to each other, we have

$$bt^{-1} = \kappa \nu C^2 t^{2b}$$

where κ is a proportionality constant. The exponents of these expressions, as well as the coefficients in front of the t-terms have to be equal. This gives

$$b = -\frac{1}{2} \qquad C = \frac{1}{\sqrt{-2\kappa\nu}}$$

We choose $\kappa = -2$ and obtain the following

$$f'' + 2\eta f' = 0 \qquad \eta = \frac{y}{2\sqrt{\nu t}}$$

where $' = \frac{d}{d\eta}$. The boundary and initial conditions also have to be compatible with the similarity assumption. We have

$$\frac{u(y,0)}{u_0} = f(\infty) = 0 \qquad \frac{u(0,t)}{u_0} = f(0) = 1 \qquad \frac{u(\infty,t)}{u_0} = f(\infty) = 0$$

This equation can be integrated twice to obtain

$$f = C_1 \int_0^\eta e^{\xi^2}\, d\xi + C_2$$

Using the boundary conditions and the definition of the error-function, we have

$$f = 1 - \frac{2}{\sqrt{\pi}}\int_0^\eta e^{\xi^2}\, d\xi = 1 - \text{erf}(\eta)$$

This solution is shown in figure 2.4, both as a function of the similarity variable η and the unscaled normal coordinate y. Note that the time dependent solution is diffusing upward.

From the velocity we can calculate the spanwise vorticity as a function of the similarity variable η and the unscaled normal coordinate y. Here the maximum of the vorticity is also changing in time, from the infinite value at $t = 0$ it is diffusing outward in time.

$$\omega_3 = \omega_z = \frac{\partial v}{\partial x} - \frac{\partial u}{\partial y} = \frac{u_0}{\sqrt{\pi\nu t}}e^{-\eta^2}$$

The vorticity is shown in figure 2.5, both as a function of the similarity variable η and the unscaled normal coordinate y. Note again that the time dependent solution is diffusing upward.

2.2 Vorticity and streamfunction

Vorticity is an important concept in fluid dynamics. It is related to the average angular momentum of a fluid particle and the swirl present in the flow. However, a flow with circular streamlines may have zero vorticity and a flow with straight streamlines may have a non-zero vorticity.
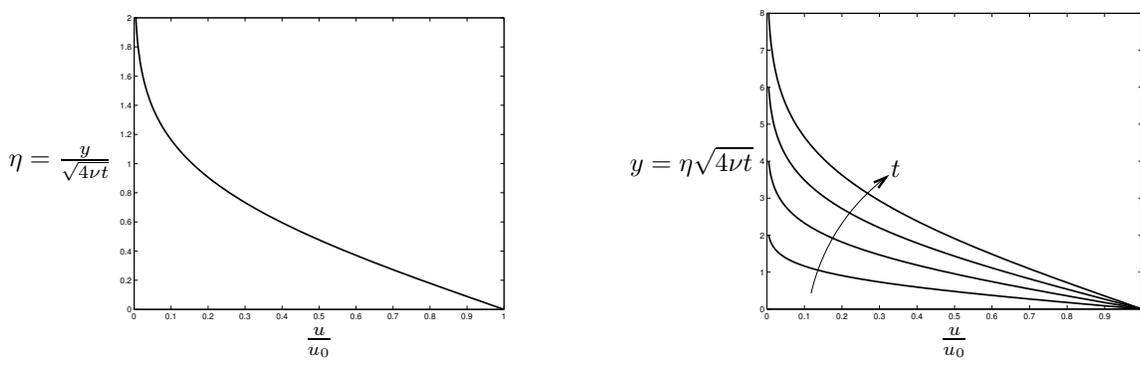
Figure 2.4: Velocity above the instantaneously started plate. a) U as a function of the similarity variable η. b) $U(y,t)$ for various times.
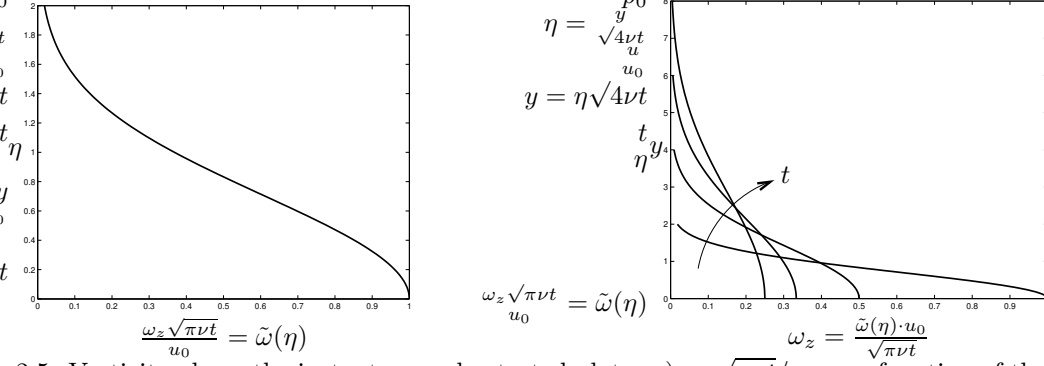
Figure 2.5: Vorticity above the instantaneously started plate. a) $\omega_z\sqrt{\pi\nu t}/u_0$ as a function of the similarity variable η. b) $\omega_z(y,t)$ for various times.

Vorticity and circulation

The vorticity is defined mathematically as the curl of the velocity field as

$$\boldsymbol{\omega} = \nabla \times \mathbf{u}$$

In tensor notation this expression becomes

$$\omega_i = \epsilon_{ijk}\frac{\partial u_k}{\partial x_j}$$

Another concept closely related to the vorticity is the circulation, which is defined as

$$\Gamma = \oint_C u_i\,\mathrm{d}x_i = \oint_C u_i t_i\,\mathrm{d}s$$

In figure 2.6 we show a closed curve C. Using Stokes theorem we can transform that integral to one over the area S as

$$\Gamma = \int_S \epsilon_{ijk}n_i\frac{\partial u_k}{\partial x_j}\,\mathrm{d}S = \int_S \omega_i n_i\,\mathrm{d}S$$

This allows us to find the following relationship between the circulation and vorticity $\mathrm{d}\Gamma = \omega_i n_i\,\mathrm{d}S$, which can also be written

$$\frac{\mathrm{d}\Gamma}{\mathrm{d}S} = \omega_i n_i$$

Thus, one interpretation is that the vorticity is the circulation per unit area for a surface perpendicular to the vorticity vector.

Example 1. The circulation of an ideal vortex. Let the azimuthal velocity be given as $u_\theta = C/r$. We can calculate the circulation of this flow as

$$\Gamma = \oint_C u_\theta r\,\mathrm{d}\theta = C\int_0^{2\pi} \mathrm{d}\theta = 2\pi C$$

Thus we have the following relationship for the ideal vortex
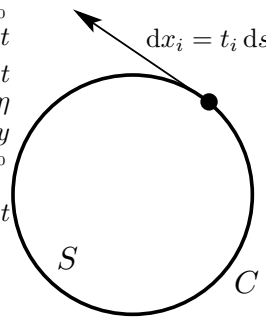
$$u_\theta = \frac{\Gamma}{2\pi r}$$

Figure 2.6: Integral along a closed curve C with enclosed area S.

The ideal vortex has its name from the fact that its vorticity is zero everywhere, except for an infinite value at the center of the vortex.

Derivation of the Vorticity Equation

We will now derive an equation for the vorticity. We start with the dimensionless momentum equations. We have

$$\frac{\partial u_i}{\partial t} + u_j \frac{\partial u_i}{\partial x_j} = -\frac{\partial p}{\partial x_i} + \frac{1}{Re}\nabla^2 u_i$$

We slightly modify this equation by introducing the following alternative form of the non-linear term

$$u_j \frac{\partial u_i}{\partial x_j} = \frac{\partial}{\partial x_i}\left(\frac{1}{2}u_j u_j\right) + \epsilon_{ijk}\omega_j u_k$$

this can readily be derived using tensor manipulation. We take the curl $(\epsilon_{pqi}\frac{\partial}{\partial x_q})$ of the momentum equations and find

$$\frac{\partial}{\partial t}\left(\epsilon_{pqi}\frac{\partial u_i}{\partial x_q}\right) + \epsilon_{pqi}\frac{\partial^2}{\partial x_q \partial x_i}\left(\frac{1}{2}u_j u_j\right) + \epsilon_{pqi}\frac{\partial}{\partial x_q}(\epsilon_{ijk}\omega_j u_k) = -\epsilon_{pqi}\frac{\partial^2 p}{\partial x_q \partial x_i} + \frac{1}{Re}\epsilon_{pqi}\nabla^2 \frac{\partial u_i}{\partial x_q}$$

The second and the fourth terms are zero, since ϵ_{pqi} is anti-symmetric in i,q and $\partial x_q \partial x_i$ is symmetric in i,q

$$\epsilon_{pqi}\frac{\partial^2}{\partial x_q \partial x_i} = 0$$

The first term and the last term can be written as derivatives of the vorticity, and we now have the following from of the vorticity equation

$$\frac{\partial \omega_p}{\partial t} + \epsilon_{pqi}\frac{\partial}{\partial x_q}(\epsilon_{ijk}\omega_j u_k) = \frac{1}{Re}\nabla^2 \omega_p$$

The second term in this equation can be written as

$$\epsilon_{ipq}\epsilon_{ijk}\frac{\partial}{\partial x_q}(\omega_j u_k) = (\delta_{pj}\delta_{qk} - \delta_{pk}\delta_{qj})\frac{\partial}{\partial x_q}(\omega_j u_k) = \frac{\partial}{\partial x_k}(\omega_p u_k) - \frac{\partial}{\partial x_j}(\omega_j u_p) =$$

$$u_k\frac{\partial \omega_p}{\partial x_k} + \omega_p\frac{\partial u_k}{\partial x_k} - u_p\frac{\partial \omega_j}{\partial x_j} - \omega_j\frac{\partial u_p}{\partial x_j}$$

Due to continuity $\frac{\partial \omega_j}{\partial x_j} = \epsilon_{jpq}\frac{\partial^2 u_q}{\partial x_j \partial x_p} = 0$ and we are left with the relation

$$\epsilon_{ipq}\epsilon_{ijk}\frac{\partial}{\partial x_q}(\omega_j u_k) = u_k\frac{\partial \omega_p}{\partial x_k} - \omega_j\frac{\partial u_p}{\partial x_j}$$

Thus, the vorticity equation becomes

$$\frac{\partial \omega_p}{\partial t} + u_k\frac{\partial \omega_p}{\partial x_k} = \omega_j\frac{\partial u_p}{\partial x_j} + \frac{1}{Re}\nabla^2 \omega_p$$

or written in vector-notation

$$\frac{D\boldsymbol{\omega}}{Dt} = (\boldsymbol{\omega}\cdot\nabla)\mathbf{u} + \frac{1}{Re}\nabla^2\boldsymbol{\omega}$$

Components in Cartesian coordinates

In cartesian coordinates the components of the vorticity vector in three-dimensions become

$$\boldsymbol{\omega} = \begin{vmatrix} \mathbf{e}_x & \mathbf{e}_y & \mathbf{e}_z \\ \frac{\partial}{\partial x} & \frac{\partial}{\partial y} & \frac{\partial}{\partial z} \\ u & v & w \end{vmatrix} = \left(\frac{\partial w}{\partial y} - \frac{\partial v}{\partial z} \right) \mathbf{e}_x + \left(\frac{\partial u}{\partial z} - \frac{\partial w}{\partial x} \right) \mathbf{e}_y + \left(\frac{\partial v}{\partial x} - \frac{\partial u}{\partial y} \right) \mathbf{e}_z$$

For two-dimensional flow it is easy to see that this reduces to a non-zero vorticity in the spanwise direction, but zero in the other two directions. We have

$$\omega_x = 0, \qquad \omega_y = 0, \qquad \omega_z = \frac{\partial v}{\partial x} - \frac{\partial u}{\partial y}$$

This simplifies the interpretation and use of the concept of vorticity greatly in two-dimensional flow.

Vorticity and viscocity

There exists a subtle relationship between flows with vorticity and flows on which viscous forces play a role. It is possible to show that

$$\nabla \times \boldsymbol{\omega} \neq 0 \iff \text{viscous forces} \neq 0$$

This means that without viscous forces there cannot be a vorticity field in the flow which varies with the coordinate directions. This is expressed by the following relationship

$$\frac{\partial \tau_{ij}}{\partial x_j} = \mu \nabla^2 u_i = -\mu \epsilon_{ijk} \frac{\partial \omega_k}{\partial x_j}$$

This can be derived in the following manner. We have

$$
\begin{aligned}
-\mu \epsilon_{ijk} \frac{\partial \omega_k}{\partial x_j} &= -\mu \epsilon_{ijk} \epsilon_{kmn} \frac{\partial}{\partial x_j} \frac{\partial}{\partial x_m} u_n \\
&= -\mu (\delta_{im}\delta_{jn} - \delta_{in}\delta_{jm}) \frac{\partial^2 u_n}{\partial x_j \partial x_m} \\
&= \mu \frac{\partial^2 u_i}{\partial x_j \partial x_j} \\
&= \mu \nabla^2 u_i
\end{aligned}
$$

Terms in the two-dimensional vorticity equation

In two dimensions the equation for the only non-zero vorticity component can be written

$$\frac{\partial \omega_3}{\partial t} + u_1 \frac{\partial \omega_3}{\partial x_1} + u_2 \frac{\partial \omega_3}{\partial x_2} = \nu \nabla^2 \omega_3$$

We will take two examples elucidating the meaning of the terms in the vorticity equation. First the diffusion of vorticity and second the advection or transport of vorticity.

Example 2. Diffusion of vorticity: the Stokes 1st problem revisited.

From the solution of Stokes 1st problem above, we find that the vorticity has the following form

$$\omega_3 = \omega_z = \omega(y, t)$$

and that it thus is a solution of the following diffusion equation

$$\frac{\partial \omega}{\partial t} = \nu \frac{\partial^2 \omega}{\partial y^2}$$

The time evolution of the vorticiy can be seen in figure 2.7, and is given by

$$\omega = \frac{u_0}{\sqrt{\pi \nu t}} e^{-\eta^2}, \qquad \text{where } \eta = \frac{y}{2\sqrt{\nu t}}$$

where the factor $\sqrt{\nu t}$ can be identified as the diffusion length scale, where we have used the following dimensional relations

$$[\nu] = \frac{L^2}{T}, \qquad [t] = T \quad \Rightarrow \quad [\sqrt{\nu t}] = L$$
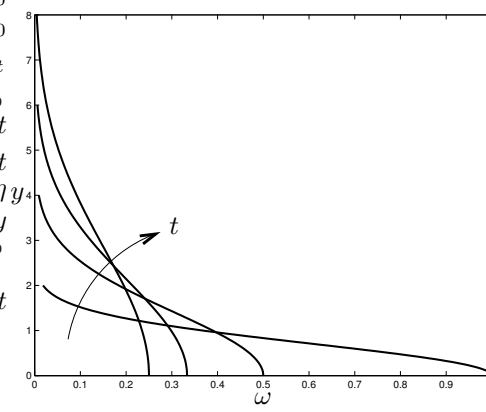
ree vectorfields // to boundary

L

h

x_1

x_2

$p_0 > p_1$

p_1

$\mathbf{u}$

$\mathbf{n}$

$\mathrm{d}S$

$\mathbf{u} \cdot \mathbf{n}\Delta t$

x

y

u_0

p_0

$\eta = \frac{y}{\sqrt{4\nu t}}$

u

u_0

$y = \eta\sqrt{4\nu t}$

t

$\eta\, y$

y

$\omega_z = \frac{\tilde{\omega}(\eta)\cdot u_0}{\sqrt{\pi\nu t}}$

t

Figure 2.7: A sketch of the evolution of vorticity in Stokes 1st problem.

$\eta = \frac{y}{\sqrt{4\nu t}}$

u

u_0

$y = \eta\sqrt{4\nu t}$

t

η

y

$\omega_z = \frac{\tilde{\omega}(\eta)\cdot u_0}{\sqrt{\pi\nu t}}$

t
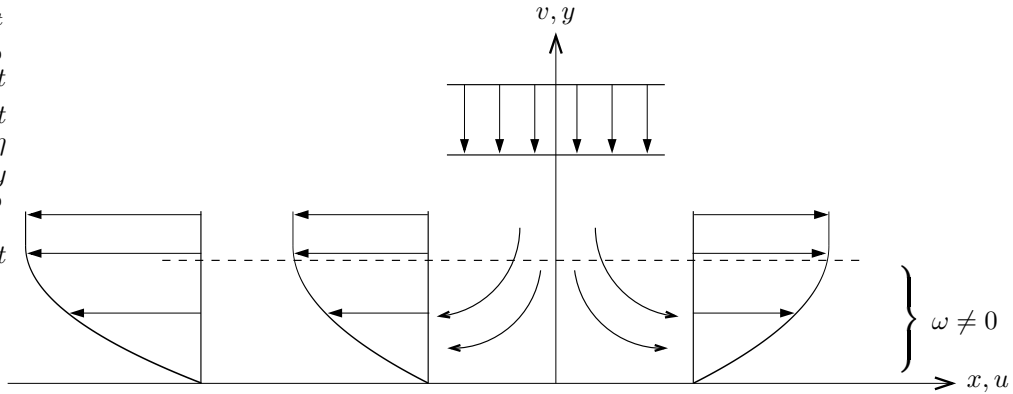
Figure 2.8: Stagnation point flow with a viscous layer close to the wall.

In this flow the streamlines are straight lines and therefore the non-linear term, or the transport/advection term, is zero. We now turn to an example where the transport of vorticity is important.

Example 3. Transport/advection of vorticity: Stagnation point flow.

The stagnation point flow is depicted in figure 2.8, and is a flow where a uniform velocity approaches a plate where it is showed down and turned to a flow parallel two the plates in both the positive and negative x-direction. At the origin we have a stagnation point.

The inviscid stagnation point flow is given as follows

$$\text{inviscid: } \begin{cases} u = cx \\ v = -cy \end{cases} \Rightarrow \quad \omega_z = \omega = \frac{\partial v}{\partial x} - \frac{\partial u}{\partial y} = 0$$

Note that this flow has zero vorticity and that it does not satisfy the no-slip condition ($u = v = 0, y = 0$). In order to satisfy this condition we introduce viscosity, or equally, vorticity. Thus close to the plate we have to fulfill the equation

$$u\frac{\partial \omega}{\partial x} + v\frac{\partial \omega}{\partial y} = \nu\left(\frac{\partial^2 \omega}{\partial x^2} + \frac{\partial^2 \omega}{\partial y^2}\right)$$

The two first terms represent advection or transport of vorticity. We will try a simple modification of the inviscid flow close to the boundary, which is written as

$$\begin{cases} u = xf'(y) \\ v = -f(y) \end{cases}$$

This satisfies the continuity equation, and will be zero on the boundary and approach the inviscid flow far above the plate if we apply the following boundary conditions

$$\begin{cases} u = v = 0, & y = 0 \\ u \propto cx, \ v \propto -cy, & y \to \infty \end{cases}$$

The vorticity can be written $\omega = -xf''(y)$. We introduce this and the above definitions of the velocity components into the vorticity equation, and find
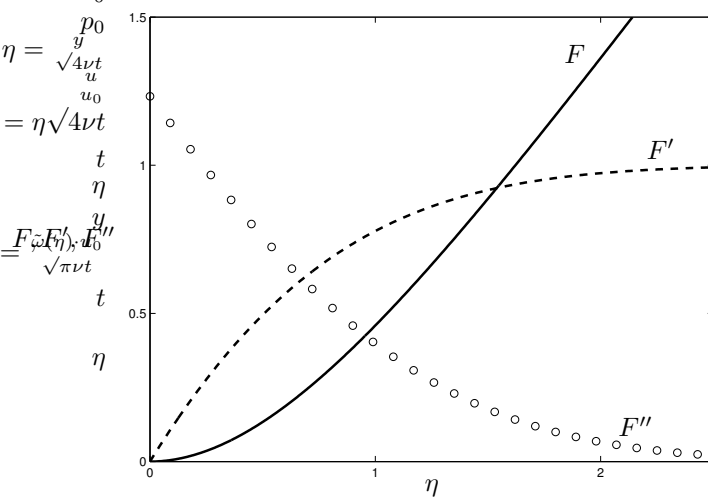
$$-f'f'' + ff''' + \nu f'''' = 0$$

Figure 2.9: Solution to the non-dimensional equation for stagnation point flow. F is proportional to the normal velocity, F' to the streamwise velocity and F'' to the vorticity.

The boundary conditions become

$$\begin{cases} f = f' = 0 & y = 0 \\ f \propto cy, \ f' \propto c, & y \to \infty \end{cases}$$

An integral to the equation exists, which can be written

$$f'^2 - ff'' - \nu f''' = K = \{\text{evaluate } y \to \infty\} = c^2$$

This is as far as we can come analytically and to make further numerical treatment simpler we make the equation non-dimensional with ν and c. Note that they have the dimensions

$$[\nu] = \frac{L^2}{T}, \quad [c] = \frac{1}{T}$$

and that we can use the length scale $\sqrt{\nu/c}$ and the velocity scale $\sqrt{\nu c}$ to scale the independent and the dependent variables as

$$\eta = \frac{y}{\sqrt{\nu/c}}$$

$$F(\eta) = \frac{f(y)}{\sqrt{\nu c}}$$

This results in the following non-dimensional equation

$$F'^2 - FF'' - F''' = 1$$

with the boundary conditions

$$\begin{cases} F = F' = 0, & \eta = 0 \\ F \propto \eta, & \eta \to \infty \end{cases}$$

In figure 2.9 a solution of the equation is shown. It can be seen that <u>diffusion</u> of vorticity from the wall is balanced by <u>transport</u> downward by v and outward by u. The thin layer of vortical flow close to the wall has the thickness $\sim \sqrt{\nu/c}$.

Stretching and tilting of vortex lines

In three-dimensions the vorticity is not restricted to a single non-zero component and the three-dimensional vorticity equation governing the vorticity vector becomes

$$\frac{\partial \omega_i}{\partial t} + \underbrace{u_j \frac{\partial \omega_i}{\partial x_j}}_{\text{advection of vorticity}} = \omega_j \frac{\partial u_i}{\partial x_j} + \underbrace{\frac{1}{Re} \nabla^2 \omega_i}_{\text{diffusion of vorticity}}$$

$$\eta = \frac{u}{\sqrt{4\nu t}}$$
$$u_0$$
$$y = \eta\sqrt{4\nu t}$$
$$t$$
$$\eta$$
$$y$$
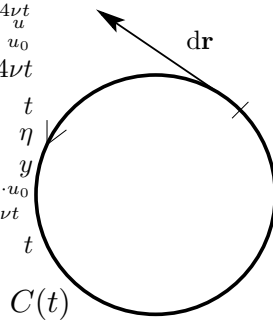$$\omega_z = \frac{\tilde{\omega}(\eta)\cdot u_0}{\sqrt{\pi\nu t}}$$
$$t$$
$$C(t)$$

Figure 2.10: A closed material curve.

The complex motion of the vorticity vector for a full three-dimensional flow can be understood by an analogy to the equation governing the evolution of a material line, discussed in the first chapter. The equation for a material line is

$$\frac{D}{Dt}\, \mathrm{d}r_i = \mathrm{d}r_j \frac{\partial u_i}{\partial x_j}$$

Note that if we disregard the diffusion term, i.e. the last term of the vorticity equation, the two equations are identical. Thus we can draw the following conclusions about the development of the vortex vector

i) Stretching of vortex lines (line $\parallel \boldsymbol{\omega}$) produce ω_i like stretching of $\mathrm{d}r_i$ produces length

ii) Tilting vortex lines produce ω_i in one direction at expense of ω_i in other direction

Helmholz and Kelvin's theorems

The analogy with the equation for the material line directly give us a proof of Helmholz theorem. We have

Theorem 1. Helmholz theorem for inviscid flow: Vortex lines are material lines in inviscid flow.

A second theorem valid in inviscid flow is Kelvin's theorem.

Theorem 2. Kelvin's theorem for inviscid flow: Circulation around a material curve is constant in inviscid flow.

Proof. We show this by considering the circulation for a closed material curve, see figure 2.10,

$$\Gamma_m = \oint_{C(t)} u_i\, \mathrm{d}r_i$$

We can evaluate the material time derivative of this expression with the use of Lagrangian coordinates as follows

$$
\begin{aligned}
\frac{D\Gamma_m}{Dt} &= \frac{D}{Dt}\oint_{C(t)} u_i\, \mathrm{d}r_i \\
&= \left\{
\begin{array}{l}
\text{Lagrange coordinates} \\
u_i = u_i(x_i^0,\hat{t}) = u_i(x_i^0(m),\hat{t}) \\
r_i = r_i(x_i^0,\hat{t}) = r_i(x_i^0(m),\hat{t})
\end{array}
\right. \\
&= \frac{\mathrm{d}}{\mathrm{d}\hat{t}}\oint_m u_i \frac{\partial r_i}{\partial m}\, \mathrm{d}m \\
&= \oint_m \frac{\partial u_i}{\partial \hat{t}}\frac{\partial r_i}{\partial m}\, \mathrm{d}m + \oint_m u_i \frac{\partial}{\partial \hat{t}}\left(\frac{\partial r_i}{\partial m}\right)\, \mathrm{d}m
\end{aligned}
$$

The last term of this expression will vanish since

$$\oint_m u_i \frac{\partial}{\partial \hat{t}}\left(\frac{\partial r_i}{\partial m}\right)\, \mathrm{d}m = \oint_m u_i \frac{\partial u_i}{\partial m}\, \mathrm{d}m = \oint_m \frac{\partial}{\partial m}\left(\frac{1}{2}u_i u_i\right)\, \mathrm{d}m = 0$$
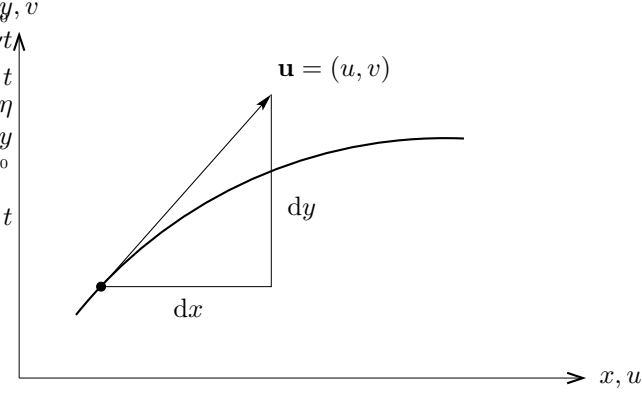
Figure 2.11: A streamline which is tangent to the velocity vector.

Thus we find the following resulting expression

$$
\begin{aligned}
\frac{D\Gamma_m}{Dt} &= \oint_{C(t)} \frac{Du_i}{Dt}\,\mathrm{d}r_i \\
&= \oint_{C(t)} \left[-\frac{\partial p}{\partial x_i} + \frac{1}{Re}\nabla^2 u_i \right]\,\mathrm{d}r_i \\
&= \frac{1}{Re}\oint_{C(t)} \nabla^2 u_i\,\mathrm{d}r_i \to 0, \qquad Re \to \infty
\end{aligned}
$$

Which shows that the circulation for a material curve changes only if the viscous force $\neq 0$ $\qquad\square$

Streamfunction

We end this section with the definition and some properties of the streamfunction. To define the stream-function we need the streamlines which are tangent to the velocity vector. In two dimensions, see figure 2.11, we have

$$
\frac{\mathrm{d}x}{\mathrm{d}y} = \frac{u}{v} \qquad \Longleftrightarrow \qquad \frac{\mathrm{d}x}{u} = \frac{\mathrm{d}y}{v} \qquad \Longleftrightarrow \qquad u\,\mathrm{d}y - v\,\mathrm{d}x = 0
$$

and in three dimensions we can write

$$
\frac{\mathrm{d}x}{u} = \frac{\mathrm{d}y}{v} = \frac{\mathrm{d}z}{w}
$$

For two-dimensional flow we can find the streamlines using a streamfunction. We can introduce a streamfunction $\psi = \psi(x,y)$ with the property that the streamfunction is constant along streamlines. We can make the following derivation

$$
\begin{aligned}
\mathrm{d}\psi &= \frac{\partial\psi}{\partial x}\,\mathrm{d}x + \frac{\partial\psi}{\partial y}\,\mathrm{d}y \\
&= \left\{ \text{assume } u = \frac{\partial\psi}{\partial y},\ v = -\frac{\partial\psi}{\partial x} \text{ and check for consistency} \right\} \\
&= u\,\mathrm{d}y - v\,\mathrm{d}x \\
&= 0, \qquad \text{on streamlines}
\end{aligned}
$$

We can also quickly check that the definition given above satisfies continuity. We have

$$
\frac{\partial u}{\partial x} + \frac{\partial v}{\partial y} = \frac{\partial^2\psi}{\partial x\partial y} - \frac{\partial^2\psi}{\partial y\partial x} = 0
$$

Another property of the streamfunction is that the volume flux between two streamlines can be found from the difference by their respective streamfunctions. We use figure 2.12 and figure 2.13 in the following derivations of the volume flux:
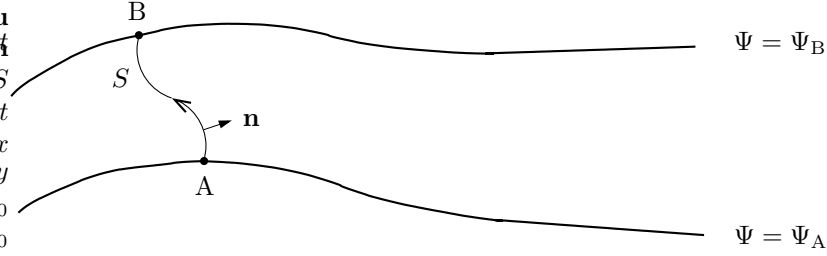
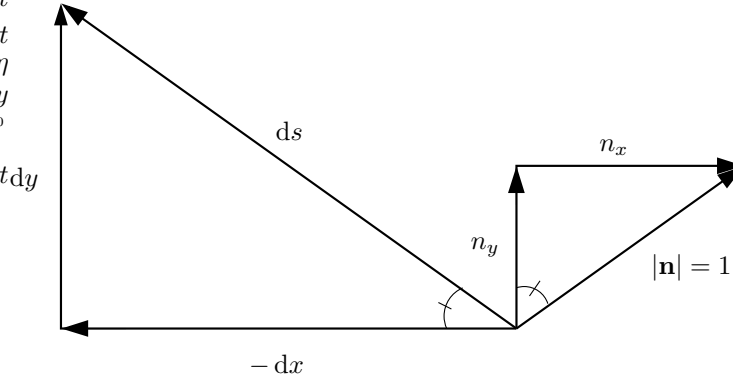Figure 2.12: Integration paths between two streamlines.

Figure 2.13: The normal vector to a line element.

$$
\begin{aligned}
Q_{AB} &= \int_A^B u_i n_i \, \mathrm{d}s \\
&= \int_A^B (n_x u + n_y v) \, \mathrm{d}s \\
&= \left\{ \frac{\mathrm{d}s}{\mathrm{d}y} = \frac{1}{n_x}, \quad -\frac{\mathrm{d}s}{\mathrm{d}x} = \frac{1}{n_y} \right\} \\
&= \int_A^B (u \, \mathrm{d}y - v \, \mathrm{d}x) = \int_A^B \mathrm{d}\psi = \psi_B - \psi_A
\end{aligned}
$$

2.3   Potential flow

Flows which can be found from the gradient of a scalar function, a so called potential, will be dealt with in this section. Working with the velocity potential, for example, will greatly simplify calculations, but also restrict the validity of the solutions. We start with a definition of the velocity potential, then discuss simplifications of the momentum equations when such potentials exist, and finally we deal with two-dimensional potential flows, where analytic function theory can be used.

Velocity potential

Assume that the velocity can be found from a potential. In three dimensions we have

$$
u_i = \frac{\partial \phi}{\partial x_i} \quad \text{or} \quad \mathbf{u} = \nabla \phi
$$

with the corresponding relations in two dimensions

$$
\left\{
\begin{aligned}
u &= \frac{\partial \phi}{\partial x} \\
v &= \frac{\partial \phi}{\partial y}
\end{aligned}
\right.
$$

There are several consequences of this definition of the velocity field.

i) Potential flow have no vorticity, which can be seen by taking the curl of the gradient of the velocity potential, i.e.

$$\omega_i = \epsilon_{ijk}\frac{\partial u_k}{\partial x_j} = \epsilon_{ijk}\frac{\partial^2 \phi}{\partial x_j \partial x_k} = 0$$

ii) Potential flow is not influenced by viscous forces, which is seen by the relationship between viscous forces and vorticity, derived earlier. We have

$$\frac{\partial \tau_{ij}}{\partial x_j} = \mu\nabla^2 u_i = -\mu\epsilon_{ijk}\frac{\partial \omega_k}{\partial x_j}$$

iii) Potential flow satisfies Laplace equation, which is a consequence of the divergence constraint applied to the gradient of the velocity potential, i.e.

$$\frac{\partial u_i}{\partial x_i} = \frac{\partial^2 \phi}{\partial x_i \partial x_i} = \nabla^2 \phi = 0$$

Bernoulli's equation

For potential flow the velocity field can thus be found by solving Laplace equation for the velocity potential. The momentum equations can then be used to find the pressure from the so called Bernoulli's equation. We start by rewriting the momentum equation

$$\frac{\partial u_i}{\partial t} + u_j\frac{\partial u_i}{\partial x_j} = -\frac{1}{\rho}\frac{\partial p}{\partial x_i} + \nu\nabla^2 u_i - g\delta_{i3}$$

using the alternative form of the non-linear terms, i.e.

$$u_j\frac{\partial u_i}{\partial x_j} = \frac{\partial}{\partial x_i}\left(\frac{1}{2}u_k u_k\right) - \epsilon_{ijk}u_j\omega_k$$

and obtain the following equation

$$\frac{\partial u_i}{\partial t} + \frac{\partial}{\partial x_i}\left(\frac{1}{2}u_k u_k + \frac{p}{\rho} + gx_3\right) = \epsilon_{ijk}u_j\omega_k + \nu\epsilon_{ijk}\frac{\partial \omega_k}{\partial x_j}$$

This equation can be integrated in for two different cases: potential flow (without vorticity) and stationary inviscid flow with vorticity.

i) Potential flow. Introduce the definition of the velocity potential $u_i = \frac{\partial \phi}{\partial x_i}$ into the momentum equation above, we have

$$\frac{\partial}{\partial x_i}\left(\frac{\partial \phi}{\partial t} + \frac{1}{2}u_k u_k + \frac{p}{\rho} + gx_3\right) = 0 \quad \Rightarrow$$

$$\frac{\partial \phi}{\partial t} + \frac{1}{2}(u_1^2 + u_2^2 + u_3^2) + \frac{p}{\rho} + gx_3 = f(t)$$

ii) Stationary, inviscid flow with vorticity. Integrate the momentum equations along a streamline, see figure 2.14. We have

$$\int t_i\frac{\partial}{\partial x_i}\left(\frac{1}{2}u_k u_k + \frac{p}{\rho} + gx_3\right)\mathrm{d}s = \int \epsilon_{ijk}\frac{u_i}{u}u_j\omega_k\,\mathrm{d}s = 0 \quad \Rightarrow$$

$$\frac{1}{2}(u_1^2 + u_2^2 + u_3^2) + \frac{p}{\rho} + gx_3 = \text{constant along streamlines}$$

Thus, Bernoulli's equation can be used to calculate the pressure when the velocity is known, for two different flow situations.

Example 4. Ideal vortex: Swirling stationary flow without vorticity. The velocity potential $\mathbf{u} = \nabla\phi$ in polar coordinates can be written

$$\begin{cases} u_r &= \dfrac{\partial \phi}{\partial r} \\[2mm] u_\theta &= \dfrac{1}{r}\dfrac{\partial \phi}{\partial \theta} \end{cases}$$
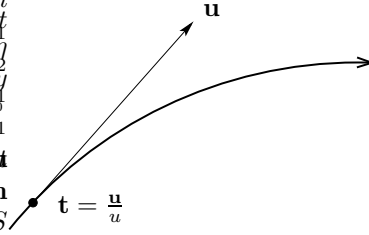
Figure 2.14: Integration of the momentum equation along a streamline.
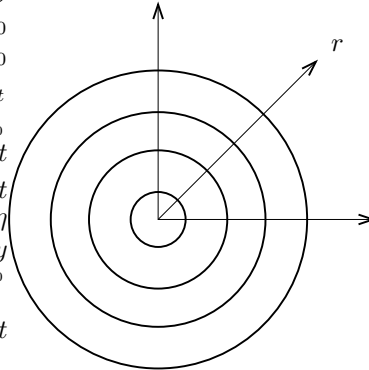

Figure 2.15: Streamlines for the ideal vortex.

The velocity potential satisfies Laplace equation, which in polar coordinates becomes

$$\nabla^2 \phi = \frac{1}{r}\frac{\partial}{\partial r}\left(\frac{1}{r}\frac{\partial \phi}{\partial r}\right) + \frac{1}{r}\frac{\partial^2 \phi}{\partial \theta^2} = 0$$

The first term vanishes since $\frac{\partial \phi}{\partial r} = u_r = 0$. Integrate the resulting equation twice and we find

$$\phi = C\theta + D$$

The constant D is arbitrary so we can set it to zero. Using the definition of the circulation we find

$$u_\theta = \frac{C}{r}, \quad C = \frac{\Gamma}{2\pi}$$

We can easily find the streamfunction for this flow. In polar coordinates the streamfunction is defined

$$\begin{cases} u_r &= \dfrac{1}{r}\dfrac{\partial \psi}{\partial \theta} \\[2mm] u_\theta &= -\dfrac{\partial \psi}{\partial r} \end{cases}$$

Note that the streamfunction satisfies continuity, i.e. $\nabla \cdot \mathbf{u} = 0$. We use the solution from the velocity potential to find the streamfunction, we have

$$\frac{\partial \psi}{\partial r} = -\frac{\Gamma}{2\pi r} \quad \Rightarrow \quad \psi = -\frac{\Gamma}{2\pi}\ln r$$

The streamfunction is constant along streamlines resulting in circular streamlines, see figure 2.15

We can now use Bernoulli's equation to calculate the pressure distribution for the ideal vortex as

$$\frac{1}{2}u_\theta^2 + p = p_\infty \quad \Rightarrow \quad p = p_\infty - \frac{\Gamma^2}{8\pi^2 r^2}$$

Note that the solution has a singularity at the origin.

Two-dimensional potential flow using analytic functions

For two-dimensional flows we can use analytic function theory, i.e. complex valued functions, to calculate the velocity potential. In fact, as we will show in the following. Any analytic function represents a two-dimensional potential flow.

We start by showing that both the velocity potential and the streamfunciton satisfy Laplace equation. Velocity potential ϕ for two-dimensional flow is defined

$$\begin{cases} u & = & \dfrac{\partial \phi}{\partial x} \\ \\ v & = & \dfrac{\partial \phi}{\partial y} \end{cases}$$

Using the continuity equation gives

$$\frac{\partial u}{\partial x} + \frac{\partial v}{\partial y} = \nabla^2 \phi = 0$$

The streamfunction ψ is defined

$$\begin{cases} u & = & \dfrac{\partial \psi}{\partial y} \\ \\ v & = & -\dfrac{\partial \psi}{\partial x} \end{cases}$$

By noting that potential flow has no vorticity we find

$$-\omega = -\frac{\partial v}{\partial x} + \frac{\partial y}{\partial y} = \nabla^2 \psi = 0$$

Thus, both the velocity potential ϕ and the streamfunction ψ satisfy Laplace equation.

We can utilize analytic function theory by introducing the complex function

$$F(z) = \phi(x, y) + i\psi(x, y)$$

where

$$z = x + iy = re^{i\theta} = r(\cos\theta + i\sin\theta)$$

which will be denoted the complex potential.

We now recall some useful results from analytic function theory.

$$F'(z) \text{ exists and is unique} \quad \Longleftrightarrow \quad F(z) \text{ is an analytic function}$$

The fact that a derivative of a complex function should be unique rests on the validity of the Cauchy–Riemann equations. We can derive those equations by requiring that a derivative of a complex function should be the same independent of the direction we take the limit in the complex plane, see figure 2.16. We have

$$\begin{aligned} F'(z) & = & \lim_{\Delta z \to 0} \frac{1}{\Delta z}[F(z + \Delta z) - F(z)] \\ \\ & = & \lim_{\Delta x \to 0} \frac{1}{\Delta x}[\phi(x + \Delta x, y) - \phi(x, y) + i\psi(x + \Delta x, y) - i\psi(x, y)] \\ \\ & = & \lim_{i\Delta y \to 0} \frac{1}{i\Delta y}[\phi(x, y + \Delta y) - \phi(x, y) + i\psi(x, y + \Delta y) - i\psi(x, y)] \end{aligned}$$

$$\Rightarrow \begin{cases} \dfrac{\partial \phi}{\partial x} = \dfrac{\partial \psi}{\partial y} & \text{real part} \\ \\ i\dfrac{\partial \psi}{\partial x} = \dfrac{1}{i}\dfrac{\partial \phi}{\partial y} \Rightarrow \dfrac{\partial \psi}{\partial x} = -\dfrac{\partial \phi}{\partial y} & \text{imaginary part} \end{cases}$$

Thus we have the Cauchy–Riemann equations as a necessary requirement for a complex function to be analytic, i.e.

$$\frac{\partial \phi}{\partial x} = \frac{\partial \psi}{\partial y} \quad \text{and} \quad \frac{\partial \phi}{\partial y} = -\frac{\partial \psi}{\partial x}$$

Using the Cauchy-Riemann equations we can show that the real ϕ and imaginary part ψ of the complex potential satisfy Laplace equations and thus that they are candidates for identification with the velocity potential and streamfunction of a two-dimensional potential flow. We have

$$\begin{cases} \dfrac{\partial^2 \phi}{\partial x^2} = \dfrac{\partial}{\partial x}\left(\dfrac{\partial \psi}{\partial y}\right) = \dfrac{\partial}{\partial y}\left(\dfrac{\partial \psi}{\partial x}\right) = -\dfrac{\partial^2 \phi}{\partial y^2} \\ \\ \dfrac{\partial^2 \psi}{\partial y^2} = \dfrac{\partial}{\partial y}\left(\dfrac{\partial \phi}{\partial x}\right) = \dfrac{\partial}{\partial x}\left(\dfrac{\partial \phi}{\partial y}\right) = -\dfrac{\partial^2 \psi}{\partial x^2} \end{cases}$$

$$\eta = \frac{y}{\sqrt{4\nu t}}$$

u_0
p_0
u
u_0

$$y = \eta\sqrt{4\nu t}$$

t
η
y

$$\omega_z = \frac{\tilde{\omega}(\eta)\cdot u_0}{\sqrt{\pi\nu t}}$$
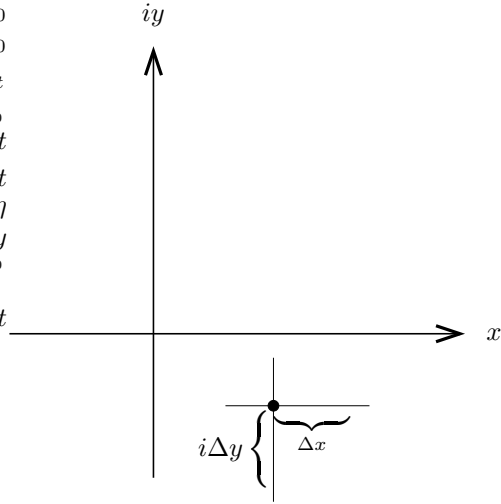
t

iy

x

$i\Delta y$

Δx

Figure 2.16: The complex plane and the definitions of analytic functions.

In addition to satisfying the Laplace equations, we also have to show that the Cauchy-Riemann equations are consistent with the definition of the velocity potential and the streamfunciton. The Cauchy–Riemann equations are

$$\begin{cases} u = \dfrac{\partial\phi}{\partial x} = \dfrac{\partial\psi}{\partial y} \\[2mm] v = \dfrac{\partial\phi}{\partial y} = -\dfrac{\partial\psi}{\partial x} \end{cases}$$

which recovers the definitions of the velocity potential and the streamfunction. Thus any analytic complex function can be identified with a potential flow, where the real part is the velocity potential and the imaginary part is the streamfunction.

We can now define the complex velocity as the complex conjugate of the velocity vector since

$$W(z) = \frac{\mathrm{d}F}{\mathrm{d}z} = \frac{\partial\phi}{\partial x} + i\frac{\partial\psi}{\partial x} = u - iv$$

It will be useful to have a similar relation for polar coordinates, see figure 2.17. In this case we have

$$\begin{cases} u = u_r\cos\theta - u_\theta\sin\theta \\ v = u_r\sin\theta + u_\theta\cos\theta \end{cases}$$

$$W(z) = u - iv = [u_r(r,\theta) - iu_\theta(r,\theta)]\underbrace{e^{-i\theta}}_{\cos\theta - i\sin\theta}$$

We will now take several examples of how potential velocity fields can be found from analytic functions.

Example 5. Calculate the velocity field from the complex potential $F = Ue^{-i\alpha}z$. The complex velocity becomes

$$W(z) = F' = Ue^{-i\alpha} = U\cos\alpha - i\sin\alpha$$

which gives us the solution for the velocity field in physical variables, see figure 2.18, as

$$\begin{cases} u = U\cos\alpha \\ v = U\sin\alpha \end{cases}$$

Example 6. Calculate the velocity field from the complex potential $F = Az^n$. In polar coordinates the complex potential becomes

$$Ar^n e^{in\theta} = Ar^n\cos(n\theta) + iAr^n\sin(n\theta)$$

Thus the velocity potential and the streamfunction can be identified as

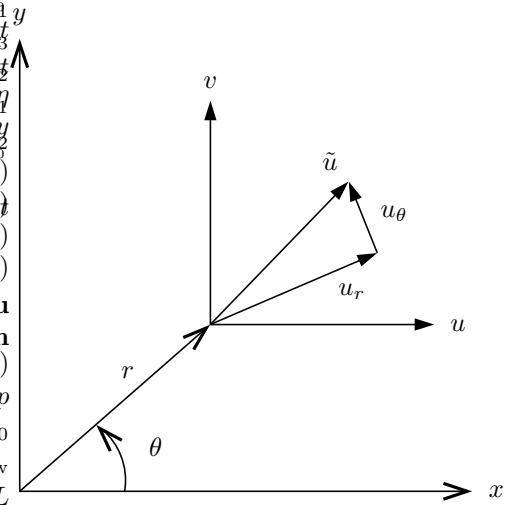$$\begin{cases} \phi = Ar^n\cos(n\theta) \\ \psi = Ar^n\sin(n\theta) \end{cases}$$
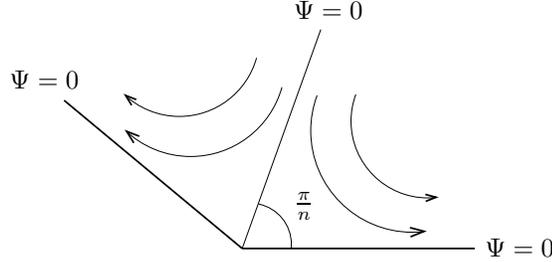
$$\Psi = 0$$
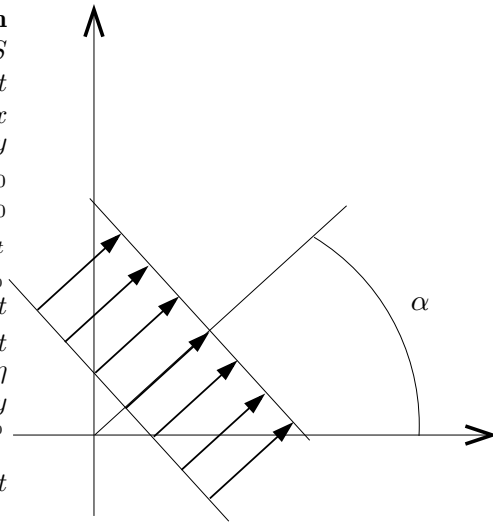
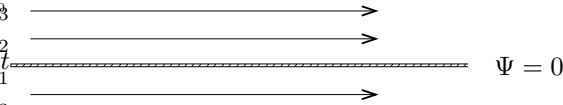Figure 2.19: Flow towards a corner.

$$\Psi = 0$$

Figure 2.20: Uniform flow over a flat plate.

and we can calculate the complex velocity as

$$
\begin{aligned}
W(z) &= F' = nAz^{n-1} \\
&= nAr^{n-1}e^{in\theta}e^{-i\theta} \\
&= nAr^{n-1}[\cos(n\theta) + i\sin(n\theta)]e^{-i\theta}
\end{aligned}
$$

This gives us the solution for the velocity in polar coordinates as

$$
\left\{
\begin{aligned}
u_r &= nAr^{n-1}\cos(n\theta) \\
u_\theta &= -nAr^{n-1}\sin(n\theta)
\end{aligned}
\right.
$$

This is a flow which approaches a corner, see figure 2.19. The streamfunction is zero on the walls and on the stagnation point streamline. By solving for the zero streamlines we can calculate the angle between a wall aligned with the x-axis and the stagnation point streamline. We have

$$\psi = Ar^n\sin(n\theta) = 0 \quad \Rightarrow \quad \theta = \frac{\pi k}{n}$$

Figure 2.20 shows the uniform flow over a flat plate which results when $n = 1$.

Figure 2.21 shows the stagnation point flow when $n = 2$. Here the analysis can be done in Cartesian coordinates

$$
\begin{aligned}
F &= Az^2 \\
W(z) &= F' = 2Az \\
&= 2A(x + iy) \\
&\Rightarrow
\left\{
\begin{aligned}
u &= 2Ax \\
v &= -2Ay
\end{aligned}
\right.
\end{aligned}
$$

Figure 2.22 shows the flow towards a wedge when $1 \le n \le 2$. The velocity along the wedge edge (x axis in figure 2.22) is

$$u_r = nAr^{n-1}\cos(n\theta) \Rightarrow \{\theta = 0\} \Rightarrow u = u_r = nAr^{n-1} = Cx^{n-1}$$

The wedge angle is
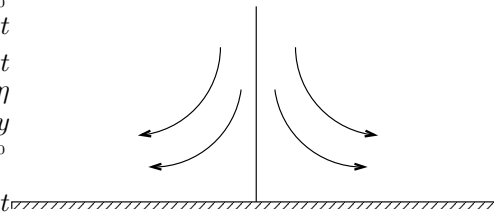
$$\varphi = 2\pi - \frac{2\pi}{n} = 2\pi\frac{n-1}{n}$$
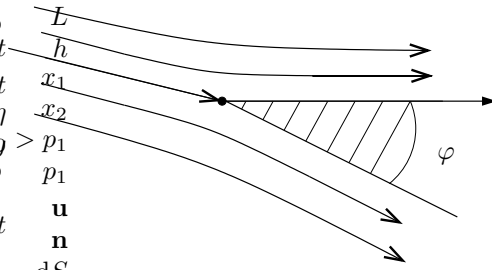
Figure 2.21: Stagnation point flow when $n = 2$.

u
u_0
L

$y = \eta\sqrt{4\nu t}$ h

t x_1

η x_2

$p_0 > p_1$

$\omega_z = \dfrac{\tilde{\omega}(\eta)\cdot u_0}{\sqrt{\pi\nu t}}$ p_1

t $\mathbf{u}$

$\mathbf{n}$

$\mathrm{d}S$

Figure 2.22: $\mathbf{u}\cdot\mathbf{n}\Delta t$: The flow over a wedge when $1 \le n \le 2$.

x

y

u_0

p_0

$\eta = \dfrac{y}{\sqrt{4\nu t}}$

u

u_0

$y = \eta\sqrt{4\nu t}$

t

η

y

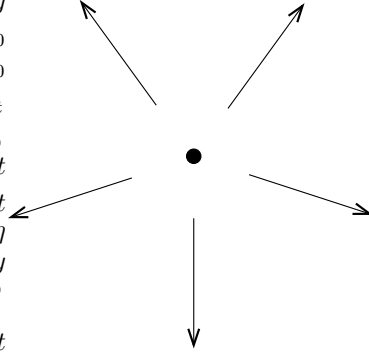$\omega_z = \dfrac{\tilde{\omega}(\eta)\cdot u_0}{\sqrt{\pi\nu t}}$

t

Figure 2.23: Line source.

We now list several other examples of potential flow fields obtained from analytic functions.

Example 7. Line source.

$$
\begin{aligned}
F(z) &= \frac{m}{2\pi}\ln z \\
&= \frac{m}{2\pi}\ln(re^{i\theta}) \\
&= \frac{m}{2\pi}[\ln r + i\theta]
\end{aligned}
$$

The velocity potential and the streamfunction become

$$
\begin{cases}
\phi = \dfrac{m}{2\pi}\ln r \\[2mm]
\psi = \dfrac{m}{2\pi}\theta
\end{cases}
$$

The complex velocity can be written as

$$
W(z) = F' = \frac{m}{2\pi z} = \frac{m}{2\pi r}e^{-i\theta}
$$

which gives the solution in polar coordinates, see figure 2.23, as

$$
\begin{cases}
u_r = \dfrac{m}{2\pi r} \\[2mm]
u_\theta = 0
\end{cases}
$$

We can now calculate the volume flux from the source as

$$
Q = \int_0^{2\pi} \frac{m}{2\pi r}r\,\mathrm{d}\theta = m
$$

Example 8. Line vortex.

$$
\begin{aligned}
F(z) &= -i\frac{\Gamma}{2\pi}\ln z \\
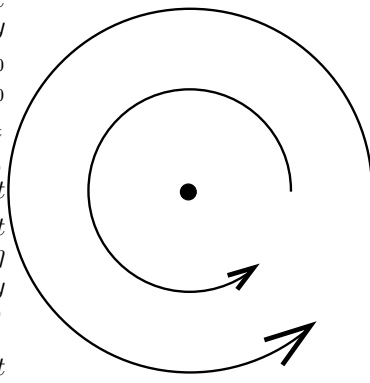&= \frac{\Gamma}{2\pi}[\theta - i\ln r]
\end{aligned}
$$

Figure 2.24: Ideal vortex.

The velocity potential and the streamfunction become

$$
\begin{cases}
\phi = \dfrac{\Gamma}{2\pi}\theta \\[2mm]
\psi = -\dfrac{\Gamma}{2\pi}\ln r
\end{cases}
$$

The complex velocity can be written as

$$
W(z) = F' = -i\frac{\Gamma}{2\pi r}e^{-i\theta}
$$

which gives the solution in polar coordinates, see figure 2.24, as

$$
\begin{cases}
u_r = 0 \\[2mm]
u_\theta = \dfrac{\Gamma}{2\pi r}
\end{cases}
$$

Example 9. The dipole has the complex potential

$$
F(z) = \frac{m\epsilon}{\pi z}
$$

Example 10. The potential flow around a cylinder has the complex potential

$$
F(z) = Uz + U\frac{r_0^2}{z}
$$

Example 11. The potential flow around a cylinder with circulation has the complex potential

$$
F(z) = Uz + U\frac{r_0^2}{z} - i\frac{\Gamma}{2\pi}\ln\frac{z}{r_0}
$$

Example 12. Airfoils. The inviscid flow around some airfoils can be calculated with conformal mappings of solutions from cylinder with circulation.

2.4   Boundary layers

For flows with high Reynolds number Re, where the viscous effects are small, most of the flow can be considered inviscid and a simpler set of equations, the Euler equations, can be solved. The Euler equations are obtained if $Re \to \infty$ in the Navier-Stokes equations. However, the highest derivatives are present in the viscous terms, thus a smaller number of boundary conditions can be satisfied when solving the Euler equations. In particular, the no flow condition can be satisfied at a solid wall but not the no slip condition. In order to satisfy the no slip condition we need to add the viscous term. Thus, there will be a layer close to the solid walls where the viscous terms are important even for very high Reynolds number flow. This layer will be very thin and the flow in that region is called boundary layer flow.
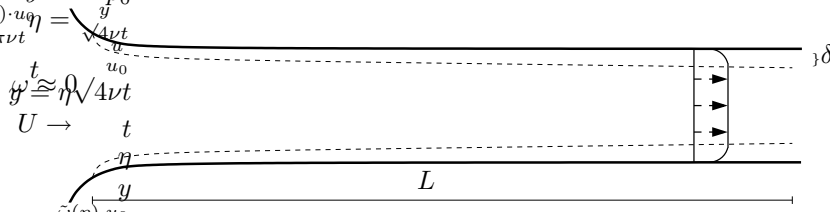
Figure 2.25: Estimate of the viscous region for an inviscid vorticity free inflow in a plane channel.
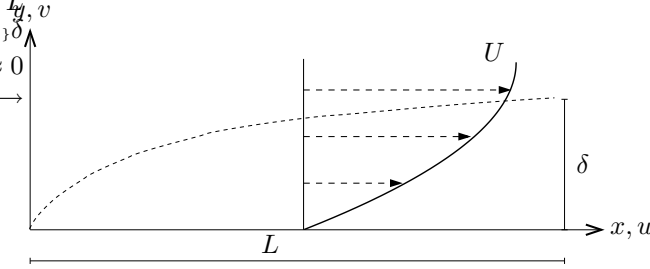

Figure 2.26: Boundary layer profile close to a solid wall.

We begin this section by estimating the thickness of the viscous region in channel with inviscid inflow (zero vorticity), see figure 2.25.

By analogy to the Stokes solution for the instantaneously starting plate, we can estimate the distance the vorticity has diffused from the wall toward the channel centerline as $\delta \sim \sqrt{\nu t_s}$. Where t_s is time of a fluid particle with velocity U has travelled length L, i.e. $t_s = \dfrac{L}{U}$. Thus we can estimate δ/L as

$$\Rightarrow \frac{\delta}{L} = \frac{\sqrt{\nu t_s}}{L} = \frac{1}{L}\left(\frac{\nu L}{U}\right)^{1/2} = \left(\frac{\nu}{UL}\right)^{1/2} = \frac{1}{\sqrt{Re}} \to 0 \text{ as } Re \to \infty$$

We will now divide the flow into a central/outer inviscid part and a boundary layer part close to walls, where the no slip condition is fulfilled. Since we expect this region to be thin for high Reynolds numbers, we expect large velocity gradients near walls.

We choose different length scales inside boundary layer and in inviscid region as indicated in figure 2.26, as

Inviscid : U velocity scale for u, v
: L length scale for x, y

BL : U velocity scale for u
: α velocity scale for v
: L length scale for x
: δ length scale for y

The pressure scale is assumed to be ρU^2 for both the inner and the outer region. The unknown velocity scale for the normal velocity α is determined using continuity

$$\underbrace{\frac{\partial u}{\partial x}}_{\mathcal{O}\left[\frac{U}{L}\right]} + \underbrace{\frac{\partial v}{\partial y}}_{\mathcal{O}\left[\frac{\alpha}{\delta}\right]} = 0$$

which implies that

$$\frac{U}{L} = \frac{\alpha}{\delta} \quad \Rightarrow \quad \alpha = \frac{\delta}{L}U$$

In this manner both terms in the continuity equation have the same size.

Let us use these scalings in the steady momentum equations and disregard small terms. We obtain the following estimates for the size of the terms in the normal momentum equation

$$\uparrow y: \quad u\frac{\partial v}{\partial x} \quad + \quad v\frac{\partial v}{\partial y} \quad = \quad -\frac{1}{\rho}\frac{\partial p}{\partial y} \quad + \quad \nu\frac{\partial^2 v}{\partial x^2} \quad + \quad \nu\frac{\partial^2 v}{\partial y^2}$$

$$U\cdot\frac{1}{L}\frac{\delta U}{L} \qquad \frac{\delta U}{L}\cdot\frac{1}{\delta}\cdot\frac{\delta U}{L} \qquad \frac{U^2}{\delta} \qquad \frac{\nu}{L^2}\cdot\frac{\delta U}{L} \qquad \frac{\nu}{\delta^2}\frac{\delta U}{L}$$

$$\left(\frac{\delta}{L}\right)^2 \qquad\qquad \left(\frac{\delta}{L}\right)^2 \qquad\qquad 1 \qquad\qquad \frac{1}{Re}\left(\frac{\delta}{L}\right)^2 \qquad\qquad \frac{1}{Re}$$

where the last line was obtained by dividing all the terms on the second line by U^2/δ. When $R \to \infty$ and δ/L is small, only pressure term $\mathcal{O}(1)$, which implies that

$$\frac{\partial p}{\partial y} = 0 \qquad \Rightarrow \qquad p = p(x)$$

Thus, the pressure is constant through the boundary layer, given by the inviscid outer solution.
Next we estimate the size of the terms in the streamwise momentum equation as

$$\to x: \quad u\frac{\partial u}{\partial x} \quad + \quad v\frac{\partial u}{\partial y} \quad = \quad -\frac{1}{\rho}\frac{\partial p}{\partial x} \quad + \quad \nu\frac{\partial^2 u}{\partial x^2} \quad + \quad \nu\frac{\partial^2 u}{\partial y^2}$$

$$\frac{U^2}{L} \qquad\qquad \frac{\delta U}{L}\cdot\frac{U}{\delta} \qquad\qquad \frac{U^2}{L} \qquad\qquad \frac{\nu}{L^2}\cdot U \qquad\qquad \frac{\nu}{\delta^2}U$$

$$1 \qquad\qquad 1 \qquad\qquad 1 \qquad\qquad \frac{1}{Re} \qquad\qquad \frac{1}{Re}\cdot\left(\frac{L}{\delta}\right)^2$$

The first three terms are order one and the fourth term negligible when the Reynolds number become large. In order to keep the last term, the only choice that gives a consistent approximation, we have to assume that

$$\frac{\delta}{L} \sim \frac{1}{\sqrt{Re}}$$

which is the same estimate as we found for the extent of the boundary layer in the channel inflow case. Thus we are left with the parabolic equation in x since the second derivative term in that direction is neglected. We have

$$u\frac{\partial u}{\partial x} + v\frac{\partial u}{\partial y} = -\frac{1}{\rho}\frac{\partial p}{\partial x} + \nu\frac{\partial^2 u}{\partial y^2}$$

In summary, the steady boundary layer equations for two-dimensional flow is

$$\begin{cases} u\dfrac{\partial u}{\partial x} + v\dfrac{\partial u}{\partial y} = -\dfrac{1}{\rho}\dfrac{\partial p}{\partial x} + \nu\dfrac{\partial^2 u}{\partial y^2} \\[2mm] \dfrac{\partial u}{\partial x} + \dfrac{\partial v}{\partial y} = 0 \end{cases}$$

with the initial (IC) and boundary conditions (BC)

IC : $\quad u(x = x_0, y) \quad = \quad u_{\text{in}}(y)$

BC : $\quad u(x, y = 0) \quad = \quad 0$
$\qquad\quad v(x, y = 0) \quad = \quad 0$
$\qquad\quad u(x, y \to \infty) \quad = \quad u_e(x)$ outer inviscid flow

where the initial condition is at $x = x_0$ and the equations are marched in the downstream direction. There are several things to note about these equations.

First, v_{in} cannot be given as its own initial condition. By using continuity one can show that once the u_0 is given the momentum equation can be written in the form

$$-\frac{\partial v}{\partial y} + f(y)\, v = g(y)$$

which can be integrated in the y-direction to give the initial normal velocity.

Second, the system of equations is a third order system in y and thus only three boundary conditions can be enforced. We have the no flow and the no slip conditions at the wall and the $u = u_e$ in the free stream. Thus no boundary condition for v in the free stream can be given.
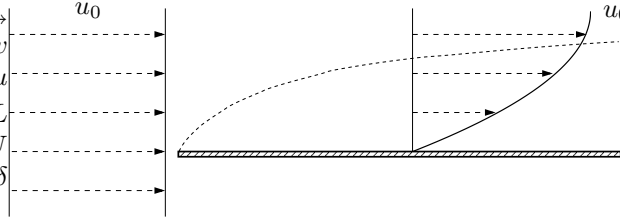
Figure 2.27: Boundary layer flow over a flat plate with zero pressure gradient.

Third, $u_e(x) = u_{inv}(x, y = 0)$, i.e. the boundary layer solution in the free stream approaches the inviscid solution evaluated at the wall, since the thickness of the boundary layer is zero from the inviscid point of view.

Fourth, the pressure gradient term in the momentum equation can be written in terms of the edge velocity u_e using the Bernoulli equation. We have

$$p(x) + \frac{1}{2}\rho u_e^2(x) = \text{const}$$

which implies that

$$-\frac{1}{\rho}\frac{dp}{dx} = u_e \frac{du_e}{dx}$$

Blasius flow over flat plate

Consider the boundary layer equations for a flow over a flat plate with zero pressure gradient, i.e. the outer inviscid flow is $u_e(x) = u_0$. The boundary layer equations become

$$\begin{cases} u\dfrac{\partial u}{\partial x} + v\dfrac{\partial u}{\partial y} = \nu\dfrac{\partial^2 u}{\partial y^2} \\ \dfrac{\partial u}{\partial x} + \dfrac{\partial v}{\partial y} = 0 \end{cases}$$

$$\begin{aligned} \text{IC}: \quad & u(x = x_0, y) & = & \quad u_0 \\ \text{BC}: \quad & u(x, y = 0) & = & \quad 0 \\ & v(x, y = 0) & = & \quad 0 \\ & u(x, y \to \infty) & = & \quad u_0 \end{aligned}$$

We introduce the two-dimensional stream function Ψ

$$u = \frac{\partial \Psi}{\partial y}, \qquad v = -\frac{\partial \Psi}{\partial x}$$

which implicitly satisfies continuity. The boundary layer equations become

$$\frac{\partial \Psi}{\partial y} \cdot \frac{\partial^2 \Psi}{\partial x \partial y} - \frac{\partial \Psi}{\partial x} \cdot \frac{\partial^2 \Psi}{\partial y^2} = \nu \frac{\partial^3 \Psi}{\partial y^3}$$

with appropriate initial and boundary conditions.

Similarity solution

We will now look for a similarity solution. Let

$$u = \frac{\partial \Psi}{\partial y} = u_0 f'(\eta), \qquad \eta = \frac{y}{\delta(x)}$$

which by integration in the y-direction implies

$$\Psi(x, y) = u_0 \delta(x) f(\eta)$$

We can now evaluate the various terms in the momentum equation. We give two below

$$v = -\frac{\partial \Psi}{\partial x} = -u_0 \left(\delta' f + \delta f' \frac{\partial \eta}{\partial x} \right) = -u_0 \left(\delta' f - \frac{y}{\delta} f' \delta' \right) = u_0 (\eta f' - f) \delta'$$
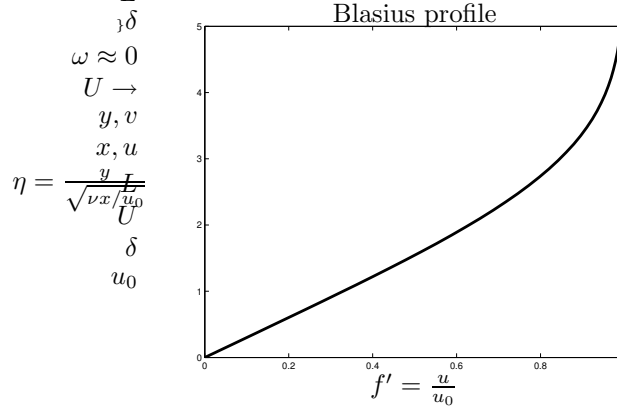
Figure 2.28: Similarity solution giving the Blasius boundary layer profile.

$$\frac{\partial^2 \Psi}{\partial x \partial y} = -u_0 f'' \frac{\eta}{\delta} \delta'$$

If these and the other corresponding terms are introduced into the momentum equation we have the following equation for f

$$-u_0^2 f' f'' \frac{\eta}{\delta} \delta' + u_0^2 (\eta f' - f) \frac{f'' \delta'}{\delta} = \nu u_0 \frac{f'''}{\delta^2}$$

which can be simplified to

$$f''' + \frac{u_0 \delta \delta'}{\nu} f f'' = 0$$

For a similarity solution to be possible, the coefficient in front of the $f f''$ term has to be constant. This implies

$$\frac{u_0 \delta \delta'}{\nu} = \frac{1}{2} \qquad \Rightarrow \qquad \int \delta \delta' \, \mathrm{d}x = \frac{1}{2} \int \frac{\nu \, \mathrm{d}x}{u_0} \qquad \Rightarrow \qquad \frac{1}{2}\delta^2 = \frac{1}{2} \frac{\nu x}{u_0}$$

which implies that $\delta(x) = \sqrt{\dfrac{\nu x}{u_0}}$, where we have chosen the constant of integration such that $\delta = 0$ when $x = 0$. We are left with the Blasius equation and boundary conditions

$$f''' + \frac{1}{2} f f'' = 0$$

$$\mathrm{BC} : \begin{cases} f(0) & = & f'(0) = 0 \\ f'(\infty) & = & 1 \end{cases}$$

The numerical solution to the Blasius equation gives the self-similar velocity profile seen in figure 2.28.

The boundary layer thickness can be evaluated as the height where the velocity has reached 99% of the free stream value. We have

$$f'(\eta_{99}) = 0.99 \qquad \Rightarrow \qquad \eta_{99} = \frac{\delta_{99}}{\sqrt{\frac{\nu x}{u_0}}} = 4.9 \qquad \Rightarrow \qquad \delta_{99} = 4.9 \sqrt{\frac{\nu x}{u_0}}$$

where it can be seen that the boundary layer thickness grows as $\sqrt{x}$.

Displacement thickness and skin friction coefficient

Another measure of the boundary layer thickness is the displacement δ^* of the wall needed in order to have the same volume flux of the inviscid flow as for the flow in the boundary layer. With the help of figure 2.29 we can evaluate this as

$$\int_0^{y_0} u \, \mathrm{d}y \equiv \int_{\delta^*}^{y} u_0 \, \mathrm{d}y = \int_0^{y} u_0 \, \mathrm{d}y - \delta^* u_0$$
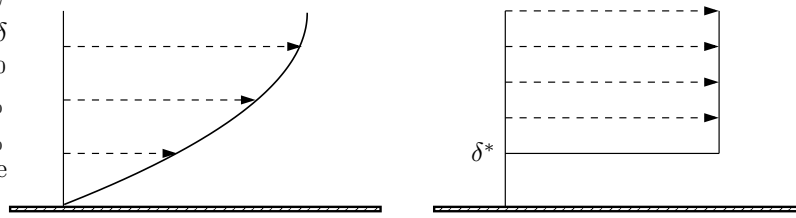
which implies that

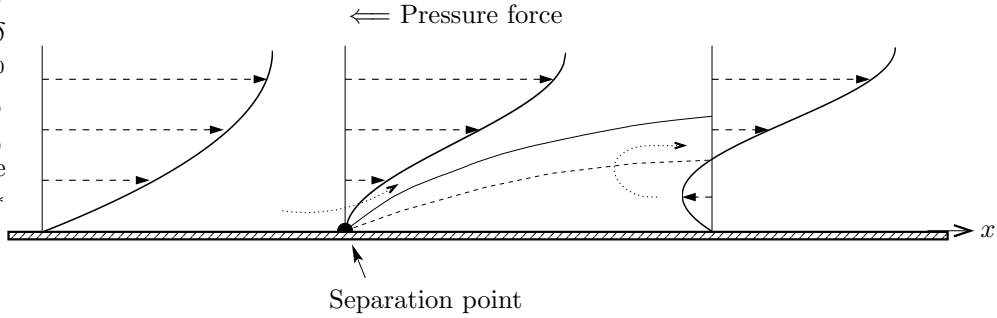Figure 2.29: The displacement thickness δ^*

Figure 2.30: Boundary layer separation caused by a pressure force directed upstream, a so called adverse pressure gradient.

$$\delta^* = \int_0^\infty \left(1 - \frac{u}{u_0}\right)\,\mathrm{d}y = \sqrt{\frac{\nu x}{u_0}}\int_0^\infty \left[1 - f'(\eta)\right]\,\mathrm{d}\eta$$

If we evaluate this expression for the Blasius boundary layer we have $\delta^* = 1.72\sqrt{\frac{\nu x}{u_0}}$.

A quantity which is of large importance in practical applications is the skin friction coefficient. The skin friction at the wall is

$$\tau_{\mathrm{w}} = \mu\frac{\partial u}{\partial y}\bigg|_{y=0} = \frac{\mu u_0}{\delta}f''(0) = \frac{\rho u_0^2}{\sqrt{\frac{u_0 x}{\nu}}}f''(0) = \frac{0.332\rho u_0^2}{\sqrt{Re_x}}$$

where the last term is the expression evaluated for Blasius flow. This can be used to evaluate the skin friction coefficient as

$$C_f = \frac{\tau_{\mathrm{w}}}{\frac{1}{2}\rho u_0^2} = \frac{0.664}{\sqrt{Re_x}}$$

where the last terms again is the Blasius value.

Boundary layer separation

A large adverse pressure gradient $\left(\frac{\partial p}{\partial x} > 0\right)$ may cause a back flow region close to wall, see figure 2.30.

The boundary layer equations cannot be integrated past a point of separation, since they become singular at that point. This can be seen from the following manipulations of the boundary layer equations. If we take the momentum equation

$$u\frac{\partial u}{\partial x} + v\frac{\partial u}{\partial y} = -\frac{1}{\rho}\frac{\mathrm{d}p}{\mathrm{d}x} + \nu\frac{\partial^2 u}{\partial y^2}$$

take the normal derivative and use continuity we have

$$u\frac{\partial^2 u}{\partial x\partial y} + v\frac{\partial^2 u}{\partial y^2} = \nu\frac{\partial^3 u}{\partial y^3}$$

If we again take the normal derivative and use continuity we can write this as

$$\frac{1}{2}\frac{\partial}{\partial x}\left(\frac{\partial u}{\partial y}\right)^2 + u\frac{\partial^3 u}{\partial x\partial y^2} - \frac{\partial u}{\partial x}\frac{\partial^2 u}{\partial y^2} + v\frac{\partial^3 u}{\partial y^3} = \nu\frac{\partial^4 u}{\partial y^4}$$

This expression evaluated at the wall, with the use of the boundary conditions, become

$$\frac{1}{2}\frac{\partial}{\partial x}\left(\left.\frac{\partial u}{\partial y}\right|_{y=0}\right)^2 = \nu \underbrace{\left.\frac{\partial^4 u}{\partial y^4}\right|_{y=0}}_{\pm\kappa^2}$$

which can be integrated to yield

$$\left(\left.\frac{\partial u}{\partial y}\right|_{y=0}\right)^2 = \pm\kappa^2 x + C$$

At the point of separation $x = x_s$, i.e. where $\left(\left.\frac{\partial u}{\partial y}\right|_{y=0} = 0\right)$ this expression is

$$\left.\frac{\partial u}{\partial y}\right|_{y=0} = \kappa\sqrt{x_s - x}$$

We can see that the boundary layer equations are not valid beyond point of separation since we have a square root singularity at that point. In addition, the point of separation is the limiting point after which there is back flow close to the wall. This means that there is information propagating upstream, invalidating the downstream parabolic nature of the equations assumed by the downstream integration of the equations.

In practical situations it is very important to be able to predict the point of separation, for example when an airfoil stalls and experience a severe loss of lift.

2.5 Turbulent flow

Reynolds average equations

Turbulent flow is inherently time dependent and chaotic. However, in applications one is not usually interested in knowing full the details of this flow, but rather satisfied with the influence of the turbulence on the averaged flow. For this purpose we define an ensemble average as

$$U_i = \overline{u}_i = \lim_{N \to \infty} \frac{1}{N} \sum_{n=1}^{N} u_i^{(n)}$$

where each member of the ensemble $u_i^{(n)}$ is regarded as an independent realization of the flow.

We are now going to derive an equation governing the mean flow U_i. Divide the total flow into an average and a fluctuating component u_i' as

$$u_i = \overline{u}_i + u_i' \qquad p = \overline{p} + p'$$

and introduce into the Navier-Stokes equations. We find

$$\frac{\partial u_i'}{\partial t} + \frac{\partial \overline{u}_i}{\partial t} + u_j'\frac{\partial \overline{u}_i}{\partial x_j} + \overline{u}_j\frac{\partial u_i'}{\partial x_j} + \overline{u}_j\frac{\partial \overline{u}_i}{\partial x_j} + u_j'\frac{\partial u_i'}{\partial x_j} = -\frac{1}{\rho}\frac{\partial p'}{\partial x_i} - \frac{1}{\rho}\frac{\partial \overline{p}}{\partial x_i} + \nu\nabla^2 u_i' + \nu\nabla^2 \overline{u}_i$$

We take the average of this equation, useing

$$\overline{u}_i' = 0 \qquad \overline{u_j'\overline{u}_i} = \overline{u}_i \cdot \overline{u_j'} = 0$$

which gives

$$\begin{cases} \dfrac{\partial \overline{u}_i}{\partial t} + \overline{u}_j\dfrac{\partial \overline{u}_i}{\partial x_j} = -\dfrac{1}{\rho}\dfrac{\partial \overline{p}}{\partial x_i} + \nu\nabla^2\overline{u}_i - \dfrac{\partial}{\partial x_j}\left(\overline{u_i'u_j'}\right) \\ \dfrac{\partial \overline{u}_i}{\partial x_i} = 0 \end{cases}$$

where the average of the continuity equation also has been added. Now, let $U_i = \overline{u}_i$, as above, and drop the $'$. We find the Reynolds average equations

$$\begin{cases} \dfrac{\partial U_i}{\partial t} + U_j \dfrac{\partial U_i}{\partial x_j} = -\dfrac{1}{\rho}\dfrac{\partial P}{\partial x_i} + \dfrac{\partial}{\partial x_j}\left(\tau_{ij} - \overline{u_i u_j}\right) \\ \dfrac{\partial U_i}{\partial x_i} \end{cases}$$

where $\overline{u_i u_j}$ is the Reynolds stress. Thus the effect of the turbulence on the mean is through an additional stress R_{ij} which explicitly written out is

$$[R_{ij}] = [\overline{u_i u_j}] = \begin{bmatrix} \overline{u^2} & \overline{uv} & \overline{uw} \\ \overline{uv} & \overline{v^2} & \overline{vw} \\ \overline{uw} & \overline{vw} & \overline{w^2} \end{bmatrix}$$

The diagonal component of this stress is the kinetic energy of the turbulent fluctuations

$$\overline{k} = R_{ii}/2 = \overline{u_i u_i}/2 = \frac{1}{2}\left(\overline{u^2} + \overline{v^2} + \overline{w^2}\right)$$

Turbulence modelling

One may derive equations for the components of the Reynolds stress tensor. However, they would involve additional new unknowns, and the equations for those would in turn involve even more unknowns. This closure problem implies that if one cannot calculate the complete turbulent flow, but is only interested in the mean, the effect of the Reynolds stress components on in the Reynolds average equations have to be modelled.

The simplest consistent model is to introduce a turbulent viscosity as a proportionality constant between the Reynolds stress components and the strain or deformation rate tensor, in analogy with the stress-strain relationship in for Newtonian fluids. We have

$$R_{ij} = \frac{2}{3}k\delta_{ij} - 2\nu_T \overline{E}_{ij}$$

The first term on the right hand side is introduced to give the correct value of the trace of R_{ij}. Here the deformation rate tensor is calculated based on the mean flow, i.e.

$$\overline{E}_{ij} = \frac{1}{2}\left(\frac{\partial U_i}{\partial x_j} + \frac{\partial U_j}{\partial x_i} - \frac{2}{3}\frac{\partial U_r}{\partial x_r}\delta{ij}\right)$$

where we have assumed incompressible flow. Introducing this into the Reynolds average equations gives

$$\frac{\partial U_i}{\partial t} + U_j \frac{\partial U_i}{\partial x_j} = \frac{\partial}{\partial x_j}\left[-\left(\frac{P}{\rho} + \frac{2}{3}k\right)\delta_{ij} + 2\left(\nu + \nu_T\right)\overline{E}_{ij}\right] = -\frac{1}{\rho}\frac{\partial P}{\partial x_i} + \left(\nu + \nu_T\right)\nabla^2 U_i$$

where the last equality assumes that ν_T is constant, an approximation only true for very simple turbulent flow. It is introduced here only to point out the analogy between the molecular viscosity and the turbulent viscosity.

The turbulent viscosity ν_T must be modelled and most numerical codes which solved the Navier-Stokes equations for practical applications uses some kind of model for ν_T.

For simple shear flows, i.e. velocity fields of the form $U(y)$, the main Reynolds stress component becomes

$$\overline{uv} = -\nu_T \frac{\partial U}{\partial y}$$

where, in analogy with kinetic gas theory, ν_T

$$\nu_T = u_T l$$

Here, u_T is a characteristic turbulent velocity scale and l is a characteristic turbulent length scale. In kinetic gas theory l would be the mean free path of the molecules and u_T the characteristic velocity of the molecules.
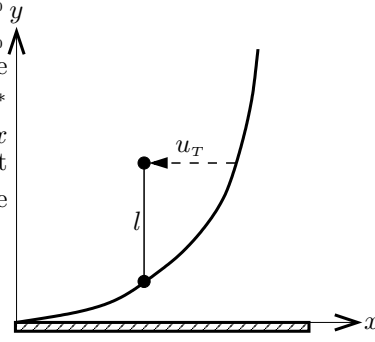
Figure 2.31: Prantdl's mixing length l is the length for which a fluid particle displaced in the normal direction can be expected to retain its horizontal momentum.

Zero-equation models

The simplest model for u_T and l is to model them algebraically.

In simple free shear flows like jets, wakes and shear layers we can take ν_T as constant in normal direction or y-direction and to vary in a self-similar manner in x.

In wall bounded shear flow we can take l as Prandtl's mixing length (1920's). This is a normal distance over which the particle retains its momentum and is depicted in figure 2.31.

We can thus evaluate u_T and find ν_T

$$u_T = l \left| \frac{\mathrm{d}U}{\mathrm{d}y} \right| \qquad \Rightarrow \qquad \nu_T = l^2 \left| \frac{\mathrm{d}U}{\mathrm{d}y} \right|$$

Define τ_w as the shear stress at the wall and $u_\tau = \sqrt{\tau_w/\rho}$ as the skin friction velocity. With

$$u_T = u_\tau, \qquad l = \kappa \cdot y$$

as Prandtl's estimation of mixing length we get

$$\frac{\mathrm{d}U}{\mathrm{d}y} = \frac{u_T}{l} = \frac{u_\tau}{\kappa y} \qquad \Rightarrow \qquad \frac{U}{u_\tau} = \frac{1}{\kappa} \ln y + C.$$

κ is the von Karman constant, approximately equal to 0.41. Thus the mixing length is proportional to the distant from the wall and the region close to the wall in a turbulent flow has a logarithmic velocity profile, called the log-region.

One-equation models

Instead of modelling the characteristic turbulent velocity algebraically, the next level of modelling uses the assumption that

$$u_T = \sqrt{k} = \sqrt{\frac{1}{2}\overline{u_i u_i}}$$

and a differential equation is used to calculate the turbulent kinetic energy. We can derive such an equation by taking the previously derived equation for $U_i + u_i$ and subtracting the equation for U, the Reynolds average equation. We find

$$\frac{\partial u_i}{\partial t} + U_j \frac{\partial u_i}{\partial x_j} = -u_j \frac{\partial U_i}{\partial x_j} - u_j \frac{\partial u_i}{\partial x_j} + \frac{\partial}{\partial x_j}\left(-\frac{p}{\rho}\delta_{ij} + \nu \frac{\partial u_i}{\partial x_j} + \overline{u_i u_j} \right)$$

We now take the average of the inner product between the turbulent fluctuations u_i and the above equation, and find

$$\frac{\partial}{\partial t}\left(\frac{1}{2}\overline{u_i u_i} \right) + U_j \frac{\partial}{\partial x_j}\left(\frac{1}{2}\overline{u_i u_i} \right) = -\overline{u_i u_j}\frac{\partial U_i}{\partial x_j} + \frac{\partial}{\partial x_j}\left(-\frac{\overline{pu_j}}{\rho} - \frac{1}{2}\overline{u_i u_i u_j} + \frac{\nu}{2}\frac{\partial}{\partial x_j}\overline{u_i u_i} \right) - \underbrace{\nu \overline{\frac{\partial u_i}{\partial x_j}\frac{\partial u_i}{\partial x_j}}}_{\epsilon}$$

where ϵ is the mean dissipation rate of the turbulent kinetic energy. We have now introduced a number of new unknowns which have to be modelled.

First, we model the Reynolds stress as previously indicated, i.e. $\overline{u_i u_j} = \frac{2}{3}\overline{k}\delta_{ij} - \nu_T \left(\frac{\partial U_i}{\partial x_j} + \frac{\partial U_j}{\partial x_i} \right)$.

Second, the turbulent dissipation is modelled purely based on dimension using $\overline{k}$ and l. We have

$$\epsilon = c_D \frac{\overline{k}^{3/2}}{l}$$

since the dimension of ϵ is $[\epsilon] = \frac{L^2}{T}$. Here c_D is a modelling constant.

Third, a gradient diffusion model is used for the transport terms, i.e.

$$-\frac{1}{2}\overline{u_i u_i u_j} - \frac{1}{\rho}\overline{p u_j} = \frac{\nu_T}{Pr_k}\frac{\partial \overline{k}}{\partial x_j}$$

where Pr_k is the turbulent Prandtl number.

For simplicity we write the resulting equation for the turbulent kinetic energy for constant ν_T. We find

$$
\underbrace{\frac{D\overline{k}}{Dt}}_{\text{rate of increase}} = \underbrace{(\nu + \nu_T)\nabla^2\overline{k}}_{\text{diffusion rate}} - \underbrace{\overline{u_i u_j}\frac{\partial U_i}{\partial x_j}}_{\text{generation rate}} - \underbrace{\epsilon}_{\text{dissipation rate}}
$$

Two-equation models

The most popular model in use in engineering applications is a two equation model, the so called $\overline{k}$-ϵ-model. This is based on the above model for $\overline{k}$ but instead of modelling ϵ a partial differential equation is derived governing the turbulent dissipation. This equation has the form as the equation for $\overline{k}$, with a diffusion term, a generation term and a dissipation term. Many new model constants need to be introduced in order to close the ϵ equation.

Once $\overline{k}$ and ϵ is calculated the turbulent viscosity is evaluated as a quotient of the two, such that the dimension is correct. We have

$$\Rightarrow \nu_T = C_\mu \cdot \frac{\overline{k}^2}{\epsilon}$$

where C_μ is a modelling constant.

T_0
U_0
Gradient fields
w_i
$\frac{\partial p}{\partial x_i}$
u_i

Chapter 3

Divergence free incompressible, tangent to boundary

L
h
x_1

Finite volume methods for incompressible flow

$p_0 > p_1$
p_1
$\mathbf{u}$
$\mathbf{n}$
$\mathrm{d}S$
$\mathbf{u} \cdot \mathbf{n} \Delta t$

3.1 Finite Volume method on arbitrary grids

Equations with 1st order derivatives: the continuity equation

u_0
p_0
$\eta = \frac{y}{\sqrt{4\nu t}}$

In finite volume methods one takes approximations of the differential equations in integral form. We start with an equation with only first order derivatives, the continuity equation. Recall that the integral from of this equation can be written

$u = u_0 \, \mathrm{erf} \frac{y}{\sqrt{4\nu t}}$

t
η
y

$$\int_V \frac{\partial}{\partial x_k} \left(u_k \right) \, \mathrm{d}V = \int_S u_k n_k \, \mathrm{d}S = 0$$

$\omega_z = \frac{\tilde{\omega}(\eta) \cdot u_0}{\sqrt{\pi \nu t}}$

Evaluating the normal vector n_i to the curve l for two-dimensional flow, see figure 3.1, we have the normal with length dl as $\mathbf{n}\,\mathrm{d}l = (\,\mathrm{d}y, -\,\mathrm{d}x)$. This implies that

$\}\delta$

$\omega \approx 0$
$U \rightarrow$
y, v

$$\int_S u_k n_k \, \mathrm{d}l = \int_S \left(u \, \mathrm{d}y - v \, \mathrm{d}x \right) = 0$$

We now apply this to an arbitrary two-dimensional grid defined as in figure 3.2.

We make use of the following definitions and approximations

x, u
L
U

$$u_{ab} \approx u_{i+\frac{1}{2},j} \approx \left(u_{i+1,j} + u_{i,j} \right)/2 \qquad \Delta x_{ab} = x_b - x_a$$

$\frac{\delta}{u_0}$

$\eta = \frac{y}{\sqrt{\nu x / u_0}}$

$$v_{ab} \approx v_{i+\frac{1}{2},j} \approx \left(v_{i+1,j} + v_{i,j} \right)/2 \qquad \Delta y_{ab} = y_b - y_a$$

$f' = \frac{u}{u_0}$

Blasius profile

δ^*
x
Separation point
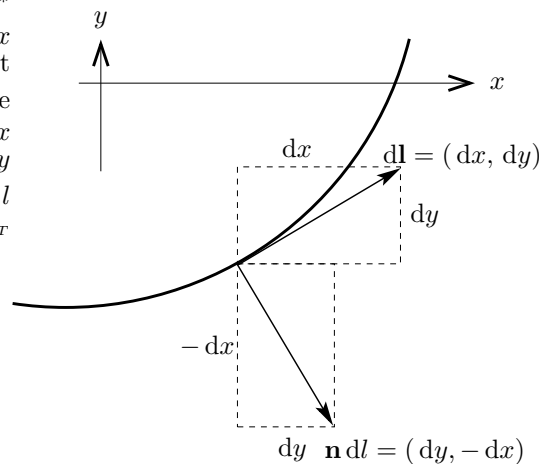$\Longleftarrow$ Pressure force
x
y
l
u_T

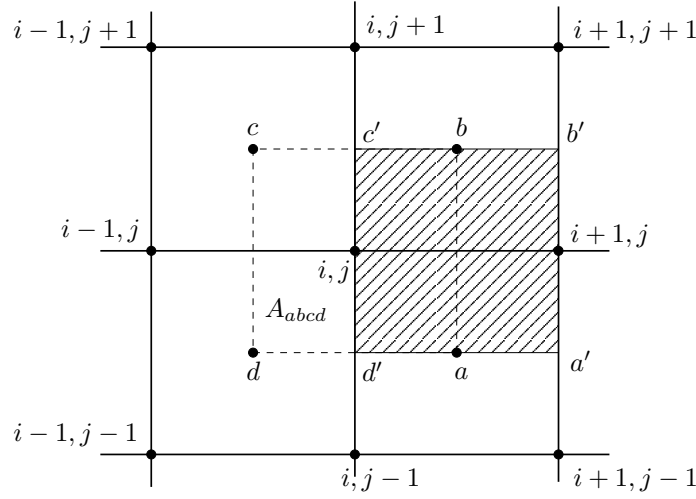Figure 3.1: Normal vector to the curve l.

Figure 3.2: Arbitrary grid. Note that the grid lines need not be parallel to the coordinate directions.

with analogous expressions for the quantities on the bc, cd and da faces. We can now evaluate the integral associated with the two-dimensional version of the continuity equation for the surface defined by the points $abcd$. We have

$$\int_S (u\,\mathrm{d}y - v\,\mathrm{d}x) \approx u_{i+\frac{1}{2},j}\Delta y_{ab} - v_{i+\frac{1}{2},j}\Delta x_{ab} + u_{i,j+\frac{1}{2}}\Delta y_{bc} - v_{i,j+\frac{1}{2}}\Delta x_{bc} +$$

$$u_{i-\frac{1}{2},j}\Delta y_{cd} - v_{i-\frac{1}{2},j}\Delta x_{cd} + u_{i,j-\frac{1}{2}}\Delta y_{da} - v_{i,j-\frac{1}{2}}\Delta x_{da}$$

On a cartesian grid we have the relations

$$\Delta x_{ab} = \Delta x_{cd} = \Delta y_{bc} = \Delta y_{da} = 0 \text{ and } \Delta y_{cd} = -\Delta y_{ab}, \Delta x_{bc} = -\Delta x_{da}$$

which implies that the approximation of the continuity equation can be written

$$\int_S (u\,\mathrm{d}y - v\,\mathrm{d}x) \approx \left(u_{i+\frac{1}{2},j} - u_{i-\frac{1}{2},j}\right)\Delta y_{ab} + \left(v_{i,j+\frac{1}{2}} + v_{i,j-\frac{1}{2}}\right)\Delta x_{da} =$$

$$\frac{1}{2}\left(u_{i+1,j} - u_{i-1,j}\right)\Delta y_{ab} + \frac{1}{2}\left(v_{i,j+1} - v_{i,j-1}\right)\Delta x_{da}$$

Note that dividing with $\Delta y_{ab} \cdot \Delta x_{da}$ gives a standard central difference discretization of the continuity equation, i.e.

$$\frac{u_{i+1,j} - u_{i-1,j}}{2\Delta x_{da}} + \frac{v_{i,j+1} - v_{i,j-1}}{2\Delta y_{ab}} = 0$$

Equations with 2nd derivatives: the Laplace equation

We use the Gauss or Greens theorem to derive the integral from of the two-dimensional Laplace equation. We find

$$0 = \int_V \frac{\partial^2 \Phi}{\partial x_j \partial x_j}\,\mathrm{d}V = \int_S \frac{\partial \phi}{\partial x_j}n_j\,\mathrm{d}S = \{2D\} = \int_S \left(\frac{\partial \Phi}{\partial x}\,\mathrm{d}y - \frac{\partial \Phi}{\partial y}\,\mathrm{d}x\right)$$

If we approximate this integral in the same manner as for the continuity equation we have

$$\left[\frac{\partial \Phi}{\partial x}\right]_{i+\frac{1}{2},j}\Delta y_{ab} - \left[\frac{\partial \Phi}{\partial y}\right]_{i+\frac{1}{2},j}\Delta x_{ab} + \left[\frac{\partial \Phi}{\partial x}\right]_{i,j+\frac{1}{2}}\Delta y_{bc} - \left[\frac{\partial \Phi}{\partial y}\right]_{i,j+\frac{1}{2}}\Delta x_{bc} +$$

$$\left[\frac{\partial \Phi}{\partial x}\right]_{i-\frac{1}{2},j}\Delta y_{cd} - \left[\frac{\partial \Phi}{\partial y}\right]_{i-\frac{1}{2},j}\Delta x_{cd} + \left[\frac{\partial \Phi}{\partial x}\right]_{i,j-\frac{1}{2}}\Delta y_{da} - \left[\frac{\partial \Phi}{\partial y}\right]_{i,j-\frac{1}{2}}\Delta x_{da}$$

First derivatives are evaluated as mean value over adjacent control volumes (areas in the two-dimensional case). We use Gauss theorem over the area defined by the points $a'b'c'd'$, see figure 3.2. For the three-dimensional case we have

$$\frac{1}{V} \int_V \frac{\partial \Phi}{\partial x_j} \, dV = \frac{1}{V} \int_S \Phi n_j \, dS \Rightarrow$$

which in the two-dimensional case is approximated by

$$\left(\left[\frac{\partial \Phi}{\partial x} \right]_{i+\frac{1}{2},j}, \left[\frac{\partial \Phi}{\partial y} \right]_{i+\frac{1}{2},j} \right) \approx \frac{1}{A_{a'b'c'd'}} \int_{a'b'c'd'} (\Phi \, dy, -\Phi \, dx)$$

where

$$\int_{a'b'c'd'} \Phi \, dy \approx \Phi_{i+1,j} \Delta y_{a'b'} + \Phi_b \Delta y_{b'c'} + \Phi_{i,j} \Delta y_{c'd'} + \Phi \Delta y_{d'a'}$$

and the area evaluated as half magnitude of cross products of diagonals, i.e.

$$A_{ab} \equiv A_{a'b'c'd'} = \frac{1}{2} \left| \Delta x_{d'b'} \cdot \Delta y_{a'c'} - \Delta y_{d'b'} \cdot \Delta x_{a'c'} \right|$$

and the value Φ_a is taken as the average

$$\Phi_a = \frac{1}{4} \left(\Phi_{i,j} + \Phi_{i+1,j} + \Phi_{i,j-1} + \Phi_{i+1,j-1} \right)$$

Evaluating the derivatives $\frac{\partial \Phi}{\partial x}, \frac{\partial \Phi}{\partial y}$ along the other cell faces and substituting back we obtain a 9 point formula which couples all of the nine points around the point i, j, of the form

$$
\begin{array}{ccccccccc}
A_{i,j} \Phi_{i+1,j+1} & + & B_{i,j} \Phi_{i+1,j} & + & C_{i,j} \Phi_{i+1,j-1} & + & D_{i,j} \Phi_{i,j+1} & + & E_{i,j} \Phi_{i,j} & + \\
F_{i,j} \Phi_{i,j-1} & + & G_{i,j} \Phi_{i-1,j+1} & + & H_{i,j} \Phi_{i-1,j} & + & I_{i,j} \Phi_{i-1,j-1} & = & 0 &
\end{array}
$$

If we have a total of $N = m \times n$ interior nodes, we obtain N equations which in matrix form can be written

$$A\mathbf{x} = \mathbf{b}$$

Here $\mathbf{x}^T = (\Phi_{11}, \Phi_{12}, \Phi_{13}, \ldots, \Phi_{mn})$ and $\mathbf{b}$ contains the boundary conditions. The matrix A is a $N \times N$ with the terms A_{ij}, B_{ij}, etc. as coefficients.

Rather than showing the general case in more detail, we instead work out the expression for cartesian grids in two-dimensions. We find

$$\int \left(\frac{\partial^2 \Phi}{\partial x^2} + \frac{\partial^2 \Phi}{\partial y^2} \right) dx \, dy = \int \left(\frac{\partial \Phi}{\partial x} \, dy - \frac{\partial \Phi}{\partial y} \, dx \right) \approx$$

$$\left(\left[\frac{\partial \Phi}{\partial x} \right]_{i+\frac{1}{2},j+} - \left[\frac{\partial \Phi}{\partial x} \right]_{i-\frac{1}{2},j} \right) \Delta y + \left(\left[\frac{\partial \Phi}{\partial y} \right]_{i,j+\frac{1}{2}} - \left[\frac{\partial \Phi}{\partial y} \right]_{i,j-\frac{1}{2}} \right) \Delta x$$

We can evaluate the derivatives as

$$\left[\frac{\partial \Phi}{\partial x} \right]_{i+\frac{1}{2},j} = (\Phi_{i+1,j} - \Phi_{i,j}) \Delta y \cdot \frac{1}{\Delta x \cdot \Delta y}$$

and so on for the rest of the terms, which implies that

$$\int \left(\frac{\partial \Phi}{\partial x} \, dy - \frac{\partial \Phi}{\partial y} \, dx \right) \approx (\Phi_{i+1,j} - 2\Phi_{i,j} + \Phi_{i-1,j}) \frac{\Delta y}{\Delta x} + (\Phi_{i,j+1} - 2\Phi_{i,j} + \Phi_{i,j-1}) \frac{\Delta x}{\Delta y}$$

Dividing with the area $\Delta x \cdot \Delta y$ we obtain the usual 5-point Laplace formula, i. e.

$$\frac{\Phi_{i+1,j} - 2\phi_{i,j} + \Phi_{i-1,j}}{\Delta x^2} + \frac{\Phi_{i,j+1} - 2\phi_{i,j} + \Phi_{i,j-1}}{\Delta y^2} = 0$$

which of course also can be written in the matrix form shown for the general case above.
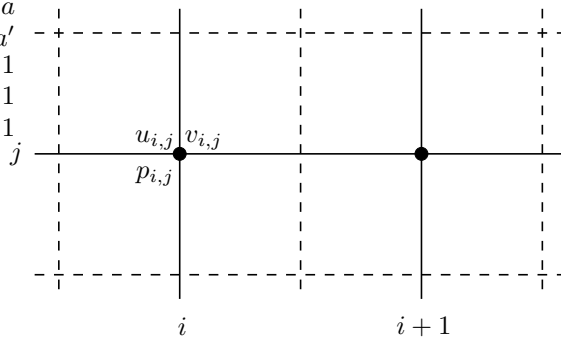
Figure 3.3: Cartesian finite-volume grid where the velocity components and the pressure are co-located.

3.2 Finite-volume discretizations of 2D NS

Co-located Cartesian grid

We will apply the finite volume discretizations to the Navier-Stokes equations in integral form, which in two-dimensions can be written

$$\int \left(u \, \mathrm{d}y - v \, \mathrm{d}x \right) = 0$$

$$\iint \frac{\partial u}{\partial t} \, \mathrm{d}S = - \int \left[u^2 \, \mathrm{d}y - uv \, \mathrm{d}x + p \, \mathrm{d}y - \frac{1}{Re} \left(\frac{\partial u}{\partial x} \, \mathrm{d}y - \frac{\partial u}{\partial y} \, \mathrm{d}x \right) \right]$$

$$\iint \frac{\partial v}{\partial t} \, \mathrm{d}S = - \int \left[uv \, \mathrm{d}y - v^2 \, \mathrm{d}x - p \, \mathrm{d}x - \frac{1}{Re} \left(\frac{\partial v}{\partial x} \, \mathrm{d}y - \frac{\partial v}{\partial y} \, \mathrm{d}x \right) \right]$$

where we have used the earlier derived result $\mathbf{n} = (\, \mathrm{d}y, -\, \mathrm{d}x)$. We start with a co-located grid which means that the finite volume used for both velocity components and the pressure is the same, see figure 3.3. In addition we choose a Cartesian grid in order to simplify the expressions. Recall that the finite volume discretization of the continuity equation becomes

$$\frac{1}{2} \left(u_{i+1,j} - u_{i-1,j} \right) \Delta y + \frac{1}{2} \left(v_{i,j+1} - v_{i,j-1} \right) \Delta x = 0$$

which is equivalent to the finite difference discretization

$$\text{or} \qquad \frac{u_{i+1,j} - u_{i-1,j}}{2\Delta x} + \frac{v_{i,j+1} - v_{i,j-1}}{2\Delta y} = 0$$

The discretization of the streamwise momentum equation needs both first and second derivatives. We have seen that the finite volume discretizations of both are equal to standard second order finite difference approximations. Thus we obtain the following result for the u-component

$$\frac{\partial u_{i,j}}{\partial t} + \frac{u_{i+1,j}^2 - u_{i-1,j}^2}{2\Delta x} + \frac{(uv)_{i,j+1} - (uv)_{i,j-1}}{2\Delta y} + \frac{p_{i+1,j} - p_{i-1,j}}{2\Delta x}$$

$$- \frac{1}{Re} \left(\frac{u_{i+1,j} - 2u_{i,j} + u_{i-1,j}}{\Delta x^2} + \frac{u_{i,j+1} - 2u_{i,j} + u_{i,j-1}}{\Delta y^2} \right) = 0$$

In a similar manner the discretization for the v-component becomes

$$\frac{\partial v_{i,j}}{\partial t} + \frac{(uv)_{i+1,j} - (uv)_{i-1,j}}{2\Delta x} + \frac{v_{i,j+1}^2 - v_{i,j-1}^2}{2\Delta y} + \frac{p_{i,j+1} - p_{i,j-1}}{2\Delta y}$$

$$- \frac{1}{Re} \left(\frac{v_{i+1,j} - 2v_{i,j} + v_{i-1,j}}{\Delta x^2} + \frac{v_{i,j+1} - 2v_{i,j} + v_{i,j-1}}{\Delta y^2} \right) = 0$$

This simple discretization cannot be used in practice without some kind of modification. The reason is that one solution to these equations are in the form of spurious checkerboard modes. Consider the following solution to the discretized equations

$$u_{i,j} = v_{i,j} = (-1)^{i+j} \cdot g(t), \qquad p = (-1)^{i+j}, \qquad \Delta x = \Delta y$$
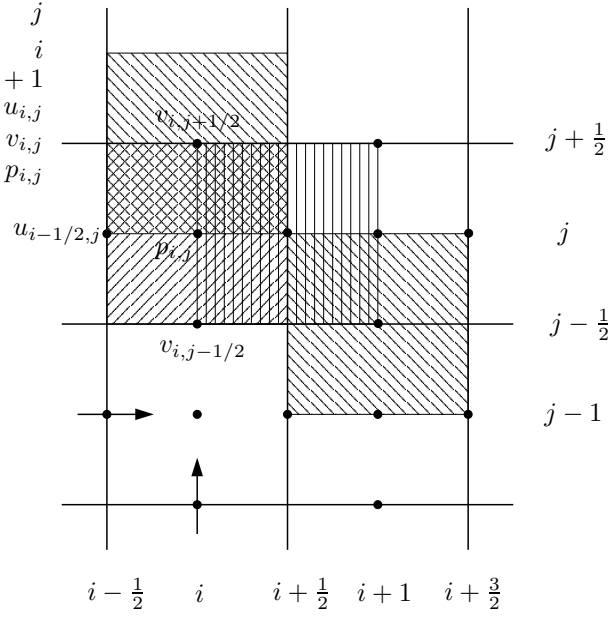
Figure 3.4: Cartesian finite-volume grid where the velocity components and the pressure uses staggered grids.

which satisfies the divergence constraint. If it is input into the equation for u and v we find the expression

$$\frac{\mathrm{d}g}{\mathrm{d}t} + \frac{8}{Re \cdot \Delta x^2} g = 0 \qquad \Rightarrow \qquad g = e^{-\frac{8t}{Re \cdot \Delta x^2}}$$

Thus we have a spurious solution consisting of checkerboard modes which are damped slowly for velocity and constant in time for the pressure. This mode will corrupt any true numerical solution and yields this discretization unusable as is. These modes are a result of the very weak coupling between nearby finite volumes or grid points, and can be avoided if they are coupled by one sided differences or if they are damped with some type of artificial viscosity.

Staggered cartesian grid

To eliminate the problem with spurious checkerboard modes, we can use a staggered grid as in figure 3.4, where the control volumes for the streamwise, spanwise and pressure are different.

The control volume for the continuity equation is centered abound the pressure point and the discretization becomes

$$\left(u_{i+\frac{1}{2},j} - u_{i-\frac{1}{2},j}\right)\Delta y + \left(v_{i,j+\frac{1}{2}} - v_{i,j-\frac{1}{2}}\right)\Delta x = 0$$

$$\text{or} \qquad \frac{u_{i+\frac{1}{2},j} - u_{i-\frac{1}{2},j}}{\Delta x} + \frac{v_{i,j+\frac{1}{2}} - v_{i,j-\frac{1}{2}}}{\Delta y} = 0$$

The control volume for the streamwise velocity is centered around the streamwise velocity point and the discretization becomes

$$\frac{\partial u_{i+1/2,j}}{\partial t} + \frac{u_{i+1,j}^2 - u_{i,j}^2}{\Delta x} + \frac{(uv)_{i+1/2,j+1/2} - (uv)_{i+1/2,j-1/2}}{\Delta y} + \frac{p_{i+1,j} - p_{i,j}}{\Delta x} -$$

$$\frac{1}{Re}\frac{u_{i+3/2,j} - 2u_{i+1/2,j} + u_{i-1/2,j}}{\Delta x^2} - \frac{1}{Re}\frac{u_{i+1/2,j+1} - 2u_{i+1/2,j} + u_{i+1/2,j-1}}{\Delta y^2} = 0$$
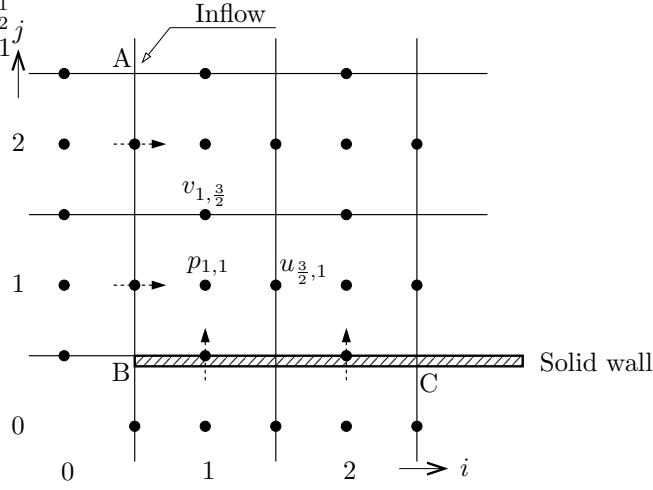
Figure 3.5: Staggered grid near the boundary.

where the $u_{i+1,j}^2, u_{i,j}^2, (uv)_{i+1/2,j+1/2}, (uv)_{i+1/2,j-1/2}$ terms need to be interpolated from the points where the corresponding velocities are defined.

The control volume for the normal velocity is centered around the normal velocity point and the discretization becomes

$$\frac{\partial v_{i,j+1/2}}{\partial t} + \frac{(uv)_{i+1/2,j+1/2} - (uv)_{i-1/2,j+1/2}}{\Delta x} + \frac{v_{i,j+1}^2 - v_{i,j}^2}{\Delta y} + \frac{p_{i,j+1} - p_{i,j}}{\Delta y} -$$

$$\frac{1}{Re} \frac{v_{i+1,j+1/2} - 2v_{i,j+1/2} + v_{i-1,j+1/2}}{\Delta x^2} - \frac{1}{Re} \frac{v_{i,j+3/2} - 2v_{i,j+1/2} + v_{i,j-1/2}}{\Delta y^2} = 0$$

where the $(uv)_{i+1/2,j+1/2}, (uv)_{i-1/2,j+1/2}, u_{i,j+1}^2, u_{i,j}^2$ terms need to be interpolated from the points where the corresponding velocities are defined.

For this discretization no checkerboard modes possible, since there is no decoupling in the divergence constraint, the pressure or the convective terms.

Boundary conditions

To close the system we need to augment the discretized equation with discrete versions of the boundary conditions. See figure 3.5 for a definition of the points near a boundary.

The boundary conditions on the solid wall, BC in figure 3.5, consists of the no flow and the no slip conditions, i.e. $u = v = 0$. The normal points are located on the boundary so that the no flow condition simply become

$$v_{1,\frac{1}{2}} = v_{2,\frac{1}{2}} = \cdots = 0$$

The evaluation of the u-equation at the point $(\frac{3}{2}, 1)$, for example, requires $u_{\frac{3}{2},0}$. We can find this value as follows

$$0 = u_{\frac{3}{2},\frac{1}{2}} = \frac{1}{2}\left(u_{\frac{3}{2},1} + u_{\frac{3}{2},0}\right) \qquad \Rightarrow \qquad u_{\frac{3}{2},0} = -u_{\frac{3}{2},1}$$

The boundary conditions on the inflow, AB in figure 3.5, consist given values of u and v, i.e. so called Dirichlet conditions. The streamwise points are located on the boundary so that the boundary condition is simply consist of the known values

$$u_{\frac{1}{2},1}, u_{\frac{1}{2},2}, \ldots$$

The evaluation of the v-equation at the point $(1, \frac{3}{2})$, for example, requires $v_{0,\frac{3}{2}}$. We can find this value as follows

$$v_{\frac{1}{2},\frac{3}{2}} = \frac{1}{2}\left(v_{1,\frac{3}{2}} + v_{0,\frac{3}{2}}\right) \qquad \Rightarrow \qquad v_{0,\frac{3}{2}} = 2v_{\frac{1}{2},\frac{3}{2}} - v_{1,\frac{3}{2}}$$

If AB in figure 3.5 is an outflow boundary, the boundary conditions may consist of $\frac{\partial u}{\partial x} = \frac{\partial v}{\partial x} = 0$, i.e. so called Neumann conditions. These conditions should be evaluated at $i = \frac{1}{2}$. For the streamwise and normal velocity we find

$$u_{-\frac{1}{2},2} = u_{\frac{3}{2},2}, \qquad v_{0,\frac{3}{2}} = v_{1,\frac{3}{2}}$$

Note that no reference is made to the pressure points outside the domain, so that in this formulation no boundary conditions for p is needed so far. However, depending on the particular discretization of the time derivative and other the details of the solution method one may need to augment the the above with boundary conditions for the pressure. If this is the case particular care has to be taken so that those conditions do not upset the divergence free condition.

3.3   Summary of the equations

The discretized equations derived for the staggered grid can be written in the following form

$$
\begin{cases}
\dfrac{\partial u_{i+\frac{1}{2},j}}{\partial t} + A_{i+\frac{1}{2},j} + \dfrac{p_{i+1,j} - p_{i,j}}{\Delta x} = 0 \\[2mm]
\dfrac{\partial v_{i,j+\frac{1}{2}}}{\partial t} + B_{i,j+\frac{1}{2}} + \dfrac{p_{i,j+1} - p_{i,j}}{\Delta y} = 0 \\[2mm]
D_{i,j} = 0
\end{cases}
$$

where the expression for the $A_{i+\frac{1}{2},j}$ can be written

$$A_{i+\frac{1}{2},j} =$$

$$
= \frac{u_{i+1,j}^2 - u_{i,j}^2}{\Delta x} + \frac{(uv)_{i+\frac{1}{2},j+\frac{1}{2}} - (uv)_{i+\frac{1}{2},j-\frac{1}{2}}}{\Delta y}
$$

$$
- \frac{1}{Re}\frac{u_{i+\frac{3}{2},j} - 2u_{i+\frac{1}{2},j} + u_{i-\frac{1}{2},j}}{\Delta x^2} - \frac{1}{Re}\frac{u_{i+\frac{1}{2},j+1} - 2u_{i+\frac{1}{2},j} + u_{i+\frac{1}{2},j-1}}{\Delta y^2}
$$

$$= \{\text{expand and interpolate using grid values}\}$$

$$
= \left[\frac{1}{2\Delta x}(u_{i+\frac{3}{2},j} - u_{i-\frac{1}{2},j}) + \frac{1}{4\Delta y}(v_{i+1,j+\frac{1}{2}} - v_{i,j+\frac{1}{2}} - v_{i+1,j-\frac{1}{2}} - v_{i,j-\frac{1}{2}}) + \frac{2}{Re}\left(\frac{1}{\Delta x^2} + \frac{1}{\Delta y^2}\right)\right] u_{i+\frac{1}{2},j}
$$

$$
+ \left(\frac{1}{4\Delta x}u_{i+\frac{3}{2},j} - \frac{1}{Re\Delta x^2}\right) u_{i+\frac{3}{2},j} + \left(\frac{1}{4\Delta x}u_{i-\frac{1}{2},j} - \frac{1}{Re\Delta x^2}\right) u_{i-\frac{1}{2},j}
$$

$$
+ \left(\frac{1}{4\Delta y}(v_{i+1,j+\frac{1}{2}} + v_{i,j+\frac{1}{2}}) - \frac{1}{Re\Delta y^2}\right) u_{i+\frac{1}{2},j+1} + \left(\frac{1}{4\Delta y}(v_{i+1,j-\frac{1}{2}} + v_{i,j-\frac{1}{2}}) - \frac{1}{Re\Delta y^2}\right) u_{i+\frac{1}{2},j-1}
$$

$$
= a(u,v)_{i+\frac{1}{2},j}u_{i+\frac{1}{2},j} + \sum_{nb} a(u,v)_{nb}u_{nb}
$$

The last line summarizes the expressions, where the sum over nb indicates a sum over the nearby nodes. The expression for $B_{i,j+\frac{1}{2}}$ can in a similar way be written

$$B_{i,j+\frac{1}{2}} =$$

$$
= \frac{(uv)_{i+\frac{1}{2},j+\frac{1}{2}} - (uv)_{i-\frac{1}{2},j+\frac{1}{2}}}{\Delta x} + \frac{v_{i,j+1}^2 - v_{i,j}^2}{\Delta y}
$$

$$
- \frac{1}{R}\frac{v_{i+1,j+\frac{1}{2}} - 2v_{i,j+\frac{1}{2}} + v_{i-1,j+\frac{1}{2}}}{\Delta x^2} - \frac{1}{R}\frac{v_{i,j+\frac{3}{2}} - 2v_{i,j+\frac{1}{2}} + v_{i,j-\frac{1}{2}}}{\Delta y^2}
$$

$$= \{\text{expand and interpolate using grid values}\}$$

$$
= b(u,v)_{i,j+\frac{1}{2}}v_{i,j+\frac{1}{2}} + \sum_{nb} b(u,v)_{nb}v_{nb}
$$

where the expressions for $b(u,v)_{i,j+\frac{1}{2}}$ and $b(u,v)_{nb}$ are analogous to $a(u,v)_{i+\frac{1}{2},j}$ and $a(u,v)_{nb}$, and therefore not explicitly written out. The expression originating from the continuity equation is

$$D_{i,j} = \frac{u_{i+\frac{1}{2},j} - u_{i-\frac{1}{2},j}}{\Delta x} + \frac{v_{i,j+\frac{1}{2}} - v_{i,j-\frac{1}{2}}}{\Delta y}$$

These equations, including the boundary conditions, can be assembled into matrix form. We have

$$\frac{\mathrm{d}}{\mathrm{d}t} \begin{pmatrix} u \\ v \\ 0 \end{pmatrix} + \begin{pmatrix} A(u,v) & 0 & G_x \\ 0 & B(u,v) & G_y \\ D_x & D_y & 0 \end{pmatrix} \begin{pmatrix} u \\ v \\ p \end{pmatrix} = \begin{pmatrix} f_u \\ f_v \\ 0 \end{pmatrix}$$

Here we we have used the definitions

u	-	vector of unknown streamwise velocities
v	-	vector of unknown normal velocities
p	-	vector of pressure unknowns
$A(u,v)$	-	non-linear algebraic operator from advective and viscous terms of u-eq.
$B(u,v)$	-	non-linear algebraic operator from advective and viscous terms of v-eq.
G_x	-	linear algebraic operator from stremwise pressure gradient
G_y	-	linear algebraic operator from normal pressure gradient
D_x	-	linear algebraic operator from x-part of divergence constraint
D_y	-	linear algebraic operator from y-part of divergence constraint
f	-	vector of source terms from BC

With obvious changes in notation, we can write the system of equations in an even more compact form as

$$\frac{\mathrm{d}}{\mathrm{d}t} \begin{pmatrix} u \\ 0 \end{pmatrix} + \begin{pmatrix} N(u) & G \\ D & 0 \end{pmatrix} \begin{pmatrix} u \\ p \end{pmatrix} = \begin{pmatrix} f \\ 0 \end{pmatrix}$$

If this is compared to the finite element discretization in the next chapter, it is seen that the form of the discretized matrix equations are the same.

3.4 Time dependent flows

The projection method

For time-dependent flow a common way to solve the discrete equations is the projection or pressure correction method. Sometimes this method and its generalizations are also called splitting methods. We illustrate the method using the system written in the compact notation defined above.

We start to discretize the time derivative with a first order explicit method

$$\begin{cases} \dfrac{u^{n+1} - u^n}{\Delta t} + N(u^n)\,u^n + G\,p^{n+1} = f(t^n) \\[2ex] Du^{n+1} = 0 \end{cases}$$

Then we make a prediction of the velocity field at the next time step u^* not satisfying continuity, and then a correction involving p such that $Du^{n+1} = 0$. We have

$$\begin{cases} \dfrac{u^* - u^n}{\Delta t} + N(u^n)\,u^n = f(t^n) \\[2ex] \dfrac{u^{n+1} - u^*}{\Delta t} + G\,p^{n+1} = 0 \\[2ex] Du^{n+1} = 0 \end{cases}$$

Next, apply the divergence operator D to the correction step

$$DG\,p^{n+1} = \frac{1}{\Delta t} D\,u^*$$

Here DG represents $divgrad$ = Laplacian, i.e. discrete version of pressure Poisson equation. The velocity at the next time level thus becomes

$$u^{n+1} = u^* - \Delta t\, G\, p^{n+1}$$

Note here that u^{n+1} is projection of u^* on divergence free space. This is a discrete version of the projection of a function on a divergence free space discussed in the section about the role of the pressure in incompressible flow.

In order to be able to discuss the boundary condition on the pressure Poisson equation we write the prediction and correction step more explicitly. Using the staggered grid discretization the prediction step can be written

$$\begin{cases} \dfrac{u^*_{i+\frac{1}{2},j} - u^n_{i+\frac{1}{2},j}}{\Delta t} + A^n_{i+\frac{1}{2},j} = 0 \\[2ex] \dfrac{v^*_{i,j+\frac{1}{2}} - v^n_{i,j+\frac{1}{2}}}{\Delta t} + B^n_{i,j+\frac{1}{2}} = 0 \end{cases}$$

and the projection step as

$$\begin{cases} \dfrac{u^{n+1}_{i+\frac{1}{2},j} - u^*_{i+\frac{1}{2},j}}{\Delta t} + \dfrac{p^{n+1}_{i+1,j} - p^{n+1}_{i,j}}{\Delta x} = 0 \\[2ex] \dfrac{v^{n+1}_{i,j+\frac{1}{2}} - v^*_{i,j+\frac{1}{2}}}{\Delta t} + \dfrac{p^{n+1}_{i,j+1} - p^{n+1}_{i,j}}{\Delta y} = 0 \end{cases}$$

By solving for $u^{n+1}_{i+\frac{1}{2},j}$ and $v^{n+1}_{i,j+\frac{1}{2}}$ above and using this, and the corresponding expressions for $u^{n+1}_{i-\frac{1}{2},j}$ and $v^{n+1}_{i,j-\frac{1}{2}}$, in the expression for the divergence constraint $D_{i,j}$ we find the following explicit expression for the discrete pressure Poisson equation

$$\frac{p^{n+1}_{i+1,j} - 2p^{n+1}_{i,j} + p^{n+1}_{i-1,j}}{\Delta x^2} + \frac{p^{n+1}_{i,j+1} - 2p^{n+1}_{i,j} + p^{n+1}_{i,j-1}}{\Delta y^2} = \frac{D^*_{i,j}}{\Delta t}$$

where $D^*_{i,j}$ is $D_{i,j}$ evaluated using the discrete velocities at the prediction step, u^* and v^*.

When the discrete pressure Poisson equation is solved we need values of the unknowns which are outside of the domain, i.e. we need additional boundary conditions. If we take the vector equation for the correction or projection step and project it normal to the solid boundary in figure 3.5 we have

$$\frac{p^{n+1}_{2,1} - p^{n+1}_{2,0}}{\Delta y} = -\frac{1}{\Delta t}\left(v^{n+1}_{2,\frac{1}{2}} - v^*_\Gamma\right)$$

where $v^*_\Gamma = v^*_{2,\frac{1}{2}}$ is an unknown value of the velocity in the prediction step at the boundary. In general it is important to choose this boundary condition such that discrete velocity after the correction step is divergence at the boundary, see the discussion in the end of the section on the role of the pressure. However, for this particular discretization it turns out that we can choose v^*_Γ arbitrarily since it completely decouples from the rest of the discrete problem. To see this we write the pressure Poisson equation, centered abound the point (2,1), close to the boundary. We find

$$\frac{p^{n+1}_{3,1} - 2p^{n+1}_{2,1} + p^{n+1}_{1,1}}{\Delta x^2} + \frac{p^{n+1}_{2,2} - 2p^{n+1}_{2,1} + p^{n+1}_{2,0}}{\Delta y^2} = \frac{1}{\Delta t}\left(\frac{u^*_{\frac{5}{2},1} - u^*_{\frac{3}{2},1}}{\Delta x} + \frac{v^*_{2,\frac{3}{2}} - v^*_\Gamma}{\Delta y}\right)$$

if we substitute the value of $p^{n+1}_{2,1} - p^{n+1}_{2,0}$ from the boundary condition obtained for the pressure into the above equation we can se that v^*_Γ cancels in the right hand side of the pressure Poisson equation. Since the discretization of the time derivative is explicit there is no other place where the values of v^* or u^* on the boundaries enter. Thus we find that we can choose the value of v^*_Γ arbitrarily. In particular, we can choose $v^*_\Gamma = v^{n+1}_{2,\frac{1}{2}}$, in which case we obtain a Neumann boundary condition for the pressure. Note, however, that this is a numerical artifact and does not imply that the real pressure gradient is zero at the boundary.

A number of other splitting methods have been devised for schemes with higher order accuracy for the time discretization. In general it is preferred to make the time discretization first for the full Navier-Stokes equations and afterward split the discrete equation into one predictor and one corrector step. See Peyret and Taylor for details.

Time step restriction

For stability it is necessary that prediction step is stable, numerical evidence indicates that this is sufficient. In the predictor case the momentum equations decouple if we linearize them abound the solution U_0, V_0. It thus suffices to consider the equation

$$\frac{\partial u}{\partial t} + U_0 \frac{\partial u}{\partial x} + V_0 \frac{\partial u}{\partial y} = \frac{1}{Re} \nabla^2 u$$

For simplicity we will here consider one-dimensional version

$$\frac{\partial u}{\partial t} + U_0 \frac{\partial u}{\partial x} = \frac{1}{Re} \frac{\partial^2 u}{\partial x^2}$$

which in discretized form can be written

$$u_j^{n+1} = u_j^n + \Delta t \left[-U_0 \frac{u_{j+1}^n - u_{j-1}^n}{2\Delta x} + \frac{1}{Re} \frac{u_{j+1}^n - 2u_j^n + u_{j-1}^n}{\Delta x^2} \right]$$

where we have chosen to call the discrete points where the u-velocity is evaluate for x_j. We introduce

$$u_j^n = Q^n \cdot e^{i \cdot \omega x_j}$$

into the discrete equation, together with the definitions

$$\lambda = \frac{U_0 \Delta t}{\Delta x}, \qquad \alpha = \frac{2\Delta t}{Re \, \Delta x^2}, \qquad \xi = \omega \cdot \Delta x$$

This implies that the amplification factor Q can be written

$$Q = 1 - i\lambda \sin(\xi) - 2\alpha \sin^2\left(\frac{\xi}{2}\right)$$

We find that the absolute value of Q satisfies

$$
\begin{aligned}
|Q| &= 1 - 4\left(\lambda^2 - \alpha^2\right) s^2 + 4\left(\lambda^2 - s^2\right) s \\
&= 1 - 4s\left[\left(\lambda^2 - \alpha^2\right) s - \lambda^2 + \alpha\right] \leq 1
\end{aligned}
$$

where $s = \sin^2\left(\frac{\xi}{2}\right)$. This implies that

$$\Phi(s) = -\left(\lambda^2 - \alpha^2\right) s + \lambda^2 - \alpha \leq 0 \qquad \forall s : 0 \leq s \leq 1$$

$\Phi(s)$ is linear function of s and thus the the limiting condition on $\Phi(s)$ is given by its values at the two end points of the s-interval. We find

$$\Phi(0) = \lambda^2 - \alpha \leq 0, \qquad \Phi(1) = \alpha^2 - \alpha \leq 0$$

which implies that

$$\Rightarrow \qquad \lambda^2 \leq \alpha \leq 1$$

substituting back the definitions of λ and α we find the following stability conditions

$$
\begin{cases}
\frac{1}{2} U_0^2 \Delta t Re & \leq \quad 1 \\
\frac{2\Delta t}{Re \Delta x^2} & \leq \quad 1
\end{cases}
$$

For the two dimensional version of the predictor step Peyret and Taylor [8] find the following stability limits

$$
\begin{cases}
\frac{1}{4}\left(U_0^2 + V_0^2\right) \Delta t \cdot Re & \leq \quad 1 \\
\frac{4\Delta t}{Re \Delta x^2} & \leq \quad 1
\end{cases}
$$

Note that this is a stronger condition than in the one-dimensional case.

3.5 General iteration methods for steady flows

Distributive iteration

For steady flows we can still use the methods introduced for unsteady flows, and iterate the solution in time to obtain a steady state. However, in many cases it is more effective to use other iteration methods. We will here introduce a general distributive iteration method and apply it to the discretized steady Navier-Stokes equations.

For the steady case the discretized equations can be written in the form

$$\left(\begin{array}{cc} N(u) & G \\ D & 0 \end{array} \right) \left(\begin{array}{c} u \\ p \end{array} \right) = \left(\begin{array}{c} f \\ 0 \end{array} \right)$$

which is of the form $A\,y = b$. Now, let $y = B\,\hat{y}$ which implies that

$$AB\,\hat{y} = b$$

and use the iteration scheme on this modified equation. We divide the matrix AB in the following manner

$$AB = M - T \qquad \Rightarrow \qquad M\,\hat{y} = T\hat{y} + b$$

and use this to define the iteration scheme

$$MB^{-1}\,y^{k+1} = TB^{-1}\,y^k + b = MB^{-1}\,y^k + b - A\,y^k$$

which can be simplified to

$$y^{k+1} = y^k + BM^{-1} \underbrace{\left(b - A\,y^k \right)}_{r^k}$$

where r^k is the residual error in the k:th step of the iteration procedure.

If $B = I$ we obtain a regular iteration method where residual r^k is used to update y^k by inverting M, a simplified part of A, as in the Gauss-Seidell method for example. For this method we have

$$\begin{aligned} A\,x &= b \\ A &= L - U \\ (L - U)\,x &= b \\ L\,x^{n+1} &= U\,x^n + b \end{aligned}$$

Application to the steady Navier-Stokes equations

When the distributive iteration method is applied to the steady Naiver-Stokes we have

$$A = \left(\begin{array}{cc} N(u) & G \\ D & 0 \end{array} \right)$$

we can obtain AB in the following block triangular form

$$AB = \left(\begin{array}{cc} N(u) & 0 \\ D & -DN(u)^{-1}G \end{array} \right)$$

if the matrix B has the form

$$B = \left(\begin{array}{cc} I & -N(u)^{-1}G \\ 0 & I \end{array} \right) \approx \left(\begin{array}{cc} I & -\tilde{N}(u)^{-1}G \\ 0 & I \end{array} \right)$$

where $\tilde{N}(u)^{-1}$ is a simple approximation of the inverse of the discrete Navier-Stokes operator. We now split $AB = M - T$ where

$$M = \left(\begin{array}{cc} Q & 0 \\ D & R \end{array} \right)$$

and where Q is an approximation of $N(u)$ and R is an approximation of $-DN^{-1}G$. Note that R is a discrete Laplace like operator.

The SIMPLE (Semi-Implicit Method for Pressure Linked Equations) by Pantankar and Spalding (1972) can be thought of as a distributive iteration method. Wesseling [10] indicates that by choosing

$$\begin{aligned}
\tilde{N}(u)^{-1} &= [\text{diag}N(u^k)]^{-1} \\
Q &= N(u^k) \\
R &= -D[\text{diag}N(u^k)]^{-1}G
\end{aligned}$$

we have a method which is essentially the original version of the SIMPLE method. Thus we have the following iteration steps

1. First, we calculate the residual

$$b - A\,y^k = \begin{pmatrix} f \\ 0 \end{pmatrix} - \begin{pmatrix} N(u^k) & G \\ D & 0 \end{pmatrix}\begin{pmatrix} u^k \\ p^k \end{pmatrix} = \begin{pmatrix} r_1^k \\ r_2^k \end{pmatrix}$$

2. Second, we calculate $M^{-1}r^k$ which implies

$$Q\,\delta\tilde{u} = r_1^k \quad \Rightarrow \quad \delta\tilde{u} = Q^{-1}\,r_1^k$$

$$R\,\delta\tilde{p} = r_2^k - D\,\delta\tilde{u}$$

3. Third, we have the distribution step $BM^{-1}\,r^k$ which becomes

$$\begin{pmatrix} \delta u \\ \delta p \end{pmatrix} = B\begin{pmatrix} \delta\tilde{u} \\ \delta\tilde{p} \end{pmatrix} = \begin{pmatrix} \delta\tilde{u} - \tilde{N}^{-1}G\,\delta\tilde{p} \\ \delta\tilde{p} \end{pmatrix}$$

4. Fourth, there is an under relaxation step, where the velocities and the pressure is updated

$$\begin{cases} u^{k+1} = u^k + \omega_u\delta u \\ p^{k+1} = p^k + \omega_p\delta p \end{cases}$$

The under relaxation is needed for the method to converge, thus ω_u and ω_p is usually substantially lower that one.

Chapter 4

Finite element methods for incompressible flow

The finite-element method (FEM) approximates an integral form of the governing equations. However, the integral form—called the *variational form*—is usually different from the one used for the finite-volume method. Moreover, different integral forms may be used for the same equation depending on circumstances such as boundary conditions. We introduce FEM first for a scalar advection–diffusion problem before discussing the Navier–Stokes equations.

4.1 FEM for an advection–diffusion problem

We consider the steady flow of an incompressible fluid in a bounded domain Ω, and we assume that its velocity field U_j is known (from a previous numerical solution, for instance). We assume that the boundary Γ of the domain can be decomposed into two portions Γ_0 and Γ_1, as in figure 4.1 for instance. We are interested to compute the temperature field u in the domain, modeled by the advection–diffusion problem

$$U_j \frac{\partial u}{\partial x_j} - \nu \nabla^2 u = f \qquad \text{in } \Omega, \tag{4.1a}$$

$$u = 0 \qquad \text{on } \Gamma_0, \tag{4.1b}$$

$$\frac{\partial u}{\partial n} = 0 \qquad \text{on } \Gamma_1. \tag{4.1c}$$

The coefficient $\nu > 0$ is the thermal diffusivity. Incompressibility yields that $\frac{\partial U_j}{\partial x_j} = 0$. We assume that Γ_1 is a solid wall, so that $n_j U_j = 0$ on Γ_1. This simplifies the analysis but is not essential. The *Dirichlet* boundary condition $u = 0$ on Γ_0 is called an *isothermal condition*, whereas the *Neumann condition* $\frac{\partial u}{\partial n} = 0$ on Γ_1 is an *adiabatic condition*.

Deriving the integral form that is used to form the finite-element discretization requires some vector calculus. The product rule of differentiation yields

$$\frac{\partial}{\partial x_i}\left(v \frac{\partial u}{\partial x_i} \right) = \frac{\partial v}{\partial x_i} \frac{\partial u}{\partial x_i} + v \nabla^2 u. \tag{4.2}$$
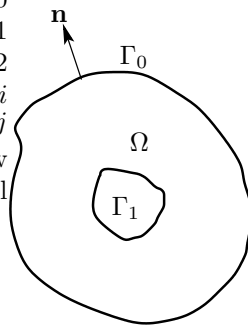
Figure 4.1: A typical domain associated with the advection–diffusion problem (4.1).

71

Recall the *divergence theorem*

$$\int_\Omega \frac{\partial w_i}{\partial x_i}\,\mathrm{d}\Omega = \int_\Gamma n_i w_i\,\mathrm{d}\Gamma. \tag{4.3}$$

Integrating expression (4.2) and applying the divergence theorem on the left side yields

$$\int_\Gamma v\frac{\partial u}{\partial n}\,\mathrm{d}\Gamma = \int_\Omega \frac{\partial v}{\partial x_i}\frac{\partial u}{\partial x_i}\,\mathrm{d}\Omega + \int_\Omega v\nabla^2 u\,\mathrm{d}\Omega. \tag{4.4}$$

(Note that

$$\frac{\partial u}{\partial n} = n_i\frac{\partial u}{\partial x_i}.)$$

Let v be any smooth function such that $v = 0$ on Γ_0. Multiplying equation (4.1a) with v, integrating over Ω, and utilizing expression (4.4) yields

$$\int_\Omega fv\,\mathrm{d}\Omega = \int_\Omega vU_j\frac{\partial u}{\partial x_j}\,\mathrm{d}\Omega - \nu\int_\Omega v\nabla^2 u\,\mathrm{d}\Omega = \int_\Omega vU_j\frac{\partial u}{\partial x_j}\,\mathrm{d}\Omega + \nu\int_\Omega \frac{\partial v}{\partial x_j}\frac{\partial u}{\partial x_j}\,\mathrm{d}\Omega - \nu\int_\Gamma v\overset{0}{\cancel{\frac{\partial u}{\partial n}}}\,\mathrm{d}\Gamma,$$

where the last term vanishes on Γ_0 due to the requirements on v, and on Γ_1 due to boundary condition (4.1c)

We have thus shown that a smooth (twice continuously differentiable) solution to problem (4.1) (also called a *classical* solution) satisfies the *varational form*

$$\int_\Omega vU_j\frac{\partial u}{\partial x_j}\,\mathrm{d}\Omega + \nu\int_\Omega \frac{\partial v}{\partial x_j}\frac{\partial u}{\partial x_j}\,\mathrm{d}\Omega = \int_\Omega fv\,\mathrm{d}\Omega \tag{4.5}$$

for each smooth function v vanishing on Γ_0

We will now "forget" about the differential equation (4.1), and directly consider the variational form (4.5). For this, we need to introduce the *function space*

$$V = \left\{ v : \int_\Omega \frac{\partial v}{\partial x_i}\frac{\partial v}{\partial x_i}\,\mathrm{d}\Omega < +\infty, v = 0 \text{ on } \Gamma_0 \right\}.$$

The space V is a *linear space*, that is, $u, v \in V \Rightarrow \alpha u + \beta v \in V \;\forall \alpha, \beta \in \mathbf{R}$. The requirement that the gradient-square of each function in V is bounded should be intepreted as a requirement that the *energy* is bounded.

The variational problem will thus be

Find $u \in V$ such that

$$\int_\Omega vU_j\frac{\partial u}{\partial x_j}\,\mathrm{d}\Omega + \nu\int_\Omega \frac{\partial v}{\partial x_j}\frac{\partial u}{\partial x_j}\,\mathrm{d}\Omega = \int_\Omega fv\,\mathrm{d}\Omega \qquad \forall v \in V. \tag{4.6}$$

A solution to variational problem (4.6) is called a *weak solution* to advection–diffusion problem (4.1). The derivation leading up to expression (4.5) shows that a classical solution is a weak solution. However, a weak solution may not be a classical solution since functions in V may fail to be twice continuously differentiable.

Note that the boundary conditions are incorporated into the variational problem. The Dirichlet boundary condition on Γ_0 is explicitly included in the definition of V and is therefore referred to as an *essential boundary condition*. The Neumann condition on Γ_1 is defined implicitly through the variational form and is therefore called a *natural boundary condition*.

4.1.1 Finite element approximation

Let us *triangulate* the domain Ω by dividing it up into triangles, as in figure 4.2. Let M be the number of triangles and N the number of nodes in $\Omega \cup \Gamma_1$, that is, the nodes on Γ_0 are excluded in the count. Let h be the largest side of any triangle.

Let V_h be the space of all functions that are
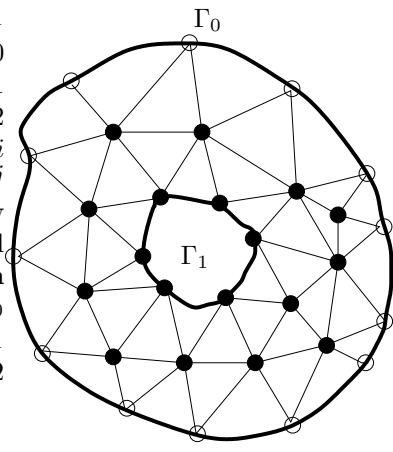
- continuous on $\overline{\Omega}$,

Figure 4.2: A triangulation. Here, the number N are the black nodes.
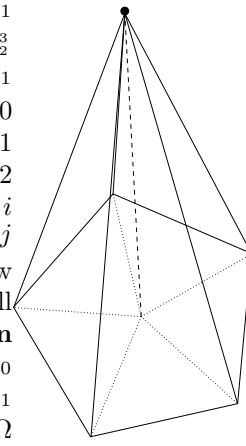

Figure 4.3: The "tent or "hat basis function associated with continuous, piece-wise linear functions.

    - linear on each triangle,

    - vanishing on Γ_0.

Note that $V_h \subset V$. We get a *finite-element approximation* of our advection-diffusion problem by simply replacing V by V_h in variational problem (4.6), that is:

Find $u_h \in V_h$ such that
$$\int_\Omega v_h U_j \frac{\partial u_h}{\partial x_j} \, d\Omega + \nu \int_\Omega \frac{\partial v_h}{\partial x_j} \frac{\partial u_h}{\partial x_j} \, d\Omega = \int_\Omega f v_h \, d\Omega \qquad \forall v_h \in V_h. \tag{4.7}$$

Restricting the function space in a variational form to a subspace is called a *Galerkin* approximation. The finite-element method is a Galerkin approximation in which the subspace is given by piecewise polynomials.

4.1.2   The algebraic problem. Assembly.

Once the value of a function u_h in V_h is known at all node points, it is easy to reconstruct it by linear interpolation. This interpolation can be written as a sum of the "tent" basis functions $\Phi^{(n)}$ (figure 4.3), which are functions in V_h that are zero at each node point except node n, where it is unity. Thus,

$$u_h(x_i) = \sum_{n=1}^N u^{(n)} \Phi^{(n)}(x_i), \tag{4.8}$$

where $u^{(n)}$ denotes the value of u_h at node n. Note that expansion (4.8) forces $u_h = 0$ on Γ_0 since it excludes the nodes on Γ_0 in the sum.

Substituting expansion (4.8) into FEM approximation (4.7) yields

$$\sum_{n=1}^N u^{(n)} \int_\Omega v_h U_j \frac{\partial \Phi^{(n)}}{\partial x_j} \, d\Omega + \nu \sum_{n=1}^N u^{(n)} \int_\Omega \frac{\partial v_h}{\partial x_j} \frac{\partial \Phi^{(n)}}{\partial x_j} \, d\Omega = \int_\Omega f v_h \, d\Omega \qquad \forall \, v_h \in V_h. \tag{4.9}$$

Since each basis function is in V_h, we may choose $v_h = \Phi^{(m)} \in V_h$ for $m = 1, \ldots, N$ in equation (4.9), which then becomes

$$\sum_{n=1}^N u^{(n)} \int_\Omega \Phi^{(m)} U_j \frac{\partial \Phi^{(n)}}{\partial x_j} \, d\Omega + \nu \sum_{n=1}^N u^{(n)} \int_\Omega \frac{\partial \Phi^{(m)}}{\partial x_j} \frac{\partial \Phi^{(n)}}{\partial x_j} \, d\Omega = \int_\Omega f \Phi^{(m)} \, d\Omega, m = 1, \, \ldots, \, N. \tag{4.10}$$

This is a linear system system $Au = b$, where $A = C + \nu K$ and

$$K_{mn} = \int_\Omega \frac{\partial \Phi^{(m)}}{\partial x_j} \frac{\partial \Phi^{(n)}}{\partial x_j} \, d\Omega, \qquad C_{mn} = \int_\Omega \Phi^{(m)} U_j \frac{\partial \Phi^{(n)}}{\partial x_j} \, d\Omega, \tag{4.11}$$
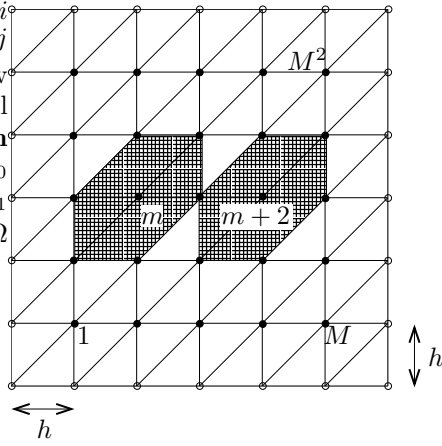
Figure 4.4: An example mesh that gives a particular simple stiffness matrix K

$$
u = \begin{pmatrix} u^{(1)} \\ \vdots \\ u^{(n)} \end{pmatrix} \qquad b = \begin{pmatrix} \int\limits_\Omega f\Phi^{(1)}\,\mathrm{d}\Omega \\ \vdots \\ \int\limits_\Omega f\Phi^{(N)}\,\mathrm{d}\Omega \end{pmatrix}
$$

The union of all triangles constitutes the domain Ω and that the triangles do not overlap. Thus, any integral over Ω can be written as a sum of integrals over each triangle,

$$
K_{mn} = \int\limits_\Omega \frac{\partial \Phi^{(m)}}{\partial x_j}\frac{\partial \Phi^{(n)}}{\partial x_j}\,\mathrm{d}\Omega = \sum_{p=1}^{M}\int\limits_{T_p} \frac{\partial \Phi^{(m)}}{\partial x_j}\frac{\partial \Phi^{(n)}}{\partial x_j}\,\mathrm{d}\Omega = \sum_{p=1}^{M} K_{mn}^{(p)}.
$$

Note that $K_{mn}^{(p)}$ vanishes as soon as m or n is not a corner node of triangle p. Thus $K_{mn}^{(p)}$ contributes to the sum only when m and n both are corner nodes of triangle p. Matrix K can thus be computed by looping all M triangles, calculating the *element contribution* $K_{mn}^{(p)}$ for m, n being the three nodes of triangle p and adding these 9 contribution to matrix K. Note that the derivatives of $\Phi^{(n)}$ are constant on each triangle, so $K_{mn}^{(p)}$ is easy to compute exactly. Matrix C and vector b can also be computed by element assembly, but numerical quadrature is usually needed, except if U_j and f happen to be particularly "easy" functions (such as constants).

4.1.3   An example

As an example, we will compute the elements of K, the "stiffness matrix" (a term borrowed from structural mechanics), for the particular case of the structured mesh depicted in figure 4.4.

Let M be the number of internal nodes in the horizontal as well as the vertical direction (the solid nodes in figure 4.4.) The width of each "panel" is then $h = 1/(M+1)$, and the area of each triangle is $|T_k| = h^2/2$. The components of K are

$$
K_{mn} = \int\limits_\Omega \frac{\partial \Phi^{(m)}}{\partial x_j}\frac{\partial \Phi^{(n)}}{\partial x_j}\,\mathrm{d}\Omega \tag{4.12}
$$

Note that K_{mn} vanishes for most m and n. For instance, $K_{m,m+2} = 0$, since basis functions $\Phi^{(m)}$ and $\Phi^{(m+2)}$ do not overlap (figure 4.4). In fact, $K_{mn} \neq 0$ *only* when m and n are associated with nodes that are nearest neighbors.

To compute matrix element (4.12), we need expressions for the gradients of basis functions $\Phi^{(m)}$ and $\Phi^{(m+1)}$. Since the functions are piecewise linear, the gradient is constant on each triangles and may thus easily be computed by finite-differences in the coordinate direction (figure 4.5). By the expressions in
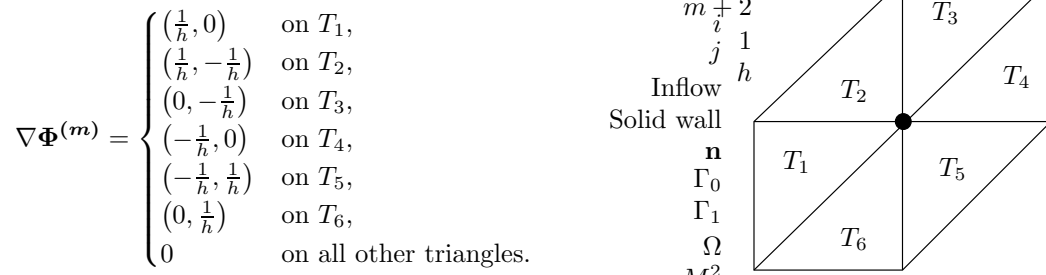
$$\nabla\mathbf{\Phi}^{(m)} = \begin{cases} \left(\frac{1}{h},0\right) & \text{on } T_1, \\ \left(\frac{1}{h},-\frac{1}{h}\right) & \text{on } T_2, \\ \left(0,-\frac{1}{h}\right) & \text{on } T_3, \\ \left(-\frac{1}{h},0\right) & \text{on } T_4, \\ \left(-\frac{1}{h},\frac{1}{h}\right) & \text{on } T_5, \\ \left(0,\frac{1}{h}\right) & \text{on } T_6, \\ 0 & \text{on all other triangles.} \end{cases}$$

Figure 4.5: The gradient of test function $\Phi^{(m)}$ for m being the (black) middle node.

$$\nabla\Phi^{(m)} = \begin{cases} \left(-\frac{1}{h},\frac{1}{h}\right) & \text{on } T_1, \\ \left(-\frac{1}{h},0\right) & \text{on } T_2, \\ 0 & \text{on all other triangles} \end{cases}$$

$$\nabla\Phi^{(m+1)} = \begin{cases} \left(\frac{1}{h},0\right) & \text{on } T_1, \\ \left(\frac{1}{h},-\frac{1}{h}\right) & \text{on } T_2. \end{cases}$$
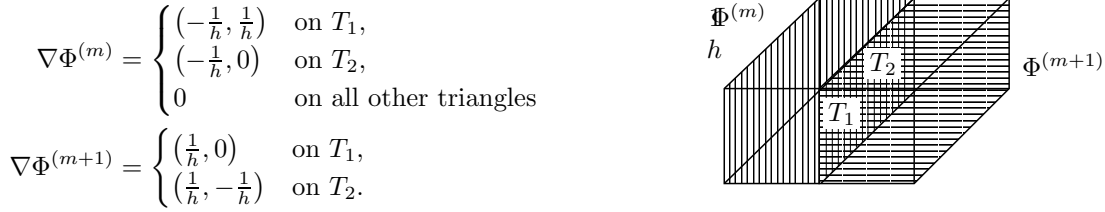
Figure 4.6: The support for basis functions Φ^m and Φ^{m+1} are marked with vertical and horizontal stripes respectively.

figure 4.5, we have

$$K_{mm} = \int_\Omega \frac{\partial\Phi^{(m)}}{\partial x_j}\frac{\partial\Phi^{(m)}}{\partial x_j}\,\mathrm{d}\Omega = \sum_{k=1}^{6}\int_{T_k}\left[\left(\frac{\partial\Phi^{(m)}}{\partial x}\right)^2 + \left(\frac{\partial\Phi^{(m)}}{\partial y}\right)^2\right]\mathrm{d}\Omega$$

$$= \frac{1}{h^2}|T_1| + 2\frac{1}{h^2}|T_2| + \frac{1}{h^2}|T_3| + \frac{1}{h^4}|T_4| + 2\frac{1}{h^2}|T_5| + \frac{1}{h^2}|T_6|$$

$$= 8\frac{1}{h^2}\frac{h^2}{2} = 4$$

The common *support* for basis functions Φ^m and Φ^{m+1} is only the two triangles marked in figure 4.6; that is, it is only on these two triangles that both functions are nonzero at the same time. Utilizing the gradient expressions given in figure 4.6 yields

$$K_{m,m+1} = \int_\Omega \nabla\Phi^{(m)}\cdot\nabla\Phi^{(m+1)}\,\mathrm{d}\Omega = \sum_{k=1}^{2}\int_{T_k}\nabla\Phi^{(m)}\cdot\nabla\Phi^{(m+1)}\,\mathrm{d}\Omega = -\frac{1}{h^2}|T_1| - \frac{1}{h^2}|T_2| = -\frac{2}{h^2}\frac{h^2}{2} = -1,$$

and in the same manner,

$$K_{m,m-1} = K_{m,m+M} = K_{m,m-M} = -1.$$

Altogether, K becomes the block-tridiagonal M^2-by-M^2 matrix

$$K = \begin{pmatrix} T & -I & & & \\ -I & T & -I & & \\ & \ddots & \ddots & \ddots & \\ & & -I & T & -I \\ & & & -I & T \end{pmatrix},$$

where I is the M-by$M$ identity matrix, and T the M-by$M$ matrix

$$T = \begin{pmatrix} 4 & -1 & & & \\ -1 & 4 & -1 & & \\ & \ddots & \ddots & \ddots & \\ & & -1 & 4 & -1 \\ & & & -1 & 4 \end{pmatrix}.$$

Thus, a typical row in the matrix–vector product Ku becomes

$$4u_m - u_{m+1} - u_{m-1} - u_{m+M} - u_{m-M}, \tag{4.13}$$

that is, after dividing expression (4.13) with h^2, we recognize the classical *five-point stencil* for the negative Laplacian $-\nabla^2$.

Thus our finite-element discretization is for this particular mesh equivalent to a finite-volume or finite-difference discretization. However, for a general unstructured mesh, the finite-element discretization will not give rise to any obvious finite-difference stencil.

4.1.4 Matrix properties and solvability

Matrix A is *sparse*: the elements of martix A are mostly zeros. At row m, matrix element $A_{mn} \neq 0$ only in the columns where n represents a nearest neighbor to node m. The number of nonzero elements on each row does *not* grow (on average) when the mesh is refined (since the number of nearest neighbors in a mesh does not grow). Thus, the matrices become sparser and sparser as the mesh is refined. A common technique in finite-element codes is therefore to use *sparse representation*, that is, to store only the nonzero elements and pointers to matrix locations.

It is immediate from expression (4.11) that $K_{mn} = K_{nm}$, that is, K is a *symmetric matrix* ($K^T = K$). Integration by parts also shows that matric C is *skew symmetric* ($C^T = -C$).

Theorem 1. K is positive definite, that is, $v^T K v > 0$ for each $v \neq 0$.

Proof. Let $v_h \in V_h$. Then $v_h = \sum_{n=1}^N v^{(N)} \Phi^{(n)}$. Denote $v = (v^{(1)}, \ldots, v^{(N)})^T$.

$$v^T K v = \sum_{m=1}^N \sum_{n=1}^N v^{(n)} \int_\Omega \frac{\partial \Phi^{(n)}}{\partial x_i} \frac{\partial \Phi^{(m)}}{\partial x_i} \, d\Omega \, v^{(m)}$$

$$= \int_\Omega \sum_{m=1}^N \frac{\partial}{\partial x_i} \left(v^{(m)} \Phi^{(m)} \right) \sum_{n=1}^N \frac{\partial}{\partial x_i} \left(v^{(m)} \Phi^{(n)} \right) \, d\Omega = \int_\Omega \frac{\partial v_h}{\partial x_i} \frac{\partial v_h}{\partial x_i} \, d\Omega \geq 0,$$

with equality if and only if $\frac{\partial v_h}{\partial x_i} = 0$, that is, if $v_h = \text{Const}$. But since $v_h|_{\Gamma_0} = 0$, $v_h \equiv 0$. $\qquad \square$

From Theorem 1 also follows that A is positive definite. To see this, note that the skew-symmetry of C yields that

$$v^T C v = \left(v^T C v \right)^T = v^T C^T v = -v^T C v$$

that is, $v^T C v = 0$ for each v. Thus

$$v^T A v = v^T \left(K + C \right) v = v^T K v + v^T C v = v^T K v > 0$$

for each $v \neq 0$, that is, A is positive definite. However, A is *not* symmetric whenever $U_j \neq 0$.

Recall that a linear system $Au = b$ has a unique solution for each b if the matrix is nonsingular. A positive-definite matrix is a particular example of a nonsingular matrix. We thus conclude that the linear system resulting from the finite-element discretization (4.7) has a unique solution.

4.1.5 Stability and accuracy

We have defined the finite-element approximation and showed that the finite-element approximation yields a linear system $Au = b$ that has a unique solution. Now the question is whether the approximation is any good. We will study the *stability* and *accuracy* of the numerical solution. FEM usually uses *integral norms* for analysis of stability and accuracy. We start by reviewing some mathematical concepts that will be used in the analysis.

Basic definitions and inequalities

The most basic integral norm is

$$\|v\|_{L^2(\Omega)} = \left(\int_\Omega v^2 \, d\Omega \right)^{1/2}$$

For the current problem, a more fundamental quantity is the *energy norm*

$$\|v\|_V = \left(\int_\Omega |\nabla v|^2 \, d\Omega \right)^{1/2} = \left(\int_\Omega \frac{\partial v}{\partial x_i} \frac{\partial v}{\partial x_i} \, d\Omega \right)^{1/2}$$

and associated inner product

$$(u, v)_V = \int_\Omega \nabla u \cdot \nabla v \, d\Omega = \int_\Omega \frac{\partial u}{\partial x_i} \frac{\partial v}{\partial x_i} \, d\Omega. \tag{4.14}$$

The *Cauchy–Schwarz* inequality for vectors $a = (a_1, \ldots, a_n)$ is

$$|a \cdot b| \leq |a||b| = |a \cdot a|^{1/2}|b \cdot b|^{1/2},$$

whereas for functions it reads

$$\left| \int_\Omega fg \, \mathrm{d}\Omega \right| \leq \left(\int_\Omega f^2 \, \mathrm{d}\Omega \right)^{1/2} \left(\int_\Omega g^2 \, \mathrm{d}\Omega \right)^{1/2}, \tag{4.15}$$

which can be denoted

$$(f, g)_{L^2(\Omega)} \leq \|f\|_{L^2(\Omega)} \|g\|_{L^2(\Omega)}.$$

The Cauchy–Schwarz inequality (4.15) implies that, for each nonzero, square-integrable g,

$$\left(\int_\Omega f^2 \, \mathrm{d}\Omega \right)^{1/2} \geq \frac{\left| \int_\Omega fg \, \mathrm{d}\Omega \right|}{\left(\int_\Omega g^2 \, \mathrm{d}\Omega \right)^{1/2}}.$$

Choosing $g = f$ yields equality in above expression. Thus

$$\|f\|_{L^2(\Omega)} = \left(\int_\Omega f^2 \, \mathrm{d}\Omega \right)^{1/2} = \max_{g \neq 0} \frac{\left| \int_\Omega fg \, \mathrm{d}\Omega \right|}{\left(\int_\Omega g^2 \, \mathrm{d}\Omega \right)^{1/2}} = \max_{g \neq 0} \frac{\left| \int_\Omega fg \, \mathrm{d}\Omega \right|}{\|g\|_{L^2(\Omega)}}$$

The rightmost expression is a "variational characterization" of the $L^2(\Omega)$ norm, that is, it expresses the norm in terms of something that is optimized. By inserting derivatives in the nominator and/or denominator of the variational characterization, various exotic norms can be defined. A norm, different from the $L^2(\Omega)$ norm and of importance for the Navier–Stokes equations is

$$\|p\|_{\text{exotic}} = \max_{w_i} \frac{\left| \int_\Omega p \left(\dfrac{\partial w_i}{\partial x_i} \right) \, \mathrm{d}\Omega \right|}{\left(\int_\Omega |\nabla w_i|^2 \, \mathrm{d}\Omega \right)^{1/2}}. \tag{4.16}$$

This norm will be of crucial importance when we analyze the stability of FEM form the Navier–Stokes equations.

The *Poincaré inequality* relates the energy and $L^2(\Omega)$ norms:

Theorem 2 (Poincaré inequality). *There is a $C > 0$ such that*

$$\int_\Omega v^2 \, \mathrm{d}\Omega \leq C \int_\Omega \frac{\partial v}{\partial x_i} \frac{\partial v}{\partial x_i} \, \mathrm{d}\Omega,$$

that is,

$$\|v\|_{L^2(\Omega)}^2 \leq C \|v\|_V^2$$

for each $v \in V$.

Remark 1. Theorem 2 says that the energy norm is *stronger* than then $L^2(\Omega)$ norm. The smallest possible value of C grows with the size of Ω. The Poincaré inequality holds only if Ω is bounded in at least one direction. Also, the inequality does not hold if $\int_{\Gamma_0} \mathrm{d}\Gamma = 0$. However, the inequality

$$\int_\Omega v^2 \, \mathrm{d}\Omega \leq C \left(\int_\Omega v^2 \, \mathrm{d}\Omega + \int_\Omega \frac{\partial v}{\partial x_i} \frac{\partial v}{\partial x_i} \, \mathrm{d}\Omega \right)$$

holds also when $\int_{\Gamma_0} \mathrm{d}\Gamma = 0$.

Stability

Choosing $v_h = u_h$ in equation (4.7) yields

$$\int_\Omega u_h U_j \frac{\partial u_h}{\partial x_j} \, \mathrm{d}\Omega + \nu \int_\Omega \frac{\partial u_h}{\partial x_j} \frac{\partial u_h}{\partial x_j} \, \mathrm{d}\Omega = \int_\Omega f u_h \, \mathrm{d}\Omega. \tag{4.17}$$

Note that

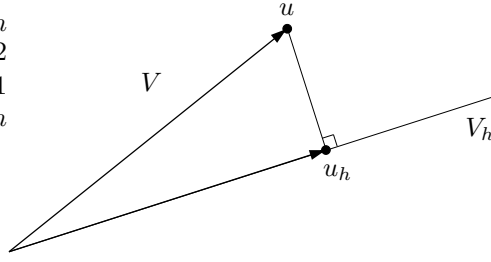$$\int_\Omega u_h U_j \frac{\partial u_h}{\partial x_j} \, \mathrm{d}\Omega = u^T C u = 0,$$

Figure 4.7: An orthogonal projection on a line. Note that the vector $u - u_h$ is the shortest of all vectors $u - v_h$ for $v_h \in V_h$, that is, $\|u - u_h\| \le \|u - v_h\| \ \forall v_h \in V_h$.

since $C = -C^T$ (using the notation of § 4.1.4).

Expression (4.17) thus becomes

$$\nu \underbrace{\int_\Omega \frac{\partial u_h}{\partial x_i} \frac{\partial u_h}{\partial x_i} \, \mathrm{d}\Omega}_{\|u_h\|_V^2} = \int_\Omega f u_h \, \mathrm{d}\Omega$$

$$(\text{Cauchy–Schwarz}) \le \left(\int_\Omega f^2 \, \mathrm{d}\Omega \right)^{1/2} \left(\int_\Omega u_h^2 \, \mathrm{d}\Omega \right)^{1/2}$$

$$(\text{Poincaré}) \le C \left(\int_\Omega f^2 \, \mathrm{d}\Omega \right)^{1/2} \left(\int_\Omega \frac{\partial u_h}{\partial x_i} \frac{\partial u_h}{\partial x_i} \, \mathrm{d}\Omega \right)^{1/2}$$

$$\le C \|f\|_{L^2(\Omega)} \|u_h\|_V.$$

Dividing with $\|u_h\|_V$ shows that

$$\|u_h\|_V \le \frac{C}{\nu} \|f\|_{L^2(\Omega)}$$

where the constant C *does not depend on* h. That is, we have shown that u_h cannot blow up as the discretization is refined, which is the same as saying that the numerical solution is stable.

Error bounds

Choosing $v = v_h \in V_h \subset V$ in variational problem (4.6) and subtracting equation (4.7) from (4.6) yields the "Galerkin orthogonality",

$$\nu \int_\Omega \frac{\partial v_h}{\partial x_i} \frac{\partial}{\partial x_i} (u - u_h) \, \mathrm{d}\Omega + \int_\Omega v_h U_j \frac{\partial}{\partial x_j} (u - u_h) \, \mathrm{d}\Omega = 0 \qquad \forall v_h \in V_h.$$

This is a "true" orthogonality condition when $U_j \equiv 0$:

$$\nu \int_\Omega \frac{\partial v_h}{\partial x_i} \frac{\partial}{\partial x_i} (u - u_h) \, \mathrm{d}\Omega = 0 \qquad \forall v_h \in V_h; \tag{4.18}$$

that is, the error $u - u_h$ is orthogonal to each $v_h \in V_h$ with respect to the inner product (4.14). Cf. two orthogonal vectors: $a \cdot b = 0$. Orthogonality relation (4.18) means that u_h is an *orthogonal projection* of u on V_h. As illustrated in figure 4.7, the orthogonal projection on a subspace yields the vector that is closest to the given element in the norm derived from the inner product in which orthogonality is defined. Orthogonality property (4.18) (cf. figure 4.7) implies that the FE approximation is *optimal* in the energy norm when $U_i \equiv 0$:

$$\|u - u_h\|_V \le \|u - v_h\|_V \qquad \forall v_h \in V_h. \tag{4.19}$$

The matrix A is *symmetric* in this case (since $C = 0$).

When $U_j \ne 0$, the FEM approximation is no longer optimal in this sense. However, there is a $C > 0$ such that *Céa's lemma* holds,

$$\|u - u_h\|_V \le \frac{C}{\nu} \|u - v_h\|_V \qquad \forall v_h \in V_h. \tag{4.20}$$

Matrix A is *nonsymmetric* in this case. Note that the approximation may be far from optimal when ν is small, as the next example illustrates.
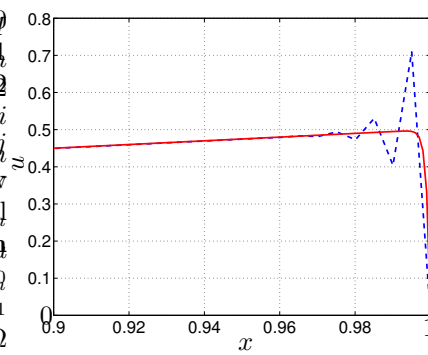
Figure 4.8: Under-resolved standard Galerkin finite-element approximations may yield oscillations for advection-dominated flows.
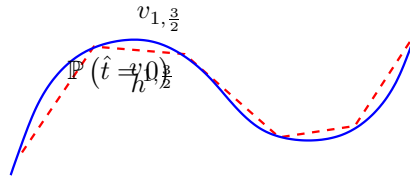

Figure 4.9: An interpolant $\Pi_h v$ interpolates v at the nodal points.

Example 1. Let us consider the above FEM applied to the 1D problem

$$-\frac{1}{500}u'' + u' = 1 \qquad \text{in } (0,1).$$
$$u(0) = u(1) = 0$$

$$(4.21)$$

The problem is *advection dominated*, that is, the viscosity coefficient in equation (4.21) is quite small: $\nu = 1/500$. A *boundary layer* with sharp gradients forms close to $x = 1$. The solid line in figure 4.8 shows the FE solution $h = 1/1000$, whereas the dashed line shows the FE approximation for $h = 1/200$. □

The result of example 1 is typical: under-resolved standard Galerkin methods may generate oscillations for advection-dominated flows in areas of sharp gradients.

An explanation of this phenomenon is that the directions of flow is not accounted for in the standard Galerkin approximation. Galerkin approximations correspond to finite-difference *central schemes. Upwinding* is used to prevent oscillations for finite-difference methods. Various methods exist to obtain similar effects in FEM, for instance *streamline diffusion* and *discontinuous Galerkin*. Both these methods modify the basic Galerkin idea to account for flow-direction effects.

Approximation and mesh quality

Estimates (4.19) and (4.20) are independent of the choice of V_h! We only used that $V_h \subset V$. Next step in assessing the error is an *approximation problem*: How well can functions in V_h approximate those in V? This step is *independent of the equation in question. Interpolants* are used to study approximation properties. The interpolant is the function $\Pi_h v \in V_h$ that interpolates the function $v \in V$ at the node points of the triangulation, as illustrated for a 1D case in figure 4.9.

Approximation theory yields that, for sufficiently smooth v,

$$\begin{aligned}
\|v - \Pi_h v\|_{L^2(\Omega)} &\leq Ch^2 &\qquad &\text{"second order error"} \\
\|v - \Pi_h v\|_V &\leq Ch &\qquad &\text{"first order error"}
\end{aligned}$$

$$(4.22)$$

The constant C contains integrals of the second derivatives of v.

A *mesh quality* assumption is needed for (4.22) to hold. The essential point is: *beware of "thin" triangles*; do not let the shape deteriorate as the mesh is refined. A strategy to preserve mesh quality when refining is to subdivide each triangle into four new triangles by joining the edge midpoints (figure 4.10).

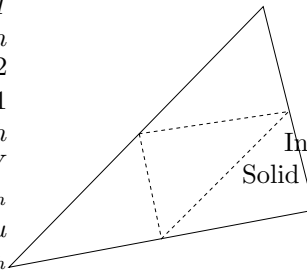Each of the conditions below is sufficient for approximation property (4.22) to hold:

M
m
$m+2$
1
h
V
V_h
u
u_h

1
2
i
j
Inflow
Solid wall
$\mathbf{n}$
Γ_0
Γ_1
Ω
M^2

Figure 4.10: A subdivision that preserves mesh quality.

(i) ("Maximum angle condition"). The largest angle of any triangle should not approach $180°$ as $h \to 0$.

(ii) ("Chunkiness parameter condition"). The quotient between the diameter of the largest circle that can be inscribed and the diameter of the triangle should not vanish as $h \to 0$.

M
m
$m+2$
1
h
V
V_h
u
u_h

Condition (ii) implies (i), but not the reverse.
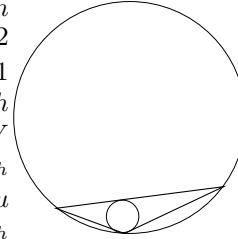
Accuracy of the FE solution

Error bounds (4.19) and (4.20) together with approximation property (4.22) implies

$$\|u - u_h\|_V \le Ch$$

Further analysis (not provided here) yields

$$\|u - u_h\|_{L^2(\Omega)} \le Ch^2.$$

This *second-order convergence rate* requires a mesh quality assumption and a sufficiently smooth solution u (since the constant C contains second derivatives of u). The convergence rate is of *optimal order*: it agrees with approximation property (4.22) and is the best *order* that in general can be obtained for, in this case, piecewise-linear functions. However, the solution may still be bad for a particular, too-crude mesh; recall example 1.

Improving Accuracy

Accuracy is improved by refining the mesh ("h-method"). This may be done *adaptively*, where it is needed (say, in areas of large gradients), to prevent the matrices to become too large. Automatic methods for adaptation are common.

An alternative is to keep the mesh fixed and increase the order of the polynomials at each triangle ("p-method"). For instance, continuous, piecewise quadratics yields a *third-order-accurate* solution (in the $L^2(\Omega)$ norm).

These strategies may be combined in the "h–p method", where the mesh is refined in certain regions and the order of approximations is increased in other.

4.1.6 Alternative Elements, 3D

A *quadrilateral* is a "skewed" rectangle: four points connected by straight lines to form a closed geometric object. Nonoverlapping quadrilaterals can be used to "triangulate" a domain, as in figure 4.11.

An example of a finite-element space V_h on quadrilaterals is globally continuous functions varying *linearly* along the edges. As in the triangular case, the functions are defined uniquely by specifying the function values at each node. The functions are defined by interpolation into the interior of each quadrilateral. This space reduces to piecewise *bilinear* functions for rectangles with edges in the coordinate directions:

$$v_h(x, y) = a + b\,x + c\,y + d\,xy$$

Quadrilaterals on a "logically rectangular domain" (a distorted rectangle, as in figure 4.11) yields a regular structure to the matrix A. This may
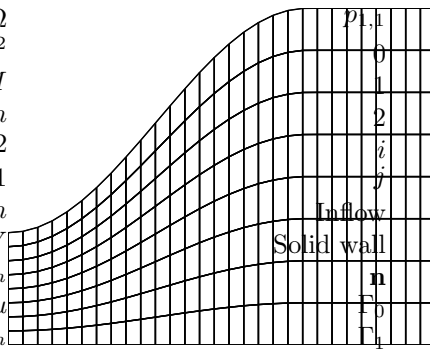
Figure 4.11: A logically rectangular domain triangulated with quadrilaterals.

Figure 4.12: In 3D, triangular and quadrilateral elements generalize to tetrahedral (left) and hexahedral (right) meshes.

- give high accuracy (particularly if the mesh is aligned with the flow), and

- allow efficient solution of the linear system (particularly for uniform, rectangular meshes).

Compared to triangular mesh, it is harder to generate quadrilateral meshes automatically for complicated geometries.

Triangular and quadrilateral meshes generalize in 3D to *tetrahedral* and *hexahedral* meshes (figure 4.12). Advantages and limitations with tetrahedral and hexahedral meshes are similar to corresponding meshes in 2D.
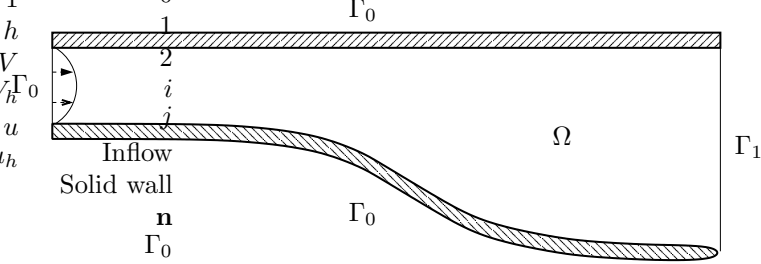
h
V
$V_h \Gamma_0$
u
u_h Inflow
Solid wall
$\mathbf{n}$
Γ_0
Γ_0
Γ_1

Γ_0

Ω

Γ_1

Figure 4.13: A simple example of a domain.

M^2
M
m
$m+2$
1
h
V
$V_h \Gamma_0$
u
u_h
Γ_0
Γ_1
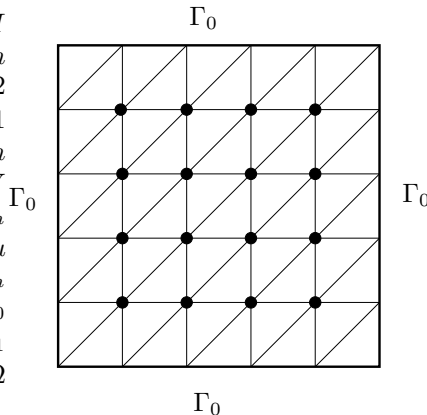Ω

Γ_0

Γ_0

Γ_0

Γ_0

Figure 4.14: The black nodes are the degrees of freedom for the velocity components, which are fewer than the number of triangles.

4.2 FEM for Navier–Stokes

We now turn to the Navier–Stokes equations for the steady flow of an incompressible fluid, and consider a situation with flow in a bounded domain Ω. A simple example domain is depicted in figure 4.13. The mathematical problem in differential form is

$$u_j \frac{\partial u_i}{\partial x_j} + \frac{\partial p}{\partial x_i} - \frac{1}{\text{Re}} \nabla^2 u_i = f_i \qquad \text{in } \Omega, \qquad (4.23\text{a})$$

$$\frac{\partial u_i}{\partial x_i} = 0 \qquad \text{in } \Omega. \qquad (4.23\text{b})$$

$$u_i = g_i \qquad \text{on } \Gamma_0 \qquad (4.23\text{c})$$

$$-\frac{1}{\text{Re}} \frac{\partial u_i}{\partial x_j} n_j + p n_i = 0 \qquad \text{on } \Gamma_1. \qquad (4.23\text{d})$$

The boundary condition on $\Gamma_1 = \partial\Omega \setminus \Gamma_0$ is of no obvious physical significance, but is useful as an artificial outflow condition.

The Navier–Stokes equations is a system of nonlinear advection–diffusion equations together with the incompressibility condition (4.23b). This condition introduces new complications not present in the advection–diffusion problem of section 4.1. Naive approximations of the Navier–Stokes equations are bound to produce disapping results, as the following example indicates.

Example 2 *("the counting argument").* Consider a case with only Dirichlet boundary conditions—that is, $\Gamma_1 = \emptyset$—and the mesh of figure 4.14. Assume that we use continuous, piecewise-linear approximations u_h, v_h for the x- and y-components of the velocity field. There are I number of panels in each direction and therefore $2(I-1)^2$ degrees of freedom (two times the number of black dots) for the velocity vector field. The left side of equation (4.23b), that is

$$\frac{\partial u_h}{\partial x} + \frac{\partial v_h}{\partial y}$$

is here constant on each triangle. Thus, demanding equation (4.23b) to be satisfied on each triangle yields $2I^2$ equations, *which is more than the degrees of freedom for the velocity*! Thus $u_h = v_h = 0$ is the only FE function satisfying the incompressibility condition (4.23b)! $\qquad\square$

Following strategies can be used to tackle the problem of example 2.

(i) Use more degrees of freedom for the velocity—for instance continuous, piecewise quadratics on each triangle—to balance the large number of equations associated with the incompressibility condition.

(ii) Accept that the discrete velocities only is approximately divergence-free.

(iii) Associate the velocity with the midpoints of *edges* instead of the vertices. This also gives more degrees of freedom for the velocities. (There are $\sim 3I^2$ edges, but only $\sim 2I^2$ vertices).

Strategies (i) and (ii) are the "standard" methods, whereas (iii) leads to "non-conforming" approximations related to finite-difference and finite-volume approximation with "staggered mesh".

4.2.1   A variational form of the Navier–Stokes equations

To derive the variational form, we need new integration-by-part formulas. The product rule of differentiation yields

$$\frac{\partial}{\partial x_j}\left(z_i\frac{\partial u_i}{\partial x_j}\right) = \frac{\partial z_i}{\partial x_j}\frac{\partial u_i}{\partial x_j} + z_i\nabla^2 u_i \tag{4.24}$$

and

$$\frac{\partial}{\partial x_j}(z_j p) = z_i\frac{\partial p}{\partial x_i} + p\frac{\partial z_j}{\partial x_j}. \tag{4.25}$$

Integrating expressions (4.24) and (4.25) and applying the the divergence theorem (4.3) on the left sides yields

$$\int_\Gamma n_j z_i\frac{\partial u_i}{\partial x_j}\,\mathrm{d}\Gamma = \int_\Omega \frac{\partial z_i}{\partial x_j}\frac{\partial u_i}{\partial x_j}\,\mathrm{d}\Omega + \int_\Omega z_i\nabla^2 u_i\,\mathrm{d}\Omega \tag{4.26}$$

and

$$\int_\Gamma n_j z_j p\,\mathrm{d}\Gamma = \int_\Omega z_i\frac{\partial p}{\partial x_i}\,\mathrm{d}\Omega + \int_\Omega p\frac{\partial z_i}{\partial x_i}\,\mathrm{d}\Omega, \tag{4.27}$$

which are the integration-by-parts formulas needed to derive our variational form.

Now, let z_i be a smooth vector-valued function on $\overline{\Omega}$ that vanishes on Γ_0. Multiply both sides of equation (4.23a) with z_i, integrating over Ω, and utilizing (4.26) and (4.27), we find that

$$\int_\Omega z_i f_i\,\mathrm{d}\Omega = \int_\Omega z_i u_j\frac{\partial u_i}{\partial x_j}\,\mathrm{d}\Omega + \int_\Omega z_i\frac{\partial p}{\partial x_i}\,\mathrm{d}\Omega - \frac{1}{\mathrm{Re}}\int_\Omega z_i\nabla^2 u_i\,\mathrm{d}\Omega$$

$$= \int_\Omega z_i u_j\frac{\partial u_i}{\partial x_j}\,\mathrm{d}\Omega + \frac{1}{\mathrm{Re}}\int_\Omega \frac{\partial z_i}{\partial x_j}\frac{\partial u_i}{\partial x_j}\,\mathrm{d}\Omega - \frac{1}{\mathrm{Re}}\int_\Gamma n_j z_i\frac{\partial u_i}{\partial x_j}\,\mathrm{d}\Gamma - \int_\Omega p\frac{\partial z_i}{\partial x_i}\,\mathrm{d}\Omega + \int_\Gamma n_j z_j p\,\mathrm{d}\Gamma \tag{4.28}$$

$$= \int_\Omega z_i u_j\frac{\partial u_i}{\partial x_j}\,\mathrm{d}\Omega + \frac{1}{\mathrm{Re}}\int_\Omega \frac{\partial z_i}{\partial x_j}\frac{\partial u_i}{\partial x_j}\,\mathrm{d}\Omega - \int_\Omega p\frac{\partial z_i}{\partial x_i}\,\mathrm{d}\Omega,$$

where, in the last equality, the boundary integrals vanish on Γ_0 since $z_i = 0$ on Γ_0 and on Γ_1 due to boundary condition (4.23d). Moreover, multiplying equation (4.23b) with a smooth function q and integrating yields

$$\int_\Omega q\frac{\partial u_i}{\partial x_i}\,\mathrm{d}\Omega = 0 \tag{4.29}$$

Thus, we conclude that a classical solution (a twice continuously differentiable solution) to the Navier–Stokes equations satisfies the variational forms (4.28) and (4.29) for all smooth functions z_i and q such that z_i vanishes on Γ_0.

Similarly as for the advection–diffusion problem, the variational form will be used to define weak solutions, without explicit reference to the differential equations. A difference with advection–diffusion problem is that we here need *different* function spaces for the velocity components and the pressure. Also note that $u_i = g_i$ on Γ_0 whereas z_i vanishes on Γ_0. To avoid this last complication and simplify the exposition, we will only consider homogeneous boundary conditions, $g_i = 0$. Thus, the equations will be "driven" only by the right-hand side f_i, which, for instance, could be gravity or magnetic forcing for a electrically conducting fluid.

The pressure space is

$$H = L^2(\Omega) = \left\{q\mid \int_\Omega q^2\,\mathrm{d}\Omega < +\infty\right\},$$

and the space of velocity components is

$$V = \left\{ u \mid \int_\Omega \frac{\partial u}{\partial x_i} \frac{\partial u}{\partial x_i} \, \mathrm{d}\Omega < +\infty \ \text{ and } u = 0 \text{ on } \Gamma_0 \right\}.$$

For the analysis in section 4.2.4, it will be convenient to work with the space V of the velocity vector $\boldsymbol{u} = (u_1, u_2)$. Saying that $\boldsymbol{u} \in V$ is equivalent to saying that that each velocity component $u_i \in V$. The energy norm for elements of V is denoted

$$\|\boldsymbol{u}\|_{\boldsymbol{V}} = \left(\int_\Omega \frac{\partial u_i}{\partial x_j} \frac{\partial u_i}{\partial x_j} \, \mathrm{d}\Omega \right)^{1/2},$$

whereas the $L^2(\Omega)$ norm is

$$\|\boldsymbol{u}\|_{L^2(\Omega)} = \left(\int_\Omega u_i u_i \, \mathrm{d}\Omega \right)^{1/2}.$$

We assume that both boundary conditions really are active. In the case of only Dirichlet boundary condition, that is, that Γ_0 constitute the whole boundary, the pressure is only possible to specify uniquely up to an additive constant.

The variational problem defining weak solutions to equation (4.23) is

Find $u_i \in V$ and $p \in H$ such that
$$\int_\Omega z_i u_j \frac{\partial u_i}{\partial x_j} \, \mathrm{d}\Omega + \frac{1}{\mathrm{Re}} \int_\Omega \frac{\partial z_i}{\partial x_j} \frac{\partial u_i}{\partial x_j} \, \mathrm{d}\Omega - \int_\Omega p \frac{\partial z_i}{\partial x_i} \, \mathrm{d}\Omega = \int_\Omega z_i f_i \, \mathrm{d}\Omega \qquad \forall z_i \in V$$
$$\int_\Omega q \frac{\partial u_i}{\partial x_i} \, \mathrm{d}\Omega = 0 \qquad \forall q \in H$$

This is a variational problem of *mixed type*: two different spaces are involved. As for the advection–diffusion problem, the boundary conditions are incorporated in the variational formulation. The *essential boundary conditions* are here that $u_i = 0$ on Γ_0 and is explicitly assigned through the definition of V. The *natural boundary conditions* are the boundary conditions on Γ_1, implicitly specified through the variational form. Note that the natural boundary condition is different than for the advection–diffusion problem.

Remark 2. The mathematical properties of the Navier–Stokes equations are complicated, and important issues are still unresolved. In fact, there is a \$ 1 000 000 prize for the person that can develop a theory that can satisfyingly explain their behavior in three space dimensions! A short summary of what is known is the following.

For the *unsteady problem* on a given, finite time interval $(0, T)$, and

- in *two* space dimensions:

  - a unique weak solution exists for any square-integrable f and for any Re,
  - smooth data yield smooth solutions, so that weak solutions are classical solutions if data is smooth enough;

- in *three* space dimensions:

  - a weak solution exists for any square-integrable f and for any Re.
  - It is not known whether the weak solution always is unique (besides during some initial interval $(0, T^*)$, where the size of T^* is unknown).
  - It is not known whether smooth data always yields a smooth solution, or if singularities can evolve from smooth data.

The *steady* problem has at least one weak solution, in 2D as well as 3D. Note that the steady problem may have several solutions, even in 2D. $\square$

Note that the natural boundary condition here not just is a Neumann condition, but the more complicated condition (4.23d).

4.2.2 Finite-element approximations

To obtain a FEM, we choose subspaces $V_h \subset V$, $H_h \subset H$ of piecewise polynomials, and replace V with V_h and H with H_h in the variational form. In 2D and in components, we obtain

Find u_h, $v_h \in V_h$ and $p_h \in H_h$ such that

$$\int_\Omega z_h \left(u_h \frac{\partial u_h}{\partial x} + v_h \frac{\partial u_h}{\partial y} \right) d\Omega + \frac{1}{\mathrm{Re}} \int_\Omega \frac{\partial z_h}{\partial x_j} \frac{\partial u_h}{\partial x_j} d\Omega - \int_\Omega p_h \frac{\partial z_h}{\partial x} d\Omega = \int_\Omega z_h f_1 \, d\Omega \qquad \forall z_h \in V_h, \quad (4.30a)$$

$$\int_\Omega z_h \left(u_h \frac{\partial v_h}{\partial x} + v_h \frac{\partial v_h}{\partial y} \right) d\Omega + \frac{1}{\mathrm{Re}} \int_\Omega \frac{\partial z_h}{\partial x_j} \frac{\partial v_h}{\partial x_j} d\Omega - \int_\Omega p_h \frac{\partial z_h}{\partial y} d\Omega = \int_\Omega z_h f_2 \, d\Omega \qquad \forall z_h \in V_h, \quad (4.30b)$$

$$\int_\Omega q_h \left(\frac{\partial u_h}{\partial x} + \frac{\partial v_h}{\partial y} \right) d\Omega = 0. \qquad (4.30c)$$

We postpone for a while the question on how to choose the subspaces V_h and H_h.

4.2.3 The algebraic problem in 2D

Expanding p_h in basis for H_h, we obtain

$$p_h(x, y) = \sum_{n=1}^{N_p} p^{(n)} \psi^{(n)}(x, y). \qquad (4.31)$$

Likewise, expanding u_h, v_h in basis for V_h yields

$$u_h(x, y) = \sum_{n=1}^{N_u} u^{(n)} \varphi^{(n)}(x, y), \qquad v_h(x, y) = \sum_{n=1}^{N_u} v^{(n)} \varphi^{(n)}(x, y). \qquad (4.32)$$

Now insert expansions (4.31) and (4.32) into equations (4.30). In (4.30a) and (4.30b), choose $z_h = \varphi^{(m)}$ for $m = 1, \ldots, N_u$; in (4.30c), choose $q_h = \psi^{(m)}$ for $m = 1, \ldots, N_p$. Then, equations (4.30) become

$$\sum_{n=1}^{N_u} u^{(n)} \int_\Omega \varphi^{(m)} \left(u_h \frac{\partial \varphi^{(n)}}{\partial x} + v_h \frac{\partial \varphi^{(n)}}{\partial y} \right) d\Omega + \frac{1}{\mathrm{Re}} \sum_{n=1}^{N_u} u^{(n)} \int_\Omega \left(\frac{\partial \varphi^{(m)}}{\partial x} \frac{\partial \varphi^{(n)}}{\partial x} + \frac{\partial \varphi^{(m)}}{\partial y} \frac{\partial \varphi^{(n)}}{\partial y} \right) d\Omega$$

$$- \sum_{n=1}^{N_p} p^{(n)} \int_\Omega \frac{\partial \varphi^{(m)}}{\partial x} \psi^{(n)} d\Omega = \int_\Omega \varphi^{(m)} f_1 \, d\Omega \qquad m = 1, \ldots, N_u$$

$$\sum_{n=1}^{N_u} v^{(n)} \int_\Omega \varphi^{(m)} \left(u_h \frac{\partial \varphi^{(n)}}{\partial x} + v_h \frac{\partial \varphi^{(n)}}{\partial y} \right) d\Omega + \frac{1}{\mathrm{Re}} \sum_{n=1}^{N_u} v^{(n)} \int_\Omega \left(\frac{\partial \varphi^{(m)}}{\partial x} \frac{\partial \varphi^{(n)}}{\partial x} + \frac{\partial \varphi^{(m)}}{\partial y} \frac{\partial \varphi^{(n)}}{\partial y} \right) d\Omega \quad (4.33)$$

$$- \sum_{n=1}^{N_p} p^{(n)} \int_\Omega \frac{\partial \varphi^{(m)}}{\partial y} \psi^{(n)} d\Omega = \int_\Omega \varphi^{(m)} f_2 \, d\Omega \qquad m = 1, \ldots, N_u$$

$$\sum_{n=1}^{N_u} u^{(n)} \int_\Omega \psi^{(m)} \frac{\partial \varphi^{(n)}}{\partial x} d\Omega + \sum_{n=1}^{N_u} v^{(n)} \int_\Omega \psi^{(m)} \frac{\partial \varphi^{(n)}}{\partial y} d\Omega = 0 \qquad m = 1, \ldots, N_p$$

Placing the coefficients into column matrices,

$$u = \left(u^{(1)}, \ldots, u^{(N_u)} \right)^T, \qquad v = \left(v^{(1)}, \ldots, v^{(N_u)} \right)^T,$$

$$p = \left(p^{(1)}, \ldots, p^{(N_p)} \right)^T,$$

we can write the system (4.33) in the matrix–vector form

$$\begin{pmatrix} C(u_h, v_h) + \frac{1}{\mathrm{Re}} K & 0 & G^{(x)} \\ 0 & C(u_h, v_h) + \frac{1}{\mathrm{Re}} K & G^{(y)} \\ -G^{(x)T} & -G^{(y)T} & 0 \end{pmatrix} \begin{pmatrix} u \\ v \\ p \end{pmatrix} = \begin{pmatrix} b^{(x)} \\ b^{(y)} \\ 0 \end{pmatrix}, \qquad (4.34)$$

where the matrix and vector components are

$$K_{mn} = \int_\Omega \left(\frac{\partial \varphi^{(m)}}{\partial x} \frac{\partial \varphi^{(n)}}{\partial x} + \frac{\partial \varphi^{(m)}}{\partial y} \frac{\partial \varphi^{(n)}}{\partial y} \right) \mathrm{d}\Omega, \qquad C_{mn}(u_h, v_h) = \int_\Omega \varphi^{(m)} \left(u_h \frac{\partial \varphi^{(n)}}{\partial x} + v_h \frac{\partial \varphi^{(n)}}{\partial y} \right) \mathrm{d}\Omega,$$

$$G_{mn}^{(x)} = -\int_\Omega \psi^{(n)} \frac{\partial \varphi^{(m)}}{\partial x} \mathrm{d}\Omega, \quad G_{mn}^{(y)} = -\int_\Omega \psi^{(n)} \frac{\partial \varphi^{(m)}}{\partial y} \mathrm{d}\Omega, \quad b_m^{(x)} = \int_\Omega \varphi^{(m)} f_1 \mathrm{d}\Omega, \quad b_m^{(y)} = \int_\Omega \varphi^{(m)} f_2 \mathrm{d}\Omega.$$

$$(4.35)$$

Matrix K represents an approximation of the discrete negative Laplacian $-\nabla^2$; $C(u_h, v_h)$ the discrete advection operator $u\frac{\partial}{\partial x} + v\frac{\partial}{\partial y}$; $G^{(x)}$ and $G^{(y)}$ the discrete gradient ∇; and $G^{(x)T}$ and $G^{(y)T}$ the discrete divergence. That is, the structure of the Navier–Stokes equations are directly reflected in the nonlinear system (4.34). We obtained the same structure of the nonlinear equation for the finite-volume discretization, except that here, it is *guaranteed* the the last block row of the matrix is the negative transpose of the last block column.

4.2.4 Stability

So far, the approximating spaces V_h and H_h have not been specified. The counting argument of example 2 indicates that not any choice is good. We will limit the discussion to the *Stokes equations*, whose finite-element formulation reads

Find $u_i^h \in V_h$ and $p_h \in H_h$ such that

$$\int_\Omega \frac{\partial z_i^h}{\partial x_j} \frac{\partial u_i^h}{\partial x_j} \mathrm{d}\Omega - \int_\Omega p_h \frac{\partial z_i^h}{\partial x_i} \mathrm{d}\Omega = \int_\Omega z_i^h f_i \mathrm{d}\Omega \qquad \forall z_i^h \in V_h, \tag{4.36a}$$

$$\int_\Omega q_h \frac{\partial u_i^h}{\partial x_i} \mathrm{d}\Omega = 0 \qquad \forall q_h \in H_h. \tag{4.36b}$$

The Stokes equations is a limit case of the Navier–Stokes equations for very low Reynolds numbers and assume that inertia can be neglected compared to viscous forces. The Stokes equations may be used to model very viscous flow, creeping flow, lubrication, but also flow of common fluids (like air and water) at the micro scale. Due to the lack of nonlinear advection, these are *linear* equations. Mathematically, the Stokes equations are much easier to analyze than the full Navier–Stokes equations. Indeed, there exists a unique weak solutions for each square-integrable f_i both in two and three space dimension. The reason to start the analysis on the Stokes equation is that a stable Stokes discretization is necessary to obtain a stable Navier–Stokes discretization.

As for the Navier–Stokes equations, we require that $V_h \subset V$ and $H_h \subset H$. Recall that each function in V and H is required to be bounded in the energy and the $L^2(\Omega)$ norm, respectively. Thus, in makes sense to require that the velocity and pressure approximations satisfy the same bounds, that is,

$$\|p_h\|_{L^2(\Omega)} = \left(\int_\Omega p_h^2 \mathrm{d}\Omega \right)^{1/2} \leq C \left(\int_\Omega f_i f_i \mathrm{d}\Omega \right)^{1/2} = C\|\boldsymbol{f}\|_{L^2(\Omega)}, \tag{4.37a}$$

$$\|\boldsymbol{u}_h\|_{\boldsymbol{V}} = \left(\int_\Omega \frac{\partial u_i^h}{\partial x_j} \frac{\partial u_i^h}{\partial x_j} \mathrm{d}\Omega \right)^{1/2} \leq C\|\boldsymbol{f}\|_{L^2(\Omega)}, \tag{4.37b}$$

where the constant C should not depend on h. This implies that the approximations will not blow up when the mesh is refined.

Choosing $z_i^h = u_i^h$ in equation (4.36a), we obtain

$$\int_\Omega \frac{\partial u_i^h}{\partial x_j} \frac{\partial u_i^h}{\partial x_j} \mathrm{d}\Omega - \int_\Omega p_h \frac{\partial u_i^h}{\partial x_i} \mathrm{d}\Omega = \int_\Omega \frac{\partial u_i^h}{\partial x_j} \frac{\partial u_i^h}{\partial x_j} \mathrm{d}\Omega = \int_\Omega u_i^h f_i \mathrm{d}\Omega,$$

where the first equality follows from equation (4.36b). Thus,

$$\|\boldsymbol{u}_h\|_{\boldsymbol{V}}^2 = \int_\Omega u_i^h f_i \mathrm{d}\Omega \leq \|\boldsymbol{u}\|_{L^2(\Omega)} \|\boldsymbol{f}\|_{L^2(\Omega)} \leq C\|\boldsymbol{u}\|_{\boldsymbol{V}} \|\boldsymbol{f}\|_{L^2(\Omega)} \tag{4.38}$$

where the Cauchy–Schwarz inequality yields the first inequality, and the Poincaré inequality the second. We thus conclude from expression (4.38) that

$$\|\boldsymbol{u}_h\|_{\boldsymbol{V}} \leq C\|\boldsymbol{f}\|_{L^2(\Omega)}, \tag{4.39}$$

that is, *any* Galerkin approximation of the velocity in the Stokes equations is stable! For bad choices of subspaces, we will of course obtain inaccurate velocity approximations, but they will *not* blow up as the mesh is refined, since their energy norm is bounded by the given data f_i.

Regarding the pressure, the situation is more complicated. Not any combination H_h and $\boldsymbol{V}_h$ yield stable pressure approximations in the sense of (4.37a). We will derive a compatibility condition between the velocity and pressure spaces, *the LBB condition*, necessary to yield stable pressure approximations.

4.2.5   The LBB condition

Rearranging equation (4.36a) implies that for each $z_i^h \in V_h$,

$$
\begin{aligned}
\int_\Omega p_h \frac{\partial z_i^h}{\partial x_i}\, \mathrm{d}\Omega &= \int_\Omega \frac{\partial z_i^h}{\partial x_j}\frac{\partial u_i^h}{\partial x_j}\, \mathrm{d}\Omega - \int_\Omega z_i^h f_i\, \mathrm{d}\Omega \\
\text{(Cauchy–Schwarz)} &\le \left(\int_\Omega \frac{\partial z_i^h}{\partial x_j}\frac{\partial z_i^h}{\partial x_j}\, \mathrm{d}\Omega\right)^{1/2}\left(\int_\Omega \frac{\partial u_i^h}{\partial x_j}\frac{\partial u_i^h}{\partial x_j}\, \mathrm{d}\Omega\right)^{1/2} + \left(\int_\Omega z_i^h z_i^h\, \mathrm{d}\Omega\right)^{1/2}\left(\int_\Omega f_i f_i\, \mathrm{d}\Omega\right)^{1/2} \\
&= \|\boldsymbol{z}_h\|_{\boldsymbol{V}}\|\boldsymbol{u}_h\|_{\boldsymbol{V}} + \|\boldsymbol{z}_h\|_{L^2(\Omega)}\|\boldsymbol{f}\|_{L^2(\Omega)} \\
\text{(Poincaré)} &\le \|\boldsymbol{z}_h\|_{\boldsymbol{V}}\|\boldsymbol{u}_h\|_{\boldsymbol{V}} + \|\boldsymbol{z}_h\|_{V}\|\boldsymbol{f}\|_{L^2(\Omega)} \\
\text{(by (4.39))} &\le C\|\boldsymbol{z}_h\|_{\boldsymbol{V}}\|\boldsymbol{f}\|_{L^2(\Omega)} + \|\boldsymbol{z}_h\|_{V}\|\boldsymbol{f}\|_{L^2(\Omega)}.
\end{aligned}
\tag{4.40}
$$

Dividing expression (4.40) with $\|\boldsymbol{z}_h\|_V$ yields that

$$
\frac{1}{\|\boldsymbol{z}_h\|_V}\int_\Omega p_h \frac{\partial z_i^h}{\partial x_i}\, \mathrm{d}\Omega \le (C+1)\|\boldsymbol{f}\|_{L^2(\Omega)}
$$

for each $z_i^h \in V_h$, from which it follows that there is a $C > 0$ such that

$$
\max_{0 \ne z_i \in V}\frac{1}{\|\boldsymbol{z}_h\|_V}\int_\Omega p_h \frac{\partial z_i^h}{\partial x_i}\, \mathrm{d}\Omega \le C\|\boldsymbol{f}\|_{L^2(\Omega)}.
\tag{4.41}
$$

We have thus found a bound on the discrete pressure in the "exotic" norm (4.16). However, we were aiming for the bound (4.37a). Thus, if it happens that

$$
\alpha\|p_h\|_{L^2(\Omega)} \le \max_{0 \ne z_i \in V_h}\frac{1}{\|\boldsymbol{z}_h\|_V}\int_\Omega p_h \frac{\partial z_i^h}{\partial x_i}\, \mathrm{d}\Omega
\tag{4.42}
$$

for some $\alpha > 0$ independent of h, then it is immediate that $\|p_h\|_{L^2(\Omega)} \le C\|\boldsymbol{f}\|_{L^2(\Omega)}$ for some $C > 0$.

Condition (4.42) says that our exotic norm is *stronger* than the $L^2(\Omega)$-norm for p_h. The LBB-condition is a condition on the pairing of spaces V_h and H_h that requires the exotic norm to be stronger than the $L^2(\Omega)$-norm for *each* function $q_h \in H_h$. The derivation above proves thus that the LBB-condition is sufficient for the pressure to be stably determined by data:

Theorem 3. *Assume that the LBB-condition holds for the spaces H_h, V_h. That is, assume that there is an $\alpha > 0$ independent of h, such that, for each $q_h \in H_h$,*

$$
\alpha\left(\int_\Omega q_h^2\, \mathrm{d}\Omega\right)^{1/2} \le \max_{0 \ne z_i \in V_h}\frac{1}{\|\boldsymbol{z}_h\|_V}\int_\Omega q_h \frac{\partial z_i^h}{\partial x_i}\, \mathrm{d}\Omega,
\tag{4.43}
$$

then there is a $C > 0$ such that

$$
\left(\int_\Omega p_h^2\, \mathrm{d}\Omega\right)^{1/2} \le C\left(\int_\Omega |\boldsymbol{f}|^2\, \mathrm{d}\Omega\right)^{1/2}
$$

holds, independently of h.

The LBB condition (4.43) is satisfied for $V_h = V$ and $H_h = H$. That is, the pressure (before discretization) is stably determined by data. The expression $\int_\Omega q_h \frac{\partial z_i^h}{\partial x_i}\, \mathrm{d}\Omega$ represents the discrete gradient of q_h (see § 4.2.3). The LBB condition thus means that a zero discrete pressure gradient implies a zero value of the pressure. Conversely, if the LBB condition is *not* satisfied, it means that the discrete pressure gradient may be small even when the pressure is not small: The discrete gradient cannot "feel" that the pressure is large, an effect that usually manifests itself as wild pressure oscillations.
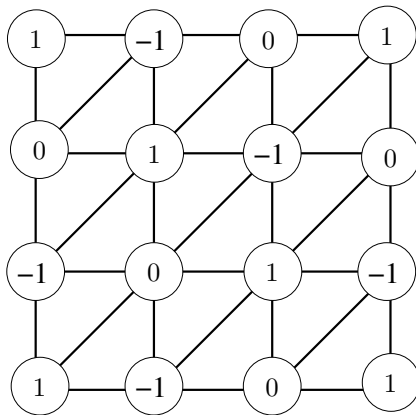
$$
\begin{array}{l}
\Omega \\
M^2 \\
M \\
m \\
m+2 \\
\\
h \\
V \\
V_h \\
u \\
u_h \\
\Gamma_0 \\
\Gamma_1 \\
\Omega
\end{array}
\qquad
\begin{array}{cccc}
\boxed{1} & \boxed{-1} & \boxed{0} & \boxed{1} \\
\boxed{0} & \boxed{1} & \boxed{-1} & \boxed{0} \\
\boxed{-1} & \boxed{0} & \boxed{1} & \boxed{-1} \\
\boxed{1} & \boxed{-1} & \boxed{0} & \boxed{1}
\end{array}
$$

Figure 4.15: A checkerboard mode for equal-order interpolation on a regular triangular mesh.

4.2.6 Mass conservation

The integral $\int_\Gamma \rho\, n_i u_i \, \mathrm{d}\Gamma$ yields the total flux of mass(in kg/s) through the boundary. There is no net mass-flux through the boundary for a constant-density flow, so $\int_\Gamma \rho\, n_i u_i \, \mathrm{d}\Gamma = 0$. A velocity approximation u_i^h is is *globally mass conservative* if

$$
\int_\Gamma n_i u_i^h \, \mathrm{d}\Gamma = 0,
$$

or, equivalently, if

$$
\int_\Omega \frac{\partial u_i^h}{\partial x_i} \, \mathrm{d}\Omega = 0,
$$

by the divergence theorem (4.3). Recall from equation (4.30c) that

$$
\int_\Omega q_h \frac{\partial u_i^h}{\partial x_i} \, \mathrm{d}\Omega = 0 \qquad \forall q_h \in H_h.
$$

A Galerkin approximation is thus globally mass conservative if $1 \in H_h$, that is, if constant functions can be represented exactly in H_h. All reasonable FE approximation satisfy this.

A finite-element approximation is *locally mass conservative* if

$$
\int_K \frac{\partial u_i^h}{\partial x_i} \, \mathrm{d}\Omega = 0,
$$

for each element K in the mesh. Not all finite-element approximations are locally mass conservative. If the pressure approximations consist of piecewise constants on each element, the FE approximation will be locally mass conservative. However, it will *not* be locally mass conservative if the pressure approximations are continuous and piecewise linear.

4.2.7 Choice of finite elements. Accuracy

Now we consider a *regular triangulation* of a 2D domain Ω, that is, a triangulation satisfying a mesh quality condition of the sort discussed in section 4.1.5.

"Equal-order interpolation"

Let us start by trying the approximation space we used for the advection–diffusion problem (section 4.1.1). That is, we use continuous functions that are linear on each triangle both for the functions in H_h and V_h.

This pair does *not* satisfy the LBB condition and yields an unstable discretization. In particular, the system matrix (4.34) is *singular*: the discrete gradient matrix G has linearly dependent columns. Thus, there is at least one nonzero N_p-vector p^c such that $Gp^c = 0$. Corresponding function $p_h^c \in H_h$, whose nodal values are equal to the elements of p^c is called a *checkerboard mode*.

Figure 4.15 depicts the nodal values of a checkerboard mode for equal-order interpolation. To see this, consider the element contribution, associated with a triangle T_n, to the ith row of vector Gp^c (notice from the expressions in figure 4.5 that $\frac{\partial \phi_i}{\partial x}$ is constant on each triangle):

$$
-\int_{T_n} p_h^c \frac{\partial \phi_i}{\partial x} \, \mathrm{d}\Omega = -\frac{\partial \phi_i}{\partial x}\bigg|_{T_n} \int_{T_n} p_h^c \, \mathrm{d}\Omega \equiv 0,
$$

$$h$$
$$V$$
$$V_h$$
$$u$$
$$u_h$$
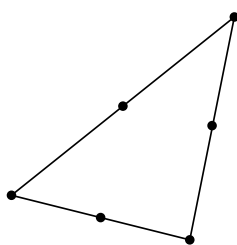$$\Gamma_0$$
$$\Gamma_1$$
$$\Omega$$

Figure 4.16: The evaluation points at each triangle for the continuous, piecewise quadratic velocity approximations of the Taylor–Hood pair.

since the mean value of the function p_h^c vanishes on each triangle, as can be seen from figure 4.15. The right side of the LBB condition (4.43) vanishes for $q_h = p_h^c$, which immediately implies that the LBB cannot hold for a space H_h that includes p_h^c. This (and other) checkerboard mode will pollute the solution of the Stokes as well as Navier–Stokes equations..

Constant pressure, (bi)linear velocities

Now we consider a triangulation either of triangles or rectangles. Let the functions in H_h be piecewise constant on each element. In case of triangular elements, the space V_h will be continuous functions, piecewise linear on each element, whereas for quadrilateral elements, continuous functions that are piecewise bilinear on each rectangle comprise V_h.

Remark 3. The pressure approximations need *not* to be continuous in order for $H_h \subset H$. However, if $V_h \subset V$, the velocity approximations cannot be discontinuous, since ∇v is not a function for discontinuous v.

This choice leads to a locally mass-conserving approximation. However, for triangular elements, the counting argument of example 2 applies here and indicates problems with this choice of elements. Indeed, the LBB conditions is not satisfied for this unstable discretization. Checkerboard modes similar as in figure 4.15 exist. Still, the constant pressure—bilinear velocity space on rectangles is in widespread engineering use! "Fixes" have been developed to take care of pressure oscillations. For instance, the checkerboard mode can be filtered out from the discrete pressures. Moreover, common iterative methods to solve the resulting discrete equations (such as the projection schemes) implies a stabilization of the discretization.

The Taylor–Hood pair

Here, the functions in H_h and V_h are globally continuous and, on each triangle,

- $p_h \in H_h$ is *linear*, whereas

- u_h, $v_h \in V_h$ is *quadratic*.

Thus, on each triangle, we have

$$u_h = a + b\,x + c\,y + d\,xy + e\,x^2 + f y^2$$

The six coefficients a–f are uniquely determined by u_h's values at the triangle vertices and midpoints (figure 4.16).

A basis $\left\{\phi^{(m)}(x_i)\right\}_{m=1}^{N_u}$ of continuous, piecewise quadratic functions interpolates the nodal values of figure 4.16, so that $u_h \in V_h$ can be expressed as $u_h(x_i) = \sum_{m=1}^{N_u} u_i \phi^{(m)}(x_i)$. There are *two* kinds of basis functions here, illustrated in figures 4.17 and 4.18.

The LBB condition is satisfied for the Taylor–Hood pair, and the following error estimates holds for a smooth solution to the Navier–Stokes equation:

$$\|u - u_h\|_{L^2(\Omega)} \leq Ch^3$$
$$\|p - p_h\|_{L^2(\Omega)} \leq Ch^2$$

The Taylor–Hood pair is globally, but not locally mass conservative.

The Taylor–Hood pair can be generalized to higher order. Then, the pressure and velocity approximations will be continuous functions, consising of piecewise polynomials of degree k for pressure and $k+1$ for velocity ($k \geq 1$) on each triangle.
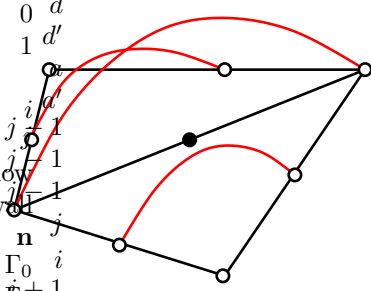
Figure 4.17: The basis function $\phi^{(m)}(x_i)$ when m corresponds to an edge-midpoint node
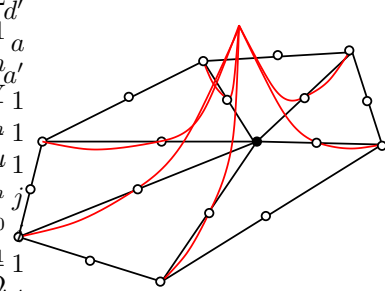

Figure 4.18: The basis function $\phi^{(m)}(x_i)$ when m corresponds to a corner node
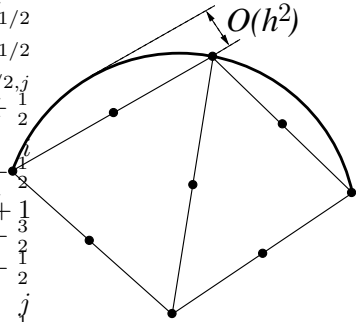

Figure 4.19: Approximating a curved boundary with a triangle sides leads to an $O(h^2)$ error of the boundary condition.
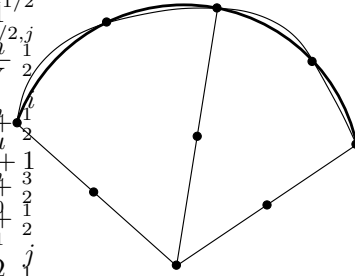

Figure 4.20: Isoparametric elements use polynomials of the same order as used for the FE approximations to approximate the shape of the boundary.

Remark 4.1. Inaccuracies in approximations of the domain boundary may reduce the convergence rate of higher-order approximations. For instance, a straight-forward triangulation of a domain with a curved boundary will lead to a boundary-condition error at the mid nodes of $O(h^2)$ (figure 4.19). This is fine for piecewise-linear approximations since the error anyway is $O(h^2)$. However, this inaccuracy at the boundary results in a *half-order* reduction of the convergence rate of piecewise quadratic approximations. Using *curved elements* restores convergence rate. The most common strategy for curved elements is known as *Isoparametric Elements*: piecewise polynomials of the same degree as used in the FE approximation are used to approximate the shape of the boundary (figure 4.20).

A stable approximation with piecewise-linear velocities and pressures

Instead of using different approximation *orders*, as in the Taylor-Hood pair, we here consider different *meshes* for velocity and pressure. Both the velocity and pressure approximations consist of continuous, piecewise-linear functions on triangles, but each pressure triangle is subdivided into four velocity triangles as in figure 4.21.

This is a stable approximation satisfying the LBB condition, and the following error estimates holds for
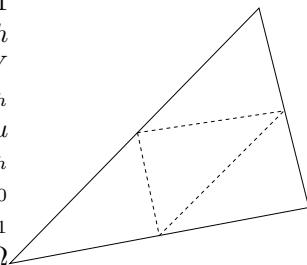

Figure 4.21: Subdividing a pressure triangle into four velocity triangles yields a stable approximation with continuous, piecewise-linear functions for both velocity and pressure.
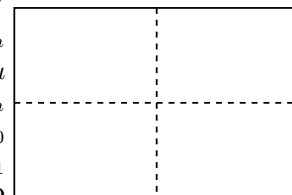
Figure 4.22: Subdividing a pressure rectangle into four velocity rectangles yields a stable approximation with continuous piecewise-bilinear functions for both velocity and pressure.
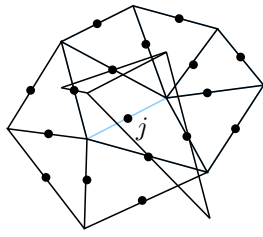
Figure 4.23: The basis functions associated with the velocity approximation for a nonconforming but stable discretization.
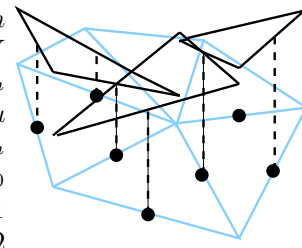

Figure 4.24: Approximations spanned by the basis functions (4.23) yields piecewise-linear functions that are continuous only along at the edge midpoints, in general.

a smooth solution to the Navier–Stokes equation:

$$\|\boldsymbol{u} - \boldsymbol{u}_h\|_{L^2(\Omega)} \leq Ch^2$$
$$\|p - p_h\|_{L^2(\Omega)} \leq Ch$$

These approximations use the same number of unknowns and the same nodal locations as for the Taylor–Hood pair, but are one order less accurate. Calculating the matrix elements (4.35) is however somewhat easier than for the Taylor–Hood pair.

There is also a version of this discretization for rectangular meshes: Each pressure rectangle is then subdivided into four velocity rectangles, as in figure 4.22. Both the velocity and pressure approximations consist of continuous and piecewise-bilinear functions.

A nonconforming method

The discussion after example 2 suggested a strategy to address the problem with the overdetermined incompressibility condition, namely to use nodal points on the *edge mid points* for the velocity. To accomplish this, consider basis functions, associated with the edges, of the type depicted in figure 4.23. Basis function ϕ_j is linear on each triangle and continuous along edge j (but discontinuous along four edges!). If x^i, y^i are the coordinates of the mid point of edge i, we have

$$\phi_j(x^i, y^i) = \begin{cases} 1 & \text{for } i = j, \\ 0 & \text{for } i \neq j. \end{cases}$$

Now define the space of the velocity components V_h from all possible expansions

$$u_h(x, y) = \sum_{j=1}^{N} u_j \phi_j(x, y), \qquad v_h(x, y) = \sum_{j=1}^{N} v_j \phi_j(x, y),$$

Here, N is the total number of edges, excluding those on Γ_1. Note that u_h will be continuous only at edge mid points in general. Thus, $V_h \not\subset V$ since ∇u_h is not a square-integrable (in fact, constant) function. Violating a property like $V_h \subset V$ is called a *variational crime*. However, ∇u_h restricted on each element is a square-integrable function. Letting H_h be piecewise constant on each triangle and V_h defined as above, we define the *nonconforming* FE approximation:

Find u_h, $v_h \in V_h$ and $p_h \in H_h$ such that

$$\sum_{n=1}^{M} \int_{T_n} z_h u_h \frac{\partial u_h}{\partial x} \, d\Omega + \sum_{n=1}^{M} \int_{T_n} z_h v_h \frac{\partial u_h}{\partial y} \, d\Omega + \frac{1}{\text{Re}} \sum_{n=1}^{M} \int_{T_n} \frac{\partial z_h}{\partial x_j} \frac{\partial u_h}{\partial x_j} \, d\Omega - \sum_{n=1}^{M} \int_{T_n} p_h \frac{\partial z_h}{\partial x} \, d\Omega = \int_{\Omega} z_h f_1 \, d\Omega \qquad \forall \, z_h \in V_h,$$

$$\sum_{n=1}^{M} \int_{T_n} z_h u_h \frac{\partial v_h}{\partial x} \, d\Omega + \sum_{n=1}^{M} \int_{T_n} z_h v_h \frac{\partial v_h}{\partial y} \, d\Omega + \frac{1}{\text{Re}} \sum_{n=1}^{M} \int_{T_n} \frac{\partial z_h}{\partial x_j} \frac{\partial v_h}{\partial x_j} \, d\Omega - \sum_{n=1}^{M} \int_{T_n} p_h \frac{\partial z_h}{\partial y} \, d\Omega = \int_{\Omega} z_h f_2 \, d\Omega \qquad \forall \, z_h \in V_h,$$

$$\sum_{n=1}^{M} \int_{T_n} q_h \left(\frac{\partial u_h}{\partial x} + \frac{\partial v_h}{\partial y} \right) d\Omega = 0 \qquad \forall \, q_h \in H_h,$$

where M is the number of triangles.

The fact that $V_h \not\subset V$ complicates the analysis of this discretization. Nevertheless, the approximation is stable, although not as accurate as the Taylor–Hood pair, for instance. Other nice properties with this method is that it is locally mass conservative, and quite easy to implement.

But maybe the most interesting with this discretization is that it allows for a construction of a *divergence free velocity basis*. In all types of discretizations discussed so far, including the present, we have used the same basis for the u_h and v_h components. By a clever combination of basis functions of the type illustrated in figure 4.23, it is possible to construct a new vector-valued basis functions $\boldsymbol{\eta}_j = (z_h^{(j)}, w_h^{(j)})$ for the velocity having the property

$$\nabla \cdot \boldsymbol{\eta}_j = \frac{\partial z_h^{(j)}}{\partial x} + \frac{\partial w_h^{(j)}}{\partial y} = 0.$$

Expanding the velocity in this basis,

$$\boldsymbol{u}_h = (u_h, v_h) = \sum_{j=1}^{M} u_j \boldsymbol{\eta}_j, \tag{4.44}$$

yields that $\nabla \cdot \boldsymbol{u}_h = 0$. Inserting expansion (4.44) into equations (4.30), and choosing $(z_h, w_h) = \boldsymbol{\eta}_i$, the continuity equation and the pressure variable vanishes, and equations (4.30) reduce to

$$\sum_{j=1}^{M} u_j \int_\Omega \boldsymbol{\eta}_i \cdot (\boldsymbol{u}_h \cdot \nabla) \boldsymbol{\eta}_j \, d\Omega + \nu \sum_{j=1}^{M} u_j \int_\Omega \nabla \boldsymbol{\eta}_i \cdot \nabla \boldsymbol{\eta}_j \, d\Omega + \sum_{j=1}^{dN_u} u_j \int_\Omega \boldsymbol{\eta}_i \cdot (\boldsymbol{u}_h \cdot \nabla) \boldsymbol{\eta}_j \, d\Omega = \int_\Omega \boldsymbol{\eta}_i \cdot \boldsymbol{f} \, d\Omega, \tag{4.45}$$

for $i = 1, \ldots, M$. The Navier–Stokes equations then reduces to a vector-valued, non-linear advection–diffusion problem, quite similar to equation (4.10). This leads to a substantial simplification when designing an algorithm to solve the discretized equations; in fact, one of the great challenges for any solver of the Navier–Stokes equations is how to treat the incompressibility condition (4.30c). Unfortunately, the construction of the basis functions $\boldsymbol{\eta}_j$ is not straightforward.

Stabilization of unstable discretizations

Stability of the choices of elements presented in sections 4.2.7–4.2.7 relied on manipulations of the local polynomial order, the meshes, or the conformity of the method. These manipulations complicate the implementation. An alternative is to use the same approximations for velocity and pressure (equal-order interpolation) combined with a *stabilization method*. This circumvents the LBB condition.

We will present a very simple idea of this sort for the Stokes equations. First choose the *same* type of approximations for the pressure and the velocity components, for instance continuous, piecewise-linear functions on a triangular mesh, and replace equations (4.36) with

Find $u_i^h \in V_h$ and $p_h \in H_h$ such that

$$\int_\Omega \frac{\partial z_i^h}{\partial x_j} \frac{\partial u_i^h}{\partial x_j} \, d\Omega - \int_\Omega p_h \frac{\partial z_i^h}{\partial x_i} \, d\Omega = \int_\Omega z_i^h f_i \, d\Omega \qquad \forall \, z_i^h \in V_h, \tag{4.46a}$$

$$\epsilon \int_\Omega \frac{\partial q_h}{\partial x_i} \frac{\partial p_h}{\partial x_i} \, d\Omega + \int_\Omega q_h \frac{\partial u_i^h}{\partial x_i} \, d\Omega = 0 \qquad \forall \, q_h \in H_h., \tag{4.46b}$$

for some small $\epsilon > 0$. Equation (4.46b) formally inconsistent by $O(\epsilon)$ with corresponding variational form. More advanced stabilization methods avoids this inconsistency by using a term that vanishes as $h \to 0$.

The main advantage with stabilization methods is the simplified implementation, but the method introduces an extra parameter that may need judicious tuning. Note also that the increased number of pressure unknowns, as compared with the discretization in section 4.2.7, does *not* increase the accuracy. The added resolution introduced is filtered away by the introduction of the stability term.

To see that approximation (4.46) is stable, choose $z_i^h = u_i^h$, $q_h = p_h$ and add equations (4.46a)

and (4.46b),

$$\int_\Omega \frac{\partial u_i^h}{\partial x_i} \frac{\partial u_i^h}{\partial x_i} \, d\Omega + \epsilon \int_\Omega \frac{\partial p_h}{\partial x_i} \frac{\partial p_h}{\partial x_i} \, d\Omega = \int_\Omega u_i^h f_i \, d\Omega$$

$$(\text{Cauchy–Schwarz}) \leq \left(\int_\Omega u_i^h u_i^h \, d\Omega \right)^{1/2} \left(\int_\Omega f_i f_i \, d\Omega \right)^{1/2}$$

$$(\text{Poincaré}) \leq C \left(\int_\Omega \frac{\partial u_i^h}{\partial x_i} \frac{\partial u_i^h}{\partial x_i} \, d\Omega \right)^{1/2} \left(\int_\Omega f_i f_i \, d\Omega \right)^{1/2}$$

$$\leq C \left(\epsilon \int_\Omega \frac{\partial p_h}{\partial x_i} \frac{\partial p_h}{\partial x_i} \, d\Omega + \int_\Omega \frac{\partial u_i^h}{\partial x_i} \frac{\partial u_i^h}{\partial x_i} \, d\Omega \right)^{1/2} \left(\int_\Omega f_i f_i \, d\Omega \right)^{1/2}.$$

Dividing and squaring yields the stability estimate

$$\int_\Omega \frac{\partial u_i^h}{\partial x_i} \frac{\partial u_i^h}{\partial x_i} \, d\Omega + \epsilon \int_\Omega \frac{\partial p_h}{\partial x_i} \frac{\partial p_h}{\partial x_i} \, d\Omega \leq C \int_\Omega f_i f_i \, d\Omega.$$

Since $C > 0$ does not depend on h, both the velocity and pressure approximations cannot blow up as $h \to 0$, even though the discretization is unstable for $\epsilon = 0$.

Appendix A

Background material

A.1   Iterative solutions to linear systems

Gauss-Seidel method

The Laplace equation on a Cartesian grids can be discretized as
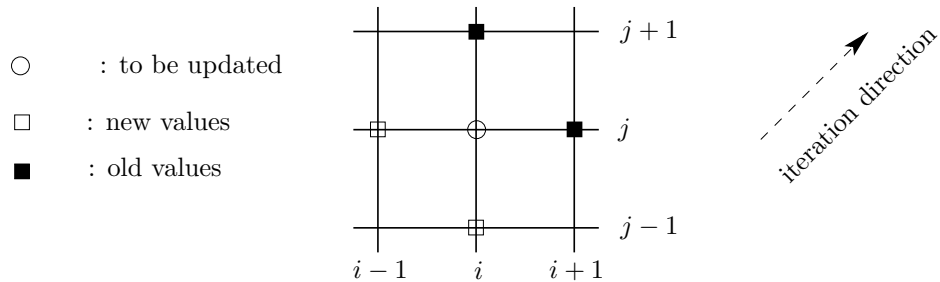
$$\Phi_{i+1,j} - 2\phi_{i,j} + \Phi_{i-1,j} + \beta^2\left(\Phi_{i,j+1} - 2\Phi_{i,j} + \Phi_{i,j-1}\right) = 0$$

where $\beta = \Delta x/\Delta y$. We can solve for $\Phi_{i,j}$,

$$\Phi_{i,j} = \frac{\Phi_{i+1,j} + \Phi_{i-1,j} + \beta^2\left(\Phi_{i,j+1} + \Phi_{i,j-1}\right)}{2\left(1 + \beta^2\right)}$$

Gauss-Seidel uses this expression to update $\Phi_{i,j}$ (using the already updated values calculated in same iteration), i.e.

$$\Phi_{i,j}^{k+1} = \frac{\Phi_{i+1,j}^{k} + \Phi_{i-1,j}^{k+1} + \beta^2\left(\Phi_{i,j+1}^{k} + \Phi_{i,j-1}^{k+1}\right)}{2\left(1 + \beta^2\right)}$$

○	: to be updated	
□	: new values	
■	: old values	

This iteration method has a slow convergence, it is possible to show

$$\|\mathbf{\Phi} - \mathbf{\Phi}^k\| \leq \rho^m \|\mathbf{\Phi} - \mathbf{\Phi}^0\|$$

where

$$\rho = 1 - \mathcal{O}\left(h^2\right) \qquad h = \Delta x = \Delta y$$

e.i. the error is reduced by $\mathcal{O}\left(h^2\right)$ each iteration. Requiring an error reduction to $\mathcal{O}\left(h^2\right)$ the number of iterations must satisfy

$$\rho^m = \mathcal{O}\left(h^2\right)$$

which implies that

$$m = \mathcal{O}\left(\frac{\ln(h)}{\ln(\rho)}\right) = \mathcal{O}\left(\frac{\ln(h)}{\ln(1 - \mathcal{O}(h^2))}\right) = \mathcal{O}\left(-h^2\ln(h)\right)$$

To proceed we note that we have $N = n^2$ unknown interior nodes, see Figure A.1. Thus

$$\Omega$$
$$M^2$$
$$M \quad h = \Delta x = \Delta y = \frac{1}{n+1} \approx n^{-1} = N^{-1/2}$$
$$m$$
which implies that
$$m+2$$
$$1$$
$$h \qquad\qquad m = \mathcal{O}\left(N \ln(N)\right)$$
and that the total work is V
$$V_h$$
$$u \qquad\qquad W = \mathcal{O}\left(N^2 \ln(N)\right)$$
since the work per iteration is $\mathcal{O}\left(N\right)$.
$$u_h$$
$$\Gamma_0$$
$$\Gamma_1$$
$$\Omega$$
: to be updated
: new values1
: old values
$$i-1$$
$$i$$
$$i+1$$
$$j-1$$
$$j$$
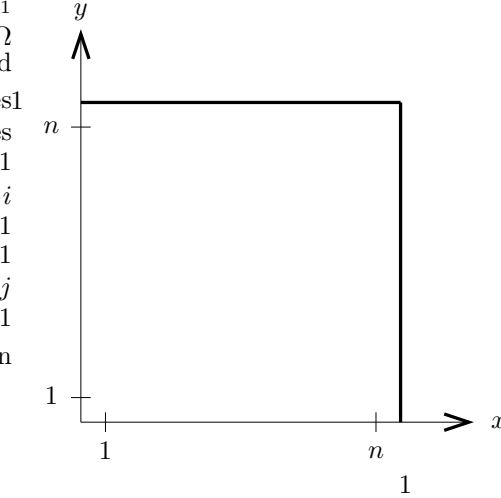$$j+1$$
iteration direction

Figure A.1: Domain for the solution of the Laplace equation.

Multigrid method

A general way to accelerate the convergence of e.g. the Gauss-Seidel method is provided by the Multigrid method. We note that the Gauss-Seidel provides good <u>smoothing</u> of the local error, but converges slowly since it takes time for boundary information to propagate into the domain. The idea behind the multigrid method is that a slowly converging low-frequency on a fine grid is a fast converging high-frequency on a coarse grid. Let

$$L\Phi_{i,j} = \frac{\Phi_{i+1,j} - 2\Phi_{i,j} + \Phi_{i-1,j}}{\Delta x^2} + \frac{\Phi_{i,j+1} - 2\Phi_{i,j} + \Phi_{i,j-1}}{\Delta y^2}$$

and define the correction to the solution to the true discrete solution in the following manner

$$
\begin{aligned}
\Phi_{i,j} &= \Phi_{i,j}^k + \Delta\Phi_{i,j} \\
\Phi_{i,j}^k &- \quad \text{solution at iteration level } k \\
\Delta\Phi_{i,j} &- \quad \text{correction to } \Phi_{i,j}^k \text{ to true discrete solution}
\end{aligned}
$$

This implies that

$$L\Delta\Phi_{i,j} = -L\Phi_{i,j}^k \equiv -R_{i,j}$$

since $L\Phi_{i,j} = 0$. Thus we are left with an equation implying that the Laplace operator on the correction is equal to the negative of the residual. This residual equation is solved on a coarser grid and the correction is interpolated onto finer grid.

In order to define the algorithm we use the following definitions

I transfer operator between grids: An example of a restriction operator I_1^2 is to
I_1^2 - restriction operator from grid 1 to grid 2
I_2^1 - prolongation operator from grid 2 to grid 1

define it as an injection, i.e. we use every other value in each direction. The prolongation operator I_2^1 may be defined by linear interpolation for the intermediate values, i.e. an average of right and left values
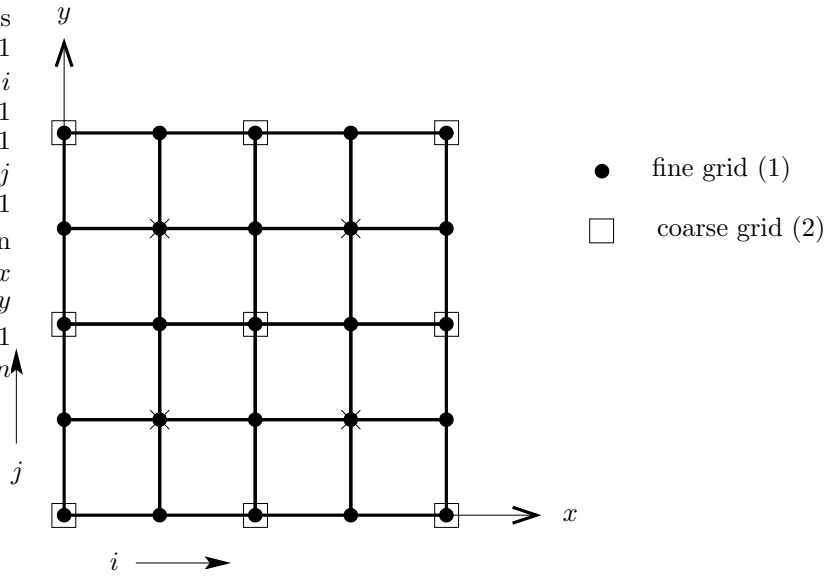
Figure A.2: Two level grid.

and top and bottom values. The values marked with $\times$ in figure A.2 are then taken as an average of the averages of the intermediate values.

Now we can define the following two level scheme:

1. $L\Phi_{i,j}$ iterated k times $\qquad \Rightarrow \qquad L\Phi_{i,j}^k = R_{i,j}$

2. $L\Delta\Phi_{i,j} = -I_1^2 R_{i,j}$ $\qquad$ iterated k times, $\Delta\Phi_{i,j}^0 = 0$ (starting value) (here $\Delta\Phi_{i,j}$ is definied on grid 2)

3. $\Phi_{i,j} = \Phi_{i,j}^k + I_2^1 \Delta\Phi_{i,j}$ $\qquad$ and goto 1.

at the end of 1. convergence is checked.

Wesseling [10] estimated the work of the multigrid method to be $W = \mathcal{O}(N \ln N)$, a substantial improvement over the Gauss-Seidel method.

A.2 Cartesian tensor notation

Tensor notation is a compact way to write vector and tensor formulas. Vectors and tensors are objects which are independent of the coordinate system they are represented in.
In the Cartesian coordinate system in Figure A.3 we have the unit vectors

$$|\mathbf{e}_k| = 1 \qquad k = 1, 2, 3$$

The scalar product of two unit vectors is the Kronecker's delta, δ_{kl}

$$\mathbf{e}_k \cdot \mathbf{e}_l = \delta_{kl} = \begin{array}{cc} 1 & k = l \\ 0 & k \neq l \end{array}$$

and the position vector $\mathbf{r}$ is

$$\mathbf{r} = x_1 \mathbf{e}_1 + x_2 \mathbf{e}_2 + x_3 \mathbf{e}_3 = \sum_{k=1}^{3} x_k \mathbf{e}_k = x_k \mathbf{e}_k.$$

The last expression make use of *Einstein's summation convention*: when an index occurs twice in the same expression, the expression is implicitly summed over all values for that index.

Example

$$\delta_{kk} = \delta_{ll} = \delta_{11} + \delta_{22} + \delta_{33} = 3$$

$$\delta_{ij} a_j = \delta_{i1} a_1 + \delta_{i2} a_2 + \delta_{i3} a_3 = a_i.$$
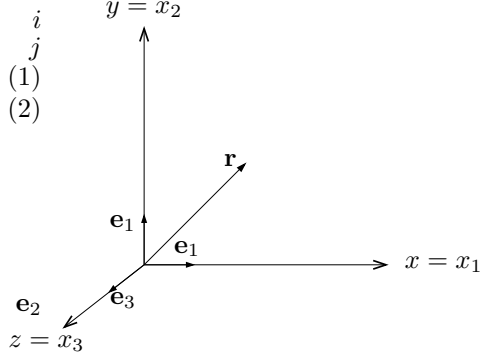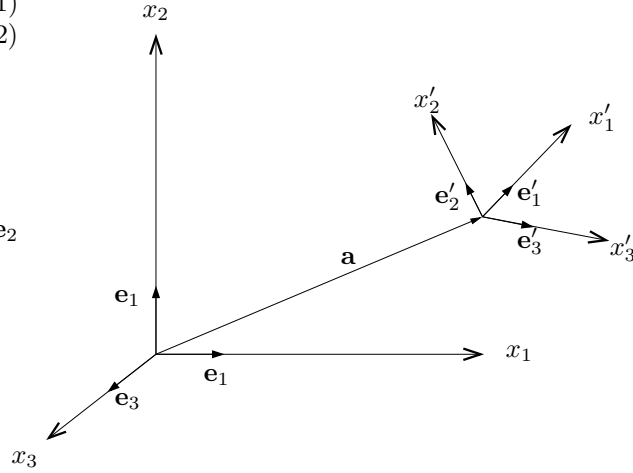
Figure A.3: Cartesian coordinate system.

Figure A.4: Two different coordinate systems.

A.2.1 Orthogonal transformation

Consider two arbitrary oriented coordinate systems as in Figure A.4. Assume identical origin, $\mathbf{a} = 0$. The unit vectors are orthogonal

$$\mathbf{e}'_k \cdot \mathbf{e}'_l = \delta_{kl}$$

and a position vector is independent of coordinate system,

$$\mathbf{r} = x_l \mathbf{e}_l = x'_l \mathbf{e}'_l.$$

Component k of $\mathbf{r}$ can be written as

$$\mathbf{e}'_k \cdot \mathbf{r} = x_l \mathbf{e}'_k \cdot \mathbf{e}_l = x'_l \mathbf{e}'_l \cdot \mathbf{e}'_k = x'_l \delta_{kl} = x'_k \qquad \Rightarrow \qquad x'_k = \mathbf{e}'_k \cdot \mathbf{e}_l x_l = c_{k'l} x_l$$

where we have the transformation tensor

$$c_{k'l} = \mathbf{e}'_k \cdot \mathbf{e}_l = \cos(x'_k, x_l).$$

Since $\cos(x'_2, x_1) \neq \cos(x'_1, x_2)$ in general, we have (for $k = 1, l = 2$)

$$c_{l'k} = \mathbf{e}'_l \cdot \mathbf{e}_k = \cos(x'_l, x_k) \neq c_{k'l}$$

From

$$\mathbf{e}_k \cdot \mathbf{r} = x_l \mathbf{e}_k \cdot \mathbf{e}_l = x'_l \mathbf{e}_k \cdot \mathbf{e}'_l \qquad \Rightarrow \qquad x_k = \mathbf{e}'_l \cdot \mathbf{e}_k x'_l = c_{l'k} x'_l = c_{lk} x'_l$$

we conclude that **first** index refer to primed system!

Example

$$
\begin{aligned}
x'_k &= c_{kl} x_l = c_{k1} x_1 + c_{k2} x_2 + c_{k3} x_3 = \cos(x'_k, x_1) x_1 + \cos(x'_k, x_2) x_2 + \cos(x'_k, x_3) x_3 \\
&= \mathbf{e}'_k \cdot \mathbf{e}_1 x_1 + \mathbf{e}'_k \cdot \mathbf{e}_2 x_2 + \mathbf{e}'_k \cdot \mathbf{e}_3 x_3
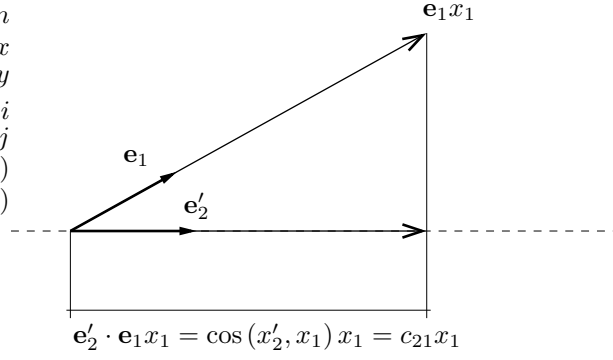\end{aligned}
$$

$$\mathbf{e}'_2 \cdot \mathbf{e}_1 x_1 = \cos\left(x'_2, x_1\right) x_1 = c_{21} x_1$$

Figure A.5: Projection of $\mathbf{e}_1 x_1$ on $\mathbf{e}'_2$.

which for component 2 reads

$$x'_2 = \mathbf{e}'_2 \cdot \mathbf{e}_1 x_1 + \mathbf{e}'_2 \cdot \mathbf{e}_2 x_2 + \mathbf{e}'_2 \cdot \mathbf{e}_3 x_3$$

$\because x'_2$ is projection of $\mathbf{e}_1 x_1, \mathbf{e}_2 x_2, \mathbf{e}_3 x_3$ on $\mathbf{e}'_2$. A visualization of the projection of $\mathbf{e}_1 x_1$ on $\mathbf{e}'_2$ can be seen in Figure A.5.

The relation between c_{kl} and c_{ml} can be studied through

$$\underbrace{x'_k}_{\delta_{km} x'_m} = c_{kl} \underbrace{x_l}_{c_{ml} x'_m} = c_{kl} c_{ml} x'_m \qquad \Rightarrow \qquad \left(c_{kl} c_{ml} - \delta_{km}\right) x'_m = 0.$$

In the same manner we have

$$\underbrace{x_k}_{\delta_{km} x_m} = c_{lk} \underbrace{x'_l}_{c_{lm} x_m} = c_{lk} c_{lm} x_m \qquad \Rightarrow \qquad \left(c_{lk} c_{lm} - \delta_{km}\right) x_m = 0.$$

A.2.2   Cartesian Tensors

Def. a Cartesian tensor of **rank** R is a set of quantities $T_{klm...}$ which transform as a vector in each of its R indices.

$$T'_{klm...} = c_{kr} c_{ls} c_{mp} \ldots T_{rsp...}$$

Example
For scalars the rank is $R = 0$

$$\mathbf{a} \cdot \mathbf{b} = a'_k \, b'_k = \underbrace{c_{kl} c_{km}}_{\delta_{lm}} a_l b_m = a_l b_l,$$

for vectors $R = 1$

$$a'_k = c_{kl} a_l$$

and for a tensor of second order we have $R = 2$

$$\delta'_{kl} = c_{km} c_{ln} \delta_{mn} = c_{km} c_{lm} = \delta_{kl}.$$

δ_{kl} is **isotropic**, i.e. identical in all coordinate systems.
An outer product generates a tensor

$$T'_{kl} S'_{rs} = c_{km} c_{ln} c_{rp} c_{sq} T_{mn} S_{pq}$$

and an inner product generates a tensor

$$T'_{kl} S'_{ls} = c_{km} \underbrace{c_{ln} c_{lp}}_{\delta_{np}} c_{sq} T_{mn} S_{pq} = c_{km} c_{sq} T_{mn} S_{nq}$$

A.2.3 Permutation tensor

$$\varepsilon_{klm} = \left\{ \begin{array}{c} 1 \\ -1 \\ 0 \end{array} \right\} \text{ if } klm \text{ is } \left\{ \begin{array}{c} \text{even} \\ \text{odd} \\ \text{no} \end{array} \right\} \text{ permutation of } (1,2,3)$$

As examples of permutations of 1,2,3 we have

(1,2,3),	(3,1,2),	(2,3,1)	even permutation	$\varepsilon_{123} = 1$
(2,1,3),	(3,2,1),	(1,3,2)	odd permutation	$\varepsilon_{213} = -1$
at least 2 subscripts equal			no permutation	$\varepsilon_{221} = 0$

A.2.4 Inner products, crossproducts and determinants

The inner product of the vectors $\mathbf{a}$ and $\mathbf{b}$ is

$$\mathbf{a} \cdot \mathbf{b} = \delta_{ij} a_i b_j = a_i b_i = a_1 b_1 + a_2 b_2 + a_3 b_3.$$

The cross product of $\mathbf{a}$ and $\mathbf{b}$ can be written as

$$\mathbf{a} \times \mathbf{b} = \begin{vmatrix} \mathbf{e}_1 & \mathbf{e}_2 & \mathbf{e}_2 \\ a_1 & a_2 & a_3 \\ b_1 & b_2 & b_3 \end{vmatrix} = (a_2 b_3 - a_3 b_2)\mathbf{e}_1 + (a_3 b_1 - a_1 b_3)\mathbf{e}_2 + (a_1 b_2 - a_2 b_1)\mathbf{e}_3 = \varepsilon_{ijk}\mathbf{e}_i a_j b_k$$

and the determinant of the tensor a_{ij} is

$$
\begin{aligned}
|\{a_{ij}\}| &= \begin{vmatrix} a_{11} & a_{12} & a_{13} \\ a_{21} & a_{22} & a_{23} \\ a_{31} & a_{32} & a_{33} \end{vmatrix} = \varepsilon_{ijk} a_{1i} a_{2j} a_{3k} \\
&= \frac{1}{6}\varepsilon_{ijk}\left(a_{i1}a_{j2}a_{k3} + a_{i3}a_{j1}a_{k2} + a_{i2}a_{j3}a_{k1} - a_{i2}a_{j1}a_{k3} - a_{i3}a_{j2}a_{k1} - a_{i1}a_{j3}a_{k2}\right) = \frac{1}{6}\varepsilon_{ijk}\varepsilon_{pqr}a_{ip}a_{jq}a_{kr}.
\end{aligned}
$$

We have the permutation relation

$$\varepsilon_{klm}\varepsilon_{ksp} = \delta_{ls}\delta_{mp} - \delta_{lp}\delta_{ms}. \tag{A.1}$$

If we set $s = l$ in (A.1) we get

$$\varepsilon_{klm}\varepsilon_{klp} = (3-1)\delta_{mp} = 2\delta_{mp}$$

and if we also use $p = m$ we end up with

$$\varepsilon_{klm}\varepsilon_{klm} = 6$$

The permutation tensor can also be used to derive the following vector relation

$$
\begin{aligned}
(\mathbf{a} \times \mathbf{b}) \cdot (\mathbf{c} \times \mathbf{d}) &= \varepsilon_{ijk} a_j b_k \varepsilon_{ilm} c_l d_m = (\delta_{jl}\delta_{km} - \delta_{jm}\delta_{lk}) a_j b_k c_l d_m \\
&= a_j c_j b_k d_k - a_j d_j b_k c_k = (\mathbf{a} \cdot \mathbf{c})(\mathbf{b} \cdot \mathbf{d}) - (\mathbf{a} \cdot \mathbf{d})(\mathbf{b} \cdot \mathbf{c})
\end{aligned}
$$

A.2.5 Second rank tensors

All second rank tensors can be decomposed into symmetric and antisymmetric parts, $T_{kl} = T_{(kl)} + T_{[kl]}$, where the antisymmetric part is

$$T_{[kl]} = -T_{[lk]} = \frac{1}{2}\left(T_{kl} - T_{lk}\right)$$

and the symmetric part

$$T_{(kl)} = T_{(lk)} = \frac{1}{2}\left(T_{kl} + T_{lk}\right).$$

The symmetric part can be decomposed into isotropic and traceless part, $T_{(kl)} = \overline{T}_{kl} + \overline{\overline{T}}_{kl}$, the isotropic part being

$$\overline{\overline{T}}_{kl} = \frac{1}{3}T_{mm}\delta_{kl}$$

and the traceless part is

$$\overline{T}_{kl} = T_{(kl)} - \frac{1}{3}T_{mm}\delta_{kl}.$$

If we project the isotropic, traceless and entisymmetric parts we get

$$S_{(kl)}T_{[kl]} = \frac{1}{2}\left(S_{(kl)}T_{[kl]} + S_{(lk)}T_{[lk]}\right) = \frac{1}{2}\left(S_{(kl)}T_{[kl]} - S_{(lk)}T_{[kl]}\right) = 0$$

$$\overline{\overline{S}}_{kl}\overline{T}_{kl} = \frac{1}{3}S_{mm}\delta_{kl}\left(T_{(kl)} - \frac{1}{3}T_{mm}\delta_{kl}\right) = \frac{1}{3}S_{mm}\left(T_{kk} - \frac{1}{3}T_{kk}\delta_{ll}\right) = 0$$

$$\Rightarrow$$

$$
\begin{aligned}
S_{kl}T_{[kl]} &= S_{[kl]}T_{[kl]} \\
S_{kl}T_{(kl)} &= S_{(kl)}T_{(kl)} \\
S_{kl}\overline{\overline{T}}_{kl} &= \overline{\overline{S}}_{kl}\overline{\overline{T}}_{kl} \\
S_{kl}\overline{T}_{kl} &= \overline{S}_{kl}\overline{T}_{kl},
\end{aligned}
$$

and each part is invariant under transformation

$$T'_{[kl]} = c_{kr}c_{ls}T_{[rs]} = -c_{kr}c_{ls}T_{[sr]} = -c_{lr}c_{ks}T_{[rs]} = -T'_{[lk]}$$

$$T'_{rr} = c_{rp}c_{rq}T_{pq} = \delta_{pq}T_{pq} = T_{pp}$$

$$\overline{T}'_{kl} = c_{kp}c_{lq}\overline{T}_{pq} = c_{kp}c_{lq}\left(T_{(pq)} - \frac{1}{3}T_{rr}\delta_{pq}\right) = T'_{(pq)} - \frac{1}{3}T_{rr}\delta_{kl}\ .$$

Since we only need three components to completely describe an antisymmetric tensor of rank $R = 2$ it can be represented by its dual vector

$$d_i = \varepsilon_{ijk}T_{jk} = \varepsilon_{ijk}T_{(jk)} + \varepsilon_{ijk}T_{[jk]}$$

The first term on the right hand side is zero since ε_{ijk} is antisymmetric in any two indecies. Multiply both sides by ε_{ilm}

$$\varepsilon_{ilm}d_i = \varepsilon_{ilm}\varepsilon_{ijk}T_{jk} = \left(\delta_{lj}\delta_{mk} - \delta_{lk}\delta_{mj}\right)T_{jk} = T_{lm} - T_{ml} = 2T_{[lm]} \qquad \Rightarrow \qquad T_{[lm]} = \frac{1}{2}\varepsilon_{ilm}d_i$$

<u>Note</u>: There are 3 independent components in $T_{[lm]}$ and d_i.

In order to sum up, an arbitrary tensor of rank 2 can be divided into the following parts

$$T_{kl} = T_{(kl)} + T_{[kl]} = \overline{\overline{T}}_{kl} + \overline{T}_{kl} + T_{[kl]} = \underbrace{\frac{1}{3}T_{rr}\delta_{kl}}_{\text{isotropic}} + \underbrace{T_{(kl)} - \frac{1}{3}T_{rr}\delta_{kl}}_{\text{traceless}} + \underbrace{\frac{1}{2}\varepsilon_{ikl}d_i}_{\text{antisymmetric}}$$

Properties of the above parts are invariant under transformation. In the Navier-Stokes equations we have the velocity gradient $\frac{\partial u_i}{\partial x_j}$. The antisymmetric part of this tensor describes rotation, the isotropic part the volume change and the traceless part describes the deformation of a fluid element.

Example

We have the second rank tensor

$$\{T_{kl}\} = \begin{bmatrix} 1 & 2 & 3 \\ 4 & 5 & 6 \\ 7 & 8 & 9 \end{bmatrix}$$

which can be divided into a symmetric part

$$\{T_{(kl)}\} = \begin{bmatrix} 1 & 3 & 5 \\ 3 & 5 & 7 \\ 5 & 7 & 9 \end{bmatrix}$$

and an antisymmetric part

$$\{T_{[kl]}\} = \begin{bmatrix} 0 & -1 & -2 \\ 1 & 0 & -1 \\ 2 & 1 & 0 \end{bmatrix}.$$

The symmetric part can then be divided into a isotropic part

$$\{\overline{\overline{T}}_{kl}\} = \begin{bmatrix} 5 & 0 & 0 \\ 0 & 5 & 0 \\ 0 & 0 & 5 \end{bmatrix}$$

and a traceless part

$$\{\overline{T}_{kl}\} = \begin{bmatrix} -4 & 3 & 5 \\ 3 & 0 & 7 \\ 5 & 7 & 4 \end{bmatrix}.$$

The dual vector of the antisymmetric tensor is

$$\{d_i\} = \begin{bmatrix} -2 \\ 4 \\ -2 \end{bmatrix}.$$

A.2.6 Tensor fields

We have the tensor field $T_{ij}(x_1, x_2, x_3) \equiv T_{ij}(x_k)$ with the following properties

- partial derivative transforms like a tensor

$$\frac{\partial}{\partial x'_p} = \frac{\partial x_k}{\partial x'_p}\frac{\partial}{\partial x_k} = c_{pk}\frac{\partial}{\partial x_k} \qquad \text{where} \qquad (x_k = c_{pk}x'_p)$$

- gradient adds one to tensor rank

$$\frac{\partial}{\partial x_k}T_{ij}$$

- divergence decreases tensor rank by one

$$\frac{\partial}{\partial x_k}T_{kl} = \frac{\partial T_{1l}}{\partial x_1} + \frac{\partial T_{2l}}{\partial x_2} + \frac{\partial T_{3l}}{\partial x_3}$$

- curl

$$(\nabla \times \mathbf{u})_i = \varepsilon_{ijk}\frac{\partial u_k}{\partial x_j}$$

which can be compared with the expression for the determinant.

Example
Show that $\nabla \cdot (\nabla \times \mathbf{\Psi}) = 0$.

$$\nabla \cdot (\nabla \times \mathbf{\Psi}) = \frac{\partial}{\partial x_k}\varepsilon_{klm}\frac{\partial \Psi_m}{\partial x_l} = \varepsilon_{klm}\frac{\partial^2}{\partial x_k \partial x_l}\Psi_m = 0$$

since ε_{klm} is antisymmetric in kl and $\frac{\partial^2}{\partial x_k \partial x_l}$ is symmetric in kl.

Example
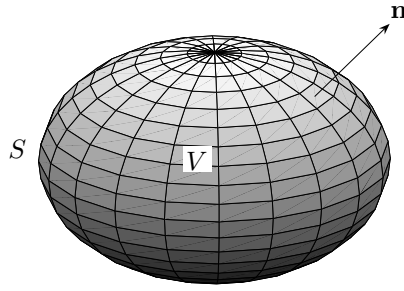*Show that $\nabla f(r) = \frac{1}{r}f'(\mathbf{r})$ where $\{\mathbf{r}\}_k = x_k$ and $r = |\mathbf{r}| = \sqrt{x_k x_k}$.*

$$\begin{aligned} \{\nabla f(r)\}_k &= \frac{\partial}{\partial x_k}f(r) = \frac{\mathrm{d}f}{\mathrm{d}r}\frac{\partial r}{\partial x_k} = f'\frac{\partial (x_p x_p)^{1/2}}{\partial x_k} = \\ &f'\frac{1}{2}(x_p x_p)^{-\frac{1}{2}}\frac{\partial}{\partial x_k}(x_p x_p) = f'\frac{1}{2r}(\delta_{pk}x_p + x_p\delta_{pk}) = \frac{1}{r}f'x_k = \left\{\frac{1}{r}f'\mathbf{r}\right\}_k \end{aligned}$$

Example
Show that $\nabla \times (\nabla \times \mathbf{F}) = \nabla(\nabla \cdot \mathbf{F}) - \Delta \mathbf{F}$.

$$\left(\nabla \times (\nabla \times \mathbf{F})\right)_i = \varepsilon_{ijk}\frac{\partial}{\partial x_j}\varepsilon_{klm}\frac{\partial}{\partial x_l}F_m = \varepsilon_{ijk}\varepsilon_{klm}\frac{\partial}{\partial x_j}\frac{\partial}{\partial x_l}F_m = \varepsilon_{kij}\varepsilon_{klm}\frac{\partial}{\partial x_j}\frac{\partial}{\partial x_l}F_m =$$

y
1
n
x
y
i
j
fine grid (1)
coarse grid (2)

S

V

$\mathbf{n}$

$$\mathrm{d}\mathbf{S} = \mathbf{n}\,\mathrm{d}S$$

Figure A.6: Volume V bounded by the close surface S.

$$(\delta_{il}\delta_{jm} - \delta_{im}\delta_{jl})\frac{\partial}{\partial x_j}\frac{\partial}{\partial x_l}F_m = \frac{\partial}{\partial x_j}\frac{\partial}{\partial x_i}F_j - \frac{\partial}{\partial x_j}\frac{\partial}{\partial x_j}F_i = \frac{\partial}{\partial x_i}\frac{\partial}{\partial x_j}F_j - \frac{\partial}{\partial x_j}\frac{\partial}{\partial x_j}F_i = \left(\nabla(\nabla \cdot \mathbf{F}) - \Delta\mathbf{F}\right)_i$$

Example

Show that if $\bar{u} = \bar{\Omega} \times \bar{r}$ then $\mathbf{\Omega} = \dfrac{\nabla \times \mathbf{u}}{2}$. This means, show that $\varepsilon_{ijk}\dfrac{\partial}{\partial x_j}u_k = 2\Omega_i$.

$$\varepsilon_{ijk}\frac{\partial}{\partial x_j}u_k = \{u_k = \varepsilon_{klm}\Omega_l r_m\} = \varepsilon_{ijk}\frac{\partial}{\partial x_j}(\varepsilon_{klm}\Omega_l r_m) = \varepsilon_{ijk}\varepsilon_{klm}\frac{\partial}{\partial x_j}\Omega_l r_m =$$

$$\varepsilon_{kij}\varepsilon_{klm}\frac{\partial}{\partial x_j}\Omega_l r_m = (\delta_{il}\delta_{jm} - \delta_{im}\delta_{jl})\frac{\partial}{\partial x_j}\Omega_l r_m =$$

$$\frac{\partial}{\partial x_m}\Omega_i r_m - \frac{\partial}{\partial x_l}\Omega_l r_i = \{\Omega \text{ independent of } x\} = \Omega_i\frac{\partial r_m}{\partial x_m} - \Omega_l\frac{\partial r_i}{\partial x_l} = \{\frac{\partial r_m}{\partial x_m} = 1 + 1 + 1 = 3 \quad \frac{\partial r_i}{\partial x_l} = \delta_{il}\} =$$

$$3\Omega_i - \Omega_l\delta_{il} = 2\Omega_i$$

A.2.7 Gauss & Stokes integral theorems

Let $\mathbf{n}$ be the outward pointing normal to the closed surface S bounding the simply-connected volume V, see Figure A.6. Gauss integral theorem then states

$$\oint_S \mathbf{a} \cdot \mathbf{n}\,\mathrm{d}S = \int_V \nabla \cdot \mathbf{a}\,\mathrm{d}V$$

or

$$\oint_S a_k n_k\,\mathrm{d}S = \int_V \frac{\partial a_k}{\partial x_k}\,\mathrm{d}V$$

for a differentiable vector field $\mathbf{a}$. This can be generalized to

$$\oint_S T_{klm}n_p\,\mathrm{d}S = \int_V \frac{\partial}{\partial x_p}T_{klm}\,\mathrm{d}V\,.$$

Example

$$\oint_S f\mathbf{n}\,\mathrm{d}S = \int_V \nabla f\,\mathrm{d}V\,.$$

$$\oint_S \mathbf{a} \times \mathbf{n}\,\mathrm{d}S = \int_V \nabla \times \mathbf{a}\,\mathrm{d}V \qquad \text{if} \qquad T_{klm}n_m = \varepsilon_{klm}a_l n_m.$$

Stokes theorem states that for a differentiable vector field $\mathbf{a}$ if an open simply-connected surface S is enclosed by a closed curve C, of which $\mathrm{d}\mathbf{l}$ is the line element as in Figure A.7, then

$$\oint_C \mathbf{a} \cdot \mathrm{d}\mathbf{l} = \int_S (\nabla \times \mathbf{a}) \cdot \mathbf{n}\,\mathrm{d}S$$
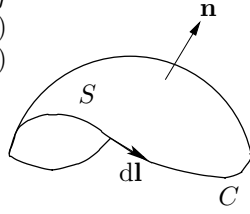
i
$i+1$ fine grid (1)
$j-1$ coarse grid (2)
j
$j+1$
iteration direction
x
y
1
n

Figure A.7: The open surface S enclosed by the contour C.

p_0

x
y
i
j
fine grid (1)
coarse grid (2)

x_3

M

$\mathbf{n}$

$\mathrm{d}V$ $\mathrm{d}m$
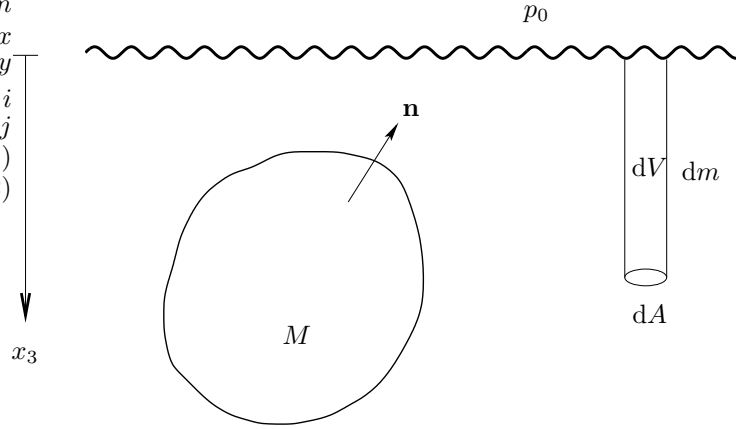
$\mathrm{d}A$

Figure A.8: An object with mass M immersed in a fluid illustrating Archimedes principle.

or

$$\oint_C a_k \, \mathrm{d}x_k = \int_S \varepsilon_{klm} n_k \frac{\partial a_m}{\partial x_k} \, \mathrm{d}S$$

this can be generalized to

$$\oint_C T_{klm} \, \mathrm{d}x_p = \int_S \varepsilon_{ijp} n_i \frac{\partial}{\partial x_j} T_{klm} \, \mathrm{d}S$$

Example

Let $T_{klm} = f$. In the generalized Stokes theorem we then get $\int_S \varepsilon_{ijp} n_i \frac{\partial f}{\partial x_j} \, \mathrm{d}S$ in right hand side

$$\oint_C f \, \mathrm{d}\mathbf{l} = \int_S \mathbf{n} \times \nabla f \, \mathrm{d}S$$

A.2.8   Archimedes principle

Gauss theorem can be used to calculate the buoyancy on an object immersed in a fluid (Archimedes circa 281–212 BC). Consider a water cylinder with volume dV and mass dm, Figure A.8.

The force from the water cylinder is

$$\mathrm{d}m \, g = \mathrm{d}V \rho g = \underbrace{x_3 \rho g}_{\text{pressure}} \, \mathrm{d}A$$

where g is the gravity constant and ρ the water density. The pressure at a distant x_3 from the surface in a fluid is then $p = \rho g x_3 + p_0$ where p_0 is the atmospheric pressure. Let $\mathbf{\Pi}$ be the buoyancy force resulting from the pressure on the object, m the mass of equivalent volume of water and M the mass of the object in Figure A.8. The force on a small element $\mathrm{d}S$ of the body resulting from the pressure is

$$\mathrm{d}\Pi_k = -g\rho x_3 n_k \, \mathrm{d}S$$

where the minus sign stems from the outward pointing normal $\mathbf{n}$. The buoyancy force can then be calculated through

$$\Pi_k = -\oint_S \rho g x_3 n_k \, \mathrm{d}S = -\rho g \int_V \frac{\partial}{\partial x_k} x_3 \, \mathrm{d}V = -\rho g \delta_{k3} V.$$
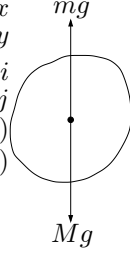
Figure A.9: The forces acting on an object immersed in a fluid. m is the mass of equivalent volume of water and M the mass of the body.
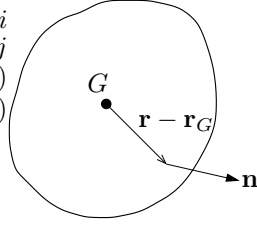

Figure A.10: Moment around G from pressure forces acting on the object.

This means that the object loses some weight as the water is displaced. The buoyancy force is

$$\Pi_3 = -\rho g V = -g\,m$$

see Figure A.9.

The moment of a force $\mathbf{F}$ at some arbitrary point with position vector $\mathbf{r}$ from the point of application of the force is $\mathbf{M} = \mathbf{r} \times \mathbf{F}$. The moment around the center of gravity G of the homogenous body produced by the pressure force $d\mathbf{\Pi}$ acting on an element dS of the body is $d\mathbf{M}_G = (\mathbf{r} - \mathbf{r}_G) \times d\mathbf{\Pi}$ as in Figure A.10. This can then be used to calculate the total moment around G form pressure forces on the body

$$
M_{G_k} = -\oint_S \rho g \varepsilon_{klm} (x_l - x_{G_l}) x_3 n_m \, dS = -\rho g \varepsilon_{klm} \int_V \left[\frac{\partial}{\partial x_m}(x_l x_3) - x_{G_l} \frac{\partial x_3}{\partial x_m} \right] dV =
$$

$$
-\rho g \varepsilon_{klm} \int_V \left[\delta_{lm} x_3 + \delta_{m3} x_l - \delta_{m3} x_{G_l} \right] dV = -\rho g \varepsilon_{kl3} \left[\int_V x_l \, dV - x_{G_l} V \right] = 0
$$

If a part of the fluid is frozen (without changing in density) this body is in <u>equilibrium</u> in the fluid: $\mathbf{F} = \mathbf{M} = 0$.

Appendix B

Supplementary material

B.1 Syllabus 2005

Computational Fluid Dynamics (5C1212), 5p.

Lecturers:

Dan Henningson (DH), *henning@mech.kth.se*, Mekanik, tel 790 9004
  Katarina Gustavsson (KG), *katarina@nada.kth.se*, NADA, tel 790 6696
  Luca Brnadt (LB), *luca@mech.kth.se*, Mekanik, tel 790 7161
  Erik Stålberg (ES), *eriks@mech.kth.se*, Mekanik, tel 790 7161

Literature:

Copies from J.C. Tannehill, D.A. Anderson, R.H. Pletcher, *Computational Fluid Mechanics and Heat Transfer*, Taylor & Francis, 1997, (TAP)
  Copies from Randall J LeVeque, *Fininte Volume Method for Hyperbolic Problems*, Cambridge University Press, 2002 (LeV)
  D. Henningson, *Lecture notes on Computational Fluid Dynamics*
  K. Gustavsson, *Lecture notes on Basic Numerics*

Grading:

Test total of 50p., homeworks (required) $3\times5 = 15$p.
Total points > 30 (3), > 40 (4), > 50 (5).

Web links

http://www.mech.kth.se/

Course plan

1. Tue 18/1 8-10, E51. Fluid dynamics I: LB

   Introduction and outline of the course.

   Derivation of the governing equations.

2. Wed 19/1 15-17, E51. Basic numerics I: KG

   Mathematical behavior of hyperbolic, parabolic and elliptic equations. Well-posedness. KG Lecture notes

3. Thu 20/1 8-10, E35. Fluid dynamics II: LB

   Derivation of the governing equations , cont.

4. Fri 21/1 15-17 L21. Basic numerics II: KG

   Discretization by finite differences. Analysis of discretized equations; order of accuracy, convergence and stability (von Neumann analysis).
   TAP: 3.1-3.3.5, 3.6, LeV: 8-8.2, 8.3.3

5. Tue 25/1 8-10, E51. Fluid dynamics III: LB

   Derivation of the governing equations , cont.

6. Wed 26/1 15-17, Q36. Basic numerics III: KG

   Numerical methods for model equations related to different levels of approximation of Navier Stokes equation: linear wave equation, Burgers equation, convection-diffusion equation. First and second order numerical methods such as upwind, Lax-Friedrichs, Lax-Wendroff, MacCormack, etc. Modified equation - dissipation and dispersion.
   TAP: 4.1-4.1.8, LeV: 8.6

7. Thu 27/1 8-10, V33. Fluid dynamics IV: LB

   Dimensionless form, fluid phenomena, simplified equations

8. Fri 28/1 15-17, L21. Basic numerics IV: KG

   Numerical methods for model equations, cont.

9. Mon 31/1 13-15, Q35. Compressible flow I: KG

   Introduction to compressible flow. Euler equations, conservative/non-conservative form. Some thermodynamics.
   LeV: 14

   Scalar conservations laws: Conservation, weak solutions, non-uniqueness, entropy conditions. Shock formation, Rankine-Hugoniot relations.
   LeV: 11

10. Wed 2/2 15-17, E52. Compressible flow II: KG

    Numerical methods for scalar conservation laws. Properties of the numerical scheme such as CFL-condition, conservation and TVD. First order methods. System of conservations laws
    LeV: 4.1-4.9, 3

11. Fri 4/2 15-17, E52. Compressible flow III: KG

    Numerical methods for Euler equations: MacCormack and artificial viscosity for non-linear systems. Numerical/physical boundary conditions. Shock tube problem.
    LeV: 3, 14

12. Tue 8/2 08-10, E51 . Compressible flow IV: KG

    High resolution schemes for conservations laws.
    LeV: 6

13. Wed 9/2 15-17, D34. Compressible flow V: KG

    Numerical methods for Euler equations. Boundary conditions, Riemann invariants. Compressible flow in 2D.
    TAP: 6.3-6.7, LeV: 14

14. Fri 11/2 15-17, E35. Compressible flow VI: KG

    Numerical methods for Euler equations, cont. Grids, algebraic mesh generation by transfinite interpolation. Flow around an airfoil.

15. Tue 15/2 08-10, E3. Finite volume and finite difference methods I: DH

    Laplace equation on arbitrary grids, equivalence with finite-differences, linear systems: Gauss-Seidel as smothers for multi-grid.

16. Wed 16/2 15-17, D34. Finite volume and finite difference methods II: DH

    Introduction to incompressible flow. Properties of the equations, role of the pressure: artificial compressibility and projection on divergence free space, Navier-Stokes in integral form.

17. Fri 18/2 15-17, E35. Finite volume and finite difference methods III: DH

Staggered grid/volume formulation + BC. Unsteady equations: projection and MAC method, discrete Poisson pressure eq.

18. Tue 22/2 8-10, Q34. Finite volume and finite difference methods IV: DH

Time step restrictions. Steady equations: distributive iteration and SIMPLE methods.

19. Thu 24/2 8-10, E35. Finite elements I: DH

An advection–diffusion problem. Variational form of the equation, weak solutions, essential and natural boundary condition. Finite-element approximations, stability and accuracy, the algebraic problem, matrix assembly.

20. Fri 25/2 15-17, E31. Finite elements II: DH

Navier–Stokes equations. Mixed variational form, Galerkin and FE approximations, the algebraic problem. Stability, the LBB condition, mass conservation.

21. Tue 1/3 13-15, E31. Finite elements III: DH

Navier–Stokes equations. Mixed variational form, Galerkin and FE approximations, the algebraic problem. Stability, the LBB condition, mass conservation.

22. Wed 2/3 15-17, Q33. Finite elements IV: DH

Navier–Stokes equations. Mixed variational form, Galerkin and FE approximations, the algebraic problem. Stability, the LBB condition, mass conservation.

23. Sat 2/4 9-13, E31. EXAM.

Homeworks

- Homework 1A, due 31/1: Homework on NS equations.

- Homework 1B, due 31/1: Numerical methods for model equations. Different schemes. Dispersion, diffusion. Stability analysis.

- Homework 2, due 15/2: Numerical methods for non-linear conservation laws. Shock-tube.

- Homework 3, due 22/2: Running compressible Euler code; flow over a bump.

- Homework 4, due 1/3: FV homework + numerical project.

- Homework 5, due 8/3: FEM homework.

B.2   Study questions

1. Define and use the Rankine-Hugoniot jump condition to compute the shock speed for the following problem

$$
\begin{aligned}
u_t + uu_x &= 0 \quad -\infty < x < \infty, \quad t > 0 \\
u(x,0) &= \begin{cases} 1 & x \le 0 \\ 0 & \text{otherwise} \end{cases}
\end{aligned}
$$

2. Define the entropy condition for a scalar conservation law.

$$
u_t + f(u)_x = 0 \quad -\infty < x < \infty, \quad t > 0
$$

with a convex flux function $f(u)$. The shock is moving with speed s and the state to the left is given by u_L and the state to the right by u_R.

Why do we need an entropy condition ?

3. Write a difference approximation (in 1D) on conservative form and define the notation.

4. Solve

$$u_t + \left(\frac{u^2}{2}\right)_x = 0, \qquad u(x,0) = \begin{cases} 1 & x < 0 \\ 0 & x \geq 0 \end{cases} \tag{B.1}$$

by the upwind scheme on the following form,

$$u_j^{n+1} = u_j^n - \frac{\Delta t}{\Delta x} u_j^n (u_j^n - u_{j-1}^n)$$

a) Will the numerical solution converge to the analytical solution?

b) If not, suggest another way of solving B.1.

5. Define a total variation decreasing (TVD) method. Why is this a desirable property ?

6. Investigate the one-sided difference scheme

$$u_j^{n+1} = u_j^n - a\frac{\Delta t}{\Delta x}(u_j^n - u_{j-1}^n)$$

for the advection equation

$$u_t + au_x = 0$$

Consider the cases $a > 0$ and $a < 0$.

a) Prove that the scheme is consistent and find the order of accuracy. Assume k/h constant.

b) Determine the stability requirement for $a > 0$ and show that it is unstable for $a < 0$.

7. Apply Lax-Friedrichs scheme to the linear wave equation

$$u_t + au_x = 0.$$

a) Write down the modified equation.

b) What type of equations is this?

c) What kind of behavior can we expect from the solution?

8. A the three-point centered scheme applied to

$$u_t + au_x = 0, \quad a > 0.$$

yields the approximation

$$u_j^{n+1} = u_j^n + \frac{a\Delta t}{2\Delta x}(u_{j+1} - u_{j-1})$$

Show that this approximation is not stable even though the CFL condition is fulfilled.

9. What does Lax's equivalence theorem state?

10. What is the condition on the $n \times n$ real matrix $A(\mathbf{u})$ for the system

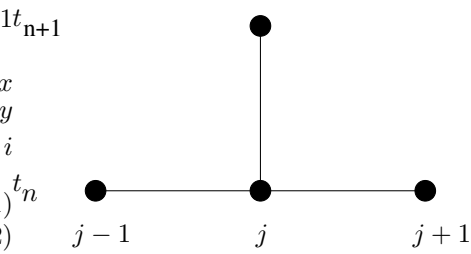$$\mathbf{u}_t + A\mathbf{u}_x = 0$$

to be hyperbolic ?

11. The barotropic gas dynamic equations

$$\rho_t + \rho u_x = 0 \tag{B.2}$$
$$u_t + uu_x + \frac{1}{\rho}p_x = 0$$

where

$$p = p(\rho) = C\rho^\gamma$$

i and C a constant, can be linearized by considering small perturbations (ρ', u') around a motionless gas.

$1t_{n+1}$

x
y
i

fine grid (1) t_n
coarse grid (2) $j-1$ j $j+1$

a) Let $\rho = \rho_0 + \rho'$ and $u = u_0 + u'$ where $u_0 = 0$. Linearize the system (B.2) and show that this yields the following linear system (the primes has been dropped)

$$\rho_t + \rho_0 u_x = 0$$
$$u_t + \frac{a^2}{\rho_0}\rho_x = 0 \qquad\qquad (B.3)$$

where a is the speed of sound. a and ρ_0 are constants.

b) Is the system given by (B.3) a hyperbolic system? Motivate your answer.

c) Determine the characteristic variables in terms of ρ and u.

d) Determine the partial differential equations the characteristic variables fulfill - characteristic formulation.

e) Given initial conditions at $t = 0$ and let $-\infty < x < \infty$ (no boundaries)

$$\rho(0, x) = sin(x) \quad u(0, x) = 0$$

determine the analytical solution to (B.3) for $t > 0$. Hint: Start from the characteristic formulation.

12. The linearized form of (B.3) is given by

$$\begin{pmatrix} \rho \\ u \end{pmatrix}_t + \underbrace{\begin{pmatrix} 0 & \rho_0 \\ a^2/\rho_0 & 0 \end{pmatrix}}_{A} \begin{pmatrix} \rho \\ u \end{pmatrix}_x = 0, \qquad\qquad (B.4)$$

where a is the speed of sound. a and ρ_0 are constants.

a) Draw the domain of dependence of the solution to the system (B.4) in a point P in the x-t plane.

b) The system is solved numerically on a grid given by $x_j = j\Delta x, j = 0, 1, 2...$ and $t_n = n\Delta t, n = 0, 1, 2, ...$ using an explicit three-point scheme, see the figure below.

Draw the domain of dependence of the numerical solution at P (in the same figure as a)) of the three-point scheme in the case when

i) the CFL condition is fulfilled

ii) the CFL condition is NOT fulfilled.

Assume that P is a grid point.

13. To solve Euler equations in 1D

$$\rho_t + \rho u_x + u\rho_x = 0$$
$$u_t + uu_x + \frac{1}{\rho}p_x = 0$$
$$p_t + \rho c^2 u_x + up_x = 0$$

How many boundary conditions must be added at (motivate your answer)

inflow boundary when the flow is

a) Supersonic

b) Subsonic

outflow boundary when the flow is

c) Supersonic

d) Subsonic

14. Describe the ideas behind a flux splitting scheme for solving a non-linear hyperbolic system of equations,
$$\mathbf{U}_t + F(\mathbf{U})_x = 0$$

15. a) Show that a vector field w_i can be decomposed into

$$w_i = u_i + \frac{\partial p}{\partial x_i}$$

where u is is divergence free and parallel to the boundary.

b) Apply this to the Navier-Stokes equations, show that the pressure term disappears and recover an equation for the pressure from the gradient part.

16. From the differential form of the Navier-Stokes equations obtain

a) the Navier-Stokes equations in integral form used in finite-volume discretizations,

b) a variational form of the Navier-Stokes equations used in finite-element discretizations.

17. a) Write down the appropriate function spaces for the pressure and velocity used to define weak solutions to the Navier-Stokes equations.

b) Explain the concept of essential and natural boundary conditions.

18. a) How is a finite-element approximation defined?

b) Explain how to convert a FEM discretization to an algebraic problem, e.g. that the Navier-Stokes equations yield

$$\begin{pmatrix} \nu\mathbf{K} + \mathbf{C}(u) & \mathbf{G} \\ \mathbf{G}^T & \mathbf{0} \end{pmatrix} \begin{pmatrix} u \\ p \end{pmatrix} = \begin{pmatrix} f \\ 0 \end{pmatrix}$$

19. a) By choosing $\mathbf{z}_h = \mathbf{u}_h$ in the finite element approximation of the Stokes problem, show that any Galerkin velocity solution is stable.

b) Describe and interpret the LBB condition.

20. Choice of elements. Discrete elements pairs

a) constant pressure-bilinear velocities,

b) the Taylor-Hood pair,

c) a stable choice with piecewise linear velocities.

21. a) Derive the finite volume (FV) discretization on arbitrary grids of the continuity equation ($\partial u_i/\partial x_i = 0$),

b) derive the FV discretization for Laplace equation on a Cartesian grid,

c) show that both are equivalent to a central difference approximation for Cartesian grids.

22. Derive the finite element (FEM) discretization for Laplace equation on a Cartesian grid and show that it is equivalent to a central difference approximation.

23. Iterative techniques for linear systems.

a) Define Gauss-Seidel iterations for the Laplace equations,

b) Define the 2-level multigrid method for the Laplace equation,

24. State the difficulties associated with the the finite-volume discretizations of the Navier-Stokes equations on a colocated grid? and show the form of the spurious solution which exist.

25. a) Define an appropriate staggered grid that can be used for the discretization of the Navier-Stokes equations,

b) write down the FV discretization of the Navier-Stokes equations on a staggered cartesian grid,

c) discuss how to treat noslip and inflow/outflow boundary conditions.

26. Time dependent flows.

a) Define a simple projection method for the time dependent Navier-Stokes equations

$$\frac{d}{dt}\begin{pmatrix} u \\ 0 \end{pmatrix} + \begin{pmatrix} \mathbf{N}(u) & \mathbf{G} \\ \mathbf{D} & \mathbf{0} \end{pmatrix}\begin{pmatrix} u \\ p \end{pmatrix} = \begin{pmatrix} f \\ g \end{pmatrix}$$

b) show in detail the equation for the pressure to be solved at each time step and discuss the boundary conditions for the pressure.

27. Time step restriction for Navier-Stokes solutions.

a) Motivate the use of an appropriate form of the advection-diffusion equation as a model equation for stability analysis,

b) derive the time step restrictions for the 1D version of that equation,

c) state the 2D equivalent of that restriction.

Bibliography

[1] D.J. Acheson, 1990, Elementary Fluid Dynamics, *Oxford University Press.*

[2] J.D. Anderson, Jr., 1995, Computational Fluid Dynamics, The basics with applications, *Mc Graw-Hill.*

[3] C.A.J. Fletcher, 1991, Computational Techniques for Fluid Dynamics Volume 1, Second Edition, *Springer-Verlag.*

[4] C.A.J. Fletcher, 1991, Computational Techniques for Fluid Dynamics, Volume 2, Second Edition, *Springer-Verlag.*

[5] M. Griebel, T. Dornseifer and T. Neunhoeffer, 1998, Numerical Simulation in Fluid Dynamics, A practical Introduction, *SIAM Monographs on Mathematical Modeling and Computation.*

[6] P.K. Kundu and I.M. Cohen, 2002, Fluid Mechanics, Second Edition, *Academic Press.*

[7] R.L. Panton, 1995, Incompressible Flow, Second Edition, *Wiley-Interscience.*

[8] R. Peyret, T.D. Taylor, 1983, Computational Methods for Fluid Flow, *Springer-Verlag.*

[9] J.C. Tannehill, D.A. Anderson and R.H. Pletcher, 1997, Computational Fluid Mechanics and Heat Transfer, Second Edition, *Taylor and Francis.*

[10] P. Wesseling, 2001, Principles of Computational Fluid Dynamics, *Springer-Verlag.*